Feeding State, Vitamin A Status and Atypical Protein Kinase C Modulate the Insulin-Regulated Gene Expression in Rat Hepatocytes

A Dissertation Presented for the

Doctor of Philosophy

Degree

The University of Tennessee, Knoxville

Wei Chen

August 2014

Copyright © 2014 by Wei Chen
All rights reserved

To my beloved mother and father

C.X. Li and Q.J. Chen

To my endearing family and friends

X. C., H. W., K. L., P. J.
C. L.; Y. W.; H. L.; J. X.
L. W.; Y. L.
Y. H.; B. H.; M. Y.; H. Z.; X. G.; G. F.
Y. D.; M. P.; Y. X.; D. G.; M. N.; J. B.; C. H.

ACKNOWLEDGEMENTS

The rewarding experience at the University of Tennessee in the past years has transformed me with a combination of intellectual guidance, hardworking, perseverance, team support, friendship, celebration and reflection. I have gained much more than I initially anticipated through my journey of becoming a person who seeks truth in the science world with a touch of curiosity and skepticism. Through the course of my study at UTK, I am blessed to come across people from all walks of life, to whom I am thankful for your unrelenting encouragements and supports. I wish to extend my gratitude to each and every one of you. Without your support, I could not have achieved what I present in this dissertation.

I would like to express special thanks to my major professor, Dr. Guoxun Chen, for his academic guidance over the years. He provided precious research opportunities and taught many technical and academic skills that are indispensible in my development as a scientist.

I would like to specifically thank Dr. Jay Whelan, Dr. Ling Zhao, Dr. Michael Karlstad and Dr. Jason Collier for their critical comments and advice regarding my research work. Their encouragements have been invaluable for making my graduate research productive and fruitful.

My special thanks also go to my dear colleagues and lab mates over the years – Meredith Howell, Rui Li, Yang Li, Yi Zhao and Pan Hu. I very much enjoyed their company inside and outside the lab. And I am grateful that they were beside me when I needed assistance in my research.

I would also like to send a final special thank you message to the Department of Nutrition at the University of Tennessee, and the China Scholarship Council, for all the financial supports that bolstered my study and research.

ABSTRACT

Hormonal and nutritional stimuli coordinately regulate the glucose and lipid metabolism in the liver. Dysregulated hormonal balance and nutrient metabolism not only disrupt the energy homeostasis, but also predispose individuals to the development of obesity and its related metabolic diseases. Research presented in this dissertation investigated the effects of a nutritional factor, vitamin A (VA), and a potential component of insulin signaling cascade, atypical protein kinase C (aPKC), on the glucose and lipid metabolic genes transcription in primary hepatocytes from Zucker lean (ZL) and fatty (ZF) rats.

To examine VA effects, we put ZL and ZF rats with different VA statuses on various feeding conditions. After the isolation of their primary hepatocytes, we analyzed the expressions of hepatic model genes in response to the treatments of insulin and retinoic acid (RA). We report that the insulin- and RA-regulated glucokinase (*Gck*), sterol regulatory element-binding protein-1c (*Srebp-1c*) and cytosolic form of phosphoenolpyruvate carboxykinase (*Pck1*) expressions are impaired in hepatocytes of ZF rats fed chow or a VA sufficient (VAS) diet ad libitum. The impairment is partially corrected when ZF rats are fed a VA deficient (VAD) diet ad libitum or pair-fed a VAS diet to the intake of their VAD counterparts in non-fasting conditions. Interestingly, in the pair-fed ZL and ZF rats, transient overeating on the last day of pair-feeding regimen changes the expression levels of some VA catabolic genes, and impairs the insulin- and RA-regulated gene expression in hepatocytes.

To investigate the roles of aPKC, PKCζ(zeta) and PKCι/λ(iota/lambda), they were overexpressed in primary hepatocytes from ZL rats using recombinant adenoviruses. aPKC overexpression in primary hepatocytes significantly attenuated the insulin-regulated expressions of *Gck*, *Srebp-1c* and *Pck1*. Additionally, aPKC overexpression increased their basal transcript levels. The impairment is associated with reduced protein level of insulin receptor substrate 1, and the phosphorylation of protein kinase B in response to insulin treatment.

Taken together, the data demonstrate that feeding state, VA status, and aPKC expression regulate the hepatic glucose and lipid metabolism at the gene expression level, and provide interesting insights into the development of metabolic diseases.

TABLE OF CONTENTS

CHAPTER I. LITERATURE REVIEW ON INSULIN SIGNALING PATHWAY, VITAMIN A AND ITS ROLES IN THE REGULATION OF MACRONUTRIENT METABOLISM. 1

1. Metabolic diseases and metabolic syndromes 2
2. Insulin signaling, insulin resistance and atypical protein kinase C 3
3. VA, carotenoids and retinoids 7
4. Physical and chemical properties of VA 11
5. The absorption, transport and metabolism of VA 12
6. VA Status assessment and VA dietary recommendation 19
7. VA, retinoid signaling pathway and gene transcription 24
8. Major physiological functions of VA 32
9. VA and metabolism 38
10. Conclusion 47

CHAPTER II. VITAMIN A AND FEEDING STATUSES MODULATE THE INSULIN-REGULATED GENE EXPRESSION IN PRIMARY RAT HEPATOCYTES 48

Abstract 49
1. Introduction 50
2. Materials and methods 51
3. Results 53
4. Discussion 78

CHAPTER III. OVEREXPRESSION OF ATYPICAL PROTEIN KINASE Cζ (PKCζ) OR ι/λ (PKCι/λ) ATTENUATES INSULIN-REGULATED GENE EXPRESSION IN PRIMARY RAT HEPATOCYTES 82

Abstract 83
1. Introduction 84
2. Materials and methods 86
3. Results 91
4. Discussion 109

CHAPTER IV. UNPUBLISHED DATA, CONCLUSION AND FUTURE DIRECTIONS 113
1. Unpublished data 114
2. Conclusion and future directions 130
LIST OF REFERENCES 134
APPENDIX 169
VITA 171

LIST OF TABLES

Table 1-1: List of common carotenoids in diets 10
Table 1-2: Calculation of EAR of vitamin A for adult 23
Table 1-3: List of physiological relevant RDHs 27
Table 1-4: List of physiological relevant RALDHs.....28
Table 1-5: List of real time PCR primers used in the dissertation.....170
Table 1-6: List of ChIP PCR primers used in the dissertation.....170

LIST OF FIGURES

Figure 1-1: Structures of representative molecules with VA activity 8
Figure 1-2: Schematic graph of the digestion, transport and absorption of molecules with vitamin A activity 13
Figure 1-3: Schematic graph of the storage and metabolism of VA.....17
Figure 1-4: Schematic graph of the retinoid signaling pathway 25
Figure 1-5: Schematic graph of NR structures and RARE in the promoter region 30
Figure 1-6: Schematic graph of the vision cycle 33
Figure 2-1: Impaired insulin-regulated gene expression in primary hepatocytes isolated from ZF, but not ZL, rats fed chow ad libitum 54
Figure 2-2: The impaired insulin-regulated gene expression in primary hepatocytes from ZF rats was partially recovered in rats fed a VAD diet for 8 weeks.....58
Figure 2-3: VAS-PF-AD ZL and ZF overate on the last day when sufficient VAS diet was provided 63
Figure 2-4: The food intake, body mass and cumulative feed efficiency over 56 days of dietary manipulation 66
Figure 2-5: Insulin-induced *Gck* expression was attenuated in hepatocytes from VAS-PF-AD, but not VAS-PF-4M rats 68
Figure 2-6: Transient overfeeding of VAS diet impaired insulin-suppressed *Pck1* expression in hepatocytes of VAS-PF-AD ZL, but not ZF, rats.....70
Figure 2-7: Transient overfeeding of VAS diet impaired insulin-induced *Srebp-1c* expression in hepatocytes of VAS-PF-AD ZL and ZF rats. 73
Figure 2-8: Differential expression levels of indicated transcripts for vitamin A metabolism in the primary hepatocytes of ZL and ZF rats. 75
Figure 3-1: ZF rats on chow ad lib had elevated expression levels of PKCζ mRNA and protein in the liver 93
Figure 3-2: Acute insulin treatment did not alter protein levels of total and phospho-aPKCs in primary rat hepatocytes.....95

Figure 3-3: Overexpression of PKCζ and PKCι/λ attenuated the insulin signaling cascade in ZL primary rat hepatocytes. 99
Figure 3-4: Overexpression of PKCζ attenuated the insulin signaling cascade in ZL primary rat hepatocytes. 100
Figure 3-5: Overexpression of PKCι/λ attenuated the insulin signaling cascade in ZL primary rat hepatocytes. 103
Figure 3-6: Overexpression of PKCζ and PKCι/λ impaired the insulin-regulated gene expression in ZL primary rat hepatocytes. 107
Figure 4-1: The effects of all-*trans*-RA on the GSIS of INS-1 cells. 116
Figure 4-2: The effects of all-*trans*-retinol, retinal and RA on the GSIS of INS-1 6D and 8E cell lines. 119
Figure 4-3: The optimization of sonication condition. 124
Figure 4-4: Comparison of whole cell and cell nuclei in the ChIP assay 124
Figure 4-5: Test of the amount of chromatin needed for each IP. 126
Figure 4-6: Test of the preclearing condition. 126
Figure 4-7: Test of different beads and the preblocking condition. 128
Figure 4-8: Test of beads amount and antibody amount. 129
Figure 4-9: Glycine interferes with the specific antibody-antigen binding. 129
Figure 4-10: Representative ChIP assay results and the densitometry analysis of three independent experiments. 131

LIST OF ABBREVIATIONS

ACC	acetyl-CoA carboxylase
Apo B_{48}	apolipoprotein B_{48}
Apo E	apolipoprotein E
ARAT	acyl-CoA:retinol acyltransferase
aPKC	atypical protein kinase C
BB-REH	brush-border retinyl ester hydrolase
BMI	body mass index
CBL	Casitas B-lineage lymphoma protein
CDK	cyclin-dependent kinase
C/EBPα	CCAAT-enhancer-binding protein α
CETP	cholesteryl ester transfer protein
CRABP	cellular-retinoic acid binding protein
CRBP	cellular-retinol binding protein
CYP	cytochrome P450 ()
DBD	DNA-binding domain
DOCK1/2	dedicator of cytokinesis protein 1/2
DMEM	Dulbecco's Modification of Eagle Medium
EAR	estimated average requirement
ER	estrogen receptor
FA	fatty acid
FAS	fatty acid synthase
FFA	free fatty acid
GAB1/2	Grb2-associated binder 1/2
GCK, *Gck*	glucokinase
GLUT4	glucose transporter type 4
GS	glycogen synthase
GSIS	glucose-stimulated insulin secretion

GSK3	glycogen synthase kinase 3
HDL	high density lipoprotein
HPLC	high performance liquid chromatography
HSPG	heparan sulfate proteoglycans
IRS	insulin receptor substrate
IU	international unit
IRBP	interphotoreceptor retinol binding protein
JAK	Janus kinase
LBD	ligand-binding domain
LDL	low density lipoprotein
LDLr	LDL receptor
LPL	lipoprotein lipase
LRAT	lecithin:retinol acyltransferase
LRP	LDL receptor related protein
LSR	lipolysis-stimulated receptor
mTORC	mammalian target of rapamycin complex
NF-κB	nuclear factor-kappaB
NHANES	National Health and Nutrition Examination Survey
NR	nuclear receptor
PDK1	phosphoinositide dependent protein kinase-1
PEPCK, *Pck1*	cytosolic form of phosphoenolpyruvate carboxykinase
PI3K	phosphatidylinositol 3-kinase
PIP2	phosphatidylinositol-4,5-bisphosphate
PIP3	phosphatidylinositol-3,4,5-triphosphate
PKB/AKT	protein kinase B
PKCζ	protein kinase C zeta
PKCι/λ	protein kinase C iota/lambda
PPAR	peroxisome proliferator-activated receptor
RA	retinoic acid
RAE	retinol activity equivalent
RALDH	retinal dehydrogenase

RAR	retinoid acid receptor
RARE	retinoic acid response element
RBP4	retinol binding protein 4
RBPR2	RBP4 receptor 2
RE	retinyl ester
REH	retinyl ester hydrolase
11-RDH	11-*cis*- retinol dehydrogenase
RDH	retinol dehydrogenase
RDR	relative dose response
RPE	retinal pigment epithelium
RXR	retinoid X receptors
SHC	Src homology 2 domain-containing transforming protein
SREBP-1c, *Srebp-1c*	sterol regulatory element-binding protein-1c
STAT	signal transducer and activator of transcription
STRA6	stimulated by retinoic acid 6
TCA cycle	tricarboxylic acid cycle
TG	triglyceride
TLR	Toll-like receptor
TTR	transthyretin
UCP	uncoupling protein
VA	vitamin A
VADD	vitamin A deficiency disorders
VAD	VA deficient
VAS	VA sufficient
VAD-AD	VAD ad libitum
VAS-PF-AD	VAS pair-feeding last day ad libitum
VAS-PF-4M	VAS pair-feeding last day 4 meals
ZL	Zucker lean
ZF	Zucker fatty

CHAPTER I. LITERATURE REVIEW ON INSULIN SIGNALING PATHWAY, VITAMIN A AND ITS ROLES IN THE REGULATION OF MACRONUTRIENT METABOLISM.

1. Metabolic diseases and metabolic syndromes

The prevalence of overweight and obesity has become a public health concern around the world [1]. According to the World Health Organization's 2010 report, 35% of adults aged 20 years and older worldwide in 2008 were clinically overweight (body mass index, BMI $\geq$ 25 kg/m^2). More than half a billion adults in the same category were obese (BMI $\geq$ 30 kg/m^2) [2]. Moreover, 2.8 million deaths are linked to raised BMI each year [2]. Overweight and obesity are associated with increased risks of developing an assortment of metabolic diseases, which mainly include hypertension, type 2 diabetes mellitus, non-alcoholic fatty liver disease, coronary heart diseases and stroke [1,3]. The implications of all those health conditions have brought gloomy biomedical and socioeconomic consequences to the well-being of the global population [3].

In clinical settings, metabolic risk factors for the development of coronary heart disease, type 2 diabetes mellitus and hypertension are collectively termed "metabolic syndromes" [4]. This concept was established as "Syndrome X" by Reaven in 1988, which mainly encompassed impaired glucose tolerance, hyperinsulinemia, and dyslipidemia [5]. Over the past 25 years, the definition of metabolic syndrome has been actively revised to reflect the latest epidemiologic and clinical data on the prevalence of major metabolic diseases [6]. In 2005, the International Diabetes Federation introduced a consensus diagnostic definition for metabolic syndromes. This definition stipulates obesity (BMI $\geq$ 30 kg/m^2) as a prerequisite factor, and the coexistence of two of the following criteria: (1) triglyceride (TG) level $\geq$ 150 mg/dL; (2) high density lipoprotein (HDL) level $\leq$ 40 mg/dL in men or $\leq$ 50 mg/dL in women; (3) systolic blood pressure $\geq$ 130 mm Hg or diastolic blood pressure $\geq$ 85 mm Hg; (4) fasting blood glucose $\geq$ 100 mg/dL; (5) previous diagnosis or treatment of the abovementioned conditions [6].

Epidemiological studies demonstrate that metabolic syndromes are important prognostic indicators for metabolic diseases [6]. An analysis of the National Health and Nutrition Examination Survey (NHANES) II data shows that metabolic syndromes strongly predict the mortality from coronary heart diseases in US adults [7]. Similar result is confirmed in the Scandinavian Simvastatin Survival Study and the Air Force/Texas Coronary Atherosclerosis Prevention Study [8]. Additionally, observations from the Framingham Offspring Study show that metabolic syndromes are associated with

significantly increased risks of developing type 2 diabetes [9]. Even though the relationships among the risk factors that define metabolic syndromes have not been fully unraveled, it appears that insulin resistance is a common link of the metabolic syndromes, and plays a central role in the development of metabolic diseases [6].

2. Insulin signaling, insulin resistance and atypical protein kinase C

2.1 Insulin signaling: IRS/PI3K/AKT and IRS/PI3K/aPKC pathways

Insulin, which is secreted from pancreatic β-cells in response to physiological stimuli, is an important peptide hormone in anabolism [10]. Upon secretion, it binds to the insulin receptor on cell membranes and exerts its actions through a signal transduction cascade mainly composed of kinases and phosphatases. The binding causes conformation changes of the insulin receptor and transphosphorylation of the β-subunit tyrosine kinase [11,12], which initiates the signal transduction cascade [13].

The insulin signal is transduced by multiple components in a complex network comprised of multiple kinases and phosphatases [14,15]. Transphosphorylated insulin receptor β subunit with open catalytic site is able to interact and phosphorylate an assortment of substrate proteins on tyrosine residues [10]. These substrate proteins include insulin receptor substrate 1~6 (IRS1~6), Src homology 2 domain-containing transforming protein (SHC), Casitas B-lineage lymphoma protein (CBL), Grb2-associated binder 1/2 (GAB1/2) and dedicator of cytokinesis protein 1/2 (DOCK1/2), which mediate distinct physiological functions *in vivo* [10,15]. Transgenic animal studies show that the majority of insulin responses are mediated by IRS1 and IRS2 [10].

Tyrosine phosphorylation of IRS1/2 leads to the association and activation of the phosphatidylinositol 3-kinase (PI3K) [10,15]. PI3K catalyzes the conversion of phosphatidylinositol-4,5-bisphosphate **(**PIP2) into phosphatidylinositol-3,4,5-triphosphate **(**PIP3) [10,15]. The latter is a lipid messenger that anchors the downstream effector proteins, e.g. phosphoinositide dependent protein kinase-1 (PDK1), protein kinase B (PKB, also known as AKT) and atypical protein kinase C (aPKC), to the cell membrane [10,15].

The interaction of PDK1 and AKT leads to the phosphorylation and activation of AKT, which is a critical node in the signaling cascade to regulate multiple downstream

physiological functions [10,15]. AKT is a member of the serine/threonine kinase family, whose activation is postulated to be a multistep process [16]: (1) the insulin-independent phosphorylation of Thr450 confers access to activation and translocation; (2) the PIP3 dependent translocation ensures the association of AKT with other kinases; (3) the insulin-dependent phosphorylation of Thr308 and Ser473 confers maximal activity. Recent data suggest that the phosphorylation of AKT at Thr308 is mediated by PDK1, and the phosphorylation of AKT at Ser473 is dependent upon mammalian target of rapamycin complex 2 (mTORC2) in *Drosophila* and human cells [17-19].

The activation of AKT regulates many downstream targets to control glucose and lipid metabolism, protein synthesis, cell survival and proliferation, apoptosis and neurophysiological functions [20]. For example in the regulation of glucose uptake into muscle cells and adipocytes, AKT promotes the translocation of glucose transporter type 4 (GLUT4) containing vesicles to the cell membrane [21]. In the hepatocytes and muscle cells, AKT activation leads to the phosphorylation and inactivation of glycogen synthase kinase 3β (GSK3β), which in turn increases glycogen synthase (GS) activity and glycogen synthesis [22]. In response to insulin and nutrient (e.g. amino acids) stimuli, the activation of AKT participates in the upregulation of protein synthesis through mTORC1 [23]. Most importantly, the activation of AKT within a cell leads to the differential regulation of metabolic genes expression, e.g. the induction of glucokinase (GCK, gene *Gck*) to promote glycolysis, the induction of sterol-regulatory element binding protein 1c (SREBP-1c, gene *Srebp-1c*) to promote lipogenesis and the suppression of phosphoenolpyruvate carboxykinase to suppress gluconeogenesis (PEPCK, gene *Pck1*) [24]. Given the important functions of AKT *in vivo*, the deregulation of AKT and its downstream pathways is associated with cancer and metabolic diseases [20].

The transduction of insulin signaling system can also be mediated by aPKC. The binding of aPKC to PIP3 prompts the conformational change in the kinase structure, which provides access to the autophosphorylation and activation of the kinase [25]. aPKC belongs to the protein kinase C family, and has two members: PKCζ and PKCι/λ [25]. It is mainly localized to the cell membrane [26], and mediates a variety of physiological events, including cell polarity establishment, cell motility, immune response and signaling transduction [25]. So far, the majority of the aPKC targets remain uncovered.

However, recent studies with transgenic mice demonstrate the role of IRS/PI3K/aPKC pathway in the regulation of metabolism. In both muscle cells and adipocytes, PI3K dependent activation of aPKC is required for the GLUT4 translocation and glucose uptake [27-29]. In hepatocytes, aPKC activation promotes the activity and expression of SREBP-1c and the attendant expression of fatty acid synthase (FAS) and acetyl-CoA carboxylase (ACC) [30-34]. aPKC activation also promotes transcription of pro-inflammatory cytokines by activating nuclear factor-kappaB (NF-κB) [34]. Additionally, the activation of PKCι was elevated at the basal level and after insulin treatment in the hepatocytes isolated from type 2 diabetic patients [35]. Treatment of these hepatocytes with PKCι inhibitors lowered the levels of lipogenic, proinflammatory and gluconeogenic enzymes [35,36]. These data collectively suggest that aPKCs are important players in the pathogenesis of obesity and type 2 diabetes.

2.2 Insulin resistance

The activation of the insulin signaling pathway results in changes in the activities and (or) the expression levels of enzymes in nutrient metabolism. These subsequently alter the metabolic state of the tissues and organs in the body. For example, insulin promotes glycolysis, glycogenesis, and lipogenesis, and at the same time, suppresses gluconeogenesis in the liver [15]. However, in individuals with metabolic abnormalities such as overweight and obesity, a certain dose of insulin only produces subnormal physiological responses. This observation is regarded as insulin resistance, which occurs concurrently with profound alterations in the glucose and lipid metabolism [10,37,38]. Even though the molecular mechanisms leading to insulin resistance has not been fully understood, it is postulated that systemic inflammation, dysregulated lipid metabolism and gastrointestinal dysbiosis, triggered by overnutrition, interplay with each other and result in the impairment of insulin action [38].

Inflammation-mediated insulin resistance is characterized by the accumulation and activation of macrophages and the other immune cells in the adipose tissue [39], and the local activation of Kupffer cells in the liver [38,40]. Certain nutrients and metabolites (e.g. free fatty acid, FFA) activate the cytokine-mediated pathways or the Toll-like receptor (TLR) pathways in these immune cells, which in turn promotes the synthesis and secretion of pro-inflammatory cytokines (e.g. tumor necrosis factor α) [38,40]. The

elevation of the pro-inflammatory cytokines *in vivo* causes systemic insulin resistance by attenuating the insulin signaling pathway in a group of organs and tissues [38,40].

The cause and effect relationship between dysregulated lipid metabolism and hyperinsulinemia is still unknown. However, it is generally accepted that the combined effects of the two factors lead to increased circulating FFAs, and lipid accumulation in the muscle and liver [38,41]. These excessive lipid molecules are considered "lipotoxic", which purportedly impact the insulin signaling cascade in the muscle cells and hepatocytes, and exacerbate hyperglycemia and hyperinsulinemia [38,41].

The gut microbiota is the collection of all microbes/microbial genomes in the gastrointestinal tract. It has been shown to influence the metabolism of the host in a profound way [38]. Despite the fact that the cause and effect relationship between dysregulated gut microbiota and metabolic disease is unknown, it is postulated that the gut microbes impact the insulin sensitivity of the host by: (1) influencing the intestinal immune system to produce pro-inflammatory factors; (2) producing metabolites (e.g. short chain fatty acid or bile acid derivatives) that cause systemic inflammation [38].

2.3 Overnutrition and metabolic diseases

Both genetic and nutritional/environmental factors are instrumental to the development of obesity and its related metabolic diseases [24,42]. Mutations in the appetite-regulating hormones (e.g. leptin and proopiomelanocortin) and their corresponding receptors (e.g. leptin receptor and melanocortin 4 receptor, respectively) result in early onset of obesity and obesity-associated metabolic dysregulations in both humans and experimental rodents [43]. Given the increasing numbers of the monogenic contributors, the majority of the obesity cases in human population are believed to be polygenic [43]. On the other hand, overnutrition related to unhealthy eating habits probably drives the rising global prevalence of overweight and obesity [44,45]. In spite of the self-evident link between overnutrition and obesity, the underlying mechanisms that the excessive intake of nutrients causes obesity and its related metabolic diseases have not been fully understood.

The utilization of dietary macronutrients requires coordinative regulation of the metabolic pathways in different organs and tissues of the body. In a fed state, excessive dietary macronutrients are conserved in the forms of glycogen and TG for future energy

needs. During fasting, glycogen and TG are respectively broken down into glucose and fatty acids (FAs) to meet the energy needs of different organs and tissues in the body. These processes are coordinately regulated by both hormonal and nutritional stimuli in response to feeding and energy states so that the body reaches energy homeostasis [24,42]. Dysregulated hormonal balance and nutrient metabolism not only disrupt the energy homeostasis, but also predispose individuals to the development of obesity and its related metabolic diseases [24].

Overnutrition provides not only excessive energy from macronutrients, but also superfluous amount of vitamins and essential factors, which have regulatory roles. How micronutrients such as vitamin A (VA, retinol) regulate the homeostasis of macronutrients is still an ongoing research topic. As an essential and lipophilic micronutrient, VA plays a key role in the general health of an individual [24]. The following sections of Chapter I overviews the nomenclature, properties, metabolism and major functions of VA, and also summarizes recent research progresses regarding the roles of VA in carbohydrate, lipid and protein metabolism.

3. VA, carotenoids and retinoids

3.1 Provitamin A and preformed VA

VA is an essential lipophilic micronutrient, which is involved in a myriad of important physiological functions, including vision formation, immune response, cell differentiation and proliferation, embryonic development and metabolism [46]. Despite its indispensable role in physiology, modern research leading to the discovery of VA started in animal husbandry in the early 20^{th} century. Pioneered by McCollum, Davis, Osborne and Mendel [47], the respective findings of provitamin A and preformed VA paved the way for the understanding of VA functions in human beings [48].

Provitamin A molecules (Figure 1-1, A) are mainly found in plant sources. The green leaves of the majority of terrestrial plants contain carotenes — a group of important photosynthetic pigment. In other yellow plant tissues and organs, cryptoxanthins can be found besides carotenes. Both cryptoxanthins and carotenes are major sources of provitamin A in the diets for herbivores and omnivores [49].

A. Provitamin A

α-carotene

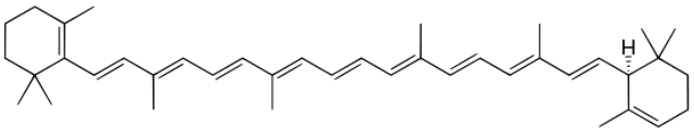

β-carotene

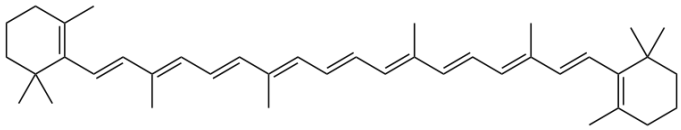

γ-carotene

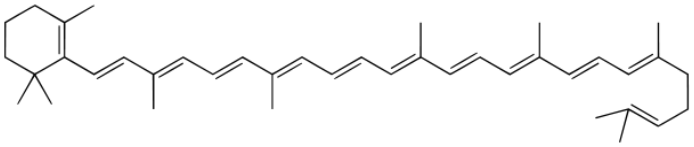

cryptoxanthin

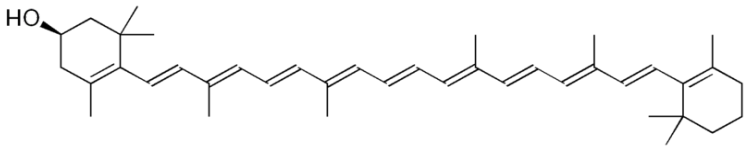

B. Preformed vitamin A

retinol

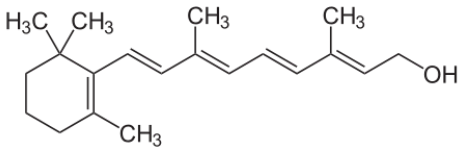

retinal

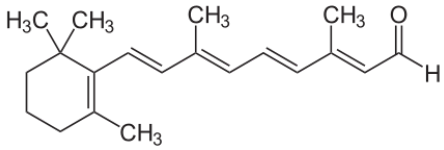

retinoic acid

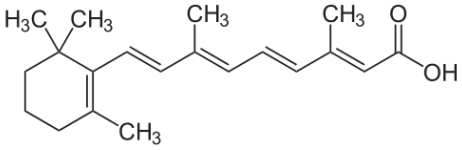

Figure 1-1: Structures of representative molecules with VA activity.

The isolation and characterization of carotene reveal three naturally occurring isomers, which are named α-, β-, and γ-carotene, respectively. β-carotene is the most abundant among the three isomers. It is also the most effective provitamin A in restoring growth stunt of VA deficient (VAD) animals [49]. In comparison, α- and γ-carotene exhibit about 25 to 50% of the activity of β-carotene [49]. Cryptoxanthins manifest 54 to 59% of the activity of β-carotene [49].

Naturally occurring preformed VA (Figure 1-1, B) is derived from provitamin A. Herbivorous and omnivorous animals convert provitamin A molecules into retinol *in vivo,* and then store it as retinyl esters in different organs and tissues depending on the species [50]. Retinol and retinyl esters are then introduced into food chain and transferred to carnivorous and omnivorous animals at the higher tiers of the food chain [49].

Retinol can be enzymatically metabolized into different VA derivatives *in vivo* for diverse physiological functions. Major derivatives include the aldehyde form of retinal, the acid form of retinoic acid (RA) and retinyl ester (RE). For this reason, VA now collectively refers to any compounds that exhibit the bioactivity of retinol regardless of their origin [51].

3.2 Carotenoids and retinoids

The isolation and purification of β-carotene result in the discovery of a group of pigments with similar structural and chemical properties, which are together termed "carotenoids" [49] (Table 1-1). Xanthophyll from green leaves and lycopene from tomatoes are two representative examples. In spite of the strong structural similarity, the majority of carotenoids were physiologically inactive in alleviating VAD symptoms in animals [49]. These carotenoids are not deemed provitamin A. Later research suggests that they function as potent anti-oxidants [52].

Chemicals with similar structural properties to retinol, retinal and RA have also been isolated from a variety of diets or synthesized from scratch for pharmaceutical purposes in the past decades. For example, 3-dehydro-retinol (also known as vitamin A_2) was found in substantial quantities in some freshwater fishes [53]. This chemical is an important dietary source of VA for some fish-eating animals, and it exhibits about 30% activity of retinol [53]. Conjugated compound such as retinoyl β-glucuronide can be found *in vivo* [51]. Additionally, RA analogues such as acitretin were synthesized to treat

Table 1-1: List of common carotenoids in diets*.

Carotenoids	Formula	Provitamin A Activity	Dietary Source
α-carotene	$C_{40}H_{56}$	~25%	Green vegetables, red palm oil
β-carotene	$C_{40}H_{56}$	100%	Green vegetables, carrots
γ-carotene	$C_{40}H_{56}$	~25%	Green vegetables
cryptoxanthin	$C_{40}H_{55}OH$	54~59%	Yellow maize
xanthophyll	$C_{40}H_{54}(OH)_2$	No activity	Green vegetables, egg yolk
lycopene	$C_{40}H_{56}$	No activity	Tomato
zeaxanthin	$C_{40}H_{54}(OH)_2$	No activity	Yellow maize
astaxanthin	$C_{40}H_{52}O_4$	No activity	Eggs, lobster

* Adapted from Moore (1957), pp.70-71, 160-161.

a series of diseases including acne [54], psoriasis [55] and cancer [56]. In order to categorize this group of compounds, the term "retinoid" is coined. However, it is important to point out that many retinoids lack the VA bioactivity [51].

4. Physical and chemical properties of VA

4.1 Structural properties of VA

Molecules with VA activity and their derivatives share common structural components, including a β-ionone ring, an isoprenoid side chain, and a polar moiety attached to the end (Figure 1-1, B).

Due to the presence of five conjugated double bonds in the isoprenoid side chain, VA molecules can exist as intra-convertible *cis*- or *trans*- isomers. The most elucidated example is the photoisomerization of 11-*cis*-retinal into all-*trans*-retinal in the rod and cone cells. The photon-driven isomerization process provides the basis for the vision cycle in both invertebrate and vertebrate animals [57]. Additionally, in some fish species up to 30% of retinol exists in the *cis*- form [49]. Furthermore, when the pure *cis*- form of retinol is used to treat VAD rats, about 89% of the VA reserve is later found in the *trans*- form in the liver. Similar result is also observed if the *trans*- form of retinol is administered as the only source [58]. These observations suggest the existence of a fine-tuned mechanism in balancing the composition of VA isomers *in vivo*. Given the difference in the spatial arrangement of chemical groups, the *cis*- and *trans*- VA isomers exhibit different biological activity. Growth tests in rats show that *cis*- retinol and RE isomers have about 25-75% of the activity compared with their *trans*- isomer counterparts [59].

The polar end of the VA molecule is labile to chemical modifications, which determine the physiological functions of the compound [46,60]. In the vision cycle, all-*trans*-retinol needs to go through esterification, isomerization and oxidation to form the 11-*cis*-retinal, which binds to opsin with high affinity via a Schiff base [57,60]. This demonstrates that the oxidation state and the chemical modification of the VA greatly affect its function *in vivo*. For the storage of retinol, the hydroxyl group of retinol is esterified with a long chain FA, so that the resulting REs can be accumulated in the stellate cells in the liver [51,60].

4.2 Physical-chemical properties of VA

The β-ionone ring and the isoprenoid side chain grant the VA molecules with high hydrophobicity, meaning that they are fat-soluble molecules. However, the presence of the polar moiety facilitates VA molecules and their derivatives to show detergent-like characteristics.

In aqueous environment, amphipathic molecules will associate with each other to form micelles. This phenomenon is observed in most VA molecules and their derivatives [51]. Especially, RA has a strong polar carboxyl group, which determines its relatively higher solubility in water compared to its counterparts. Free RA forms micelles at the micromolar concentration level [61]. Retinol and its derivatives usually bind to proteins in *vivo*. This is to prevent forming micelles, which are disruptive of the cell membrane and cell function [62].

4.3 Chemical properties of VA

The abundance of double bonds in the VA molecule structure determines its susceptibility to oxidation and photodegradation [49]. In the open air, VA is quickly oxidized into retrovitamin A, anhydrovitamin A and isoanhydravitamin A [63]. In the organic solvents, the oxidation rate of VA is slower but steady. Comparably, VA will remain stable for a longer time in natural fats due to the presence of antioxidants (e.g. tocopherols) [49].

5. The absorption, transport and metabolism of VA

5.1 General information about the digestion and absorption of VA molecules

Dietary VA molecules are released from the digested food matrix in the gastrointestinal tract (Figure 1-2). Due to their lipophilic characteristic, VA molecules are incorporated into lipid micelles in the intestinal lumen prior to the absorption. The formation of lipid micelles is an important step, in that bile and dietary fat have been shown to facilitate the optimal absorption of VA molecules [49]. Additionally, lecithin and vitamin E aid the absorption of VA molecules [49]. The former is a fantastic emulsifier which improves the emulsification of fat droplets, and the latter protects VA molecules from oxidation in the small intestine [64].

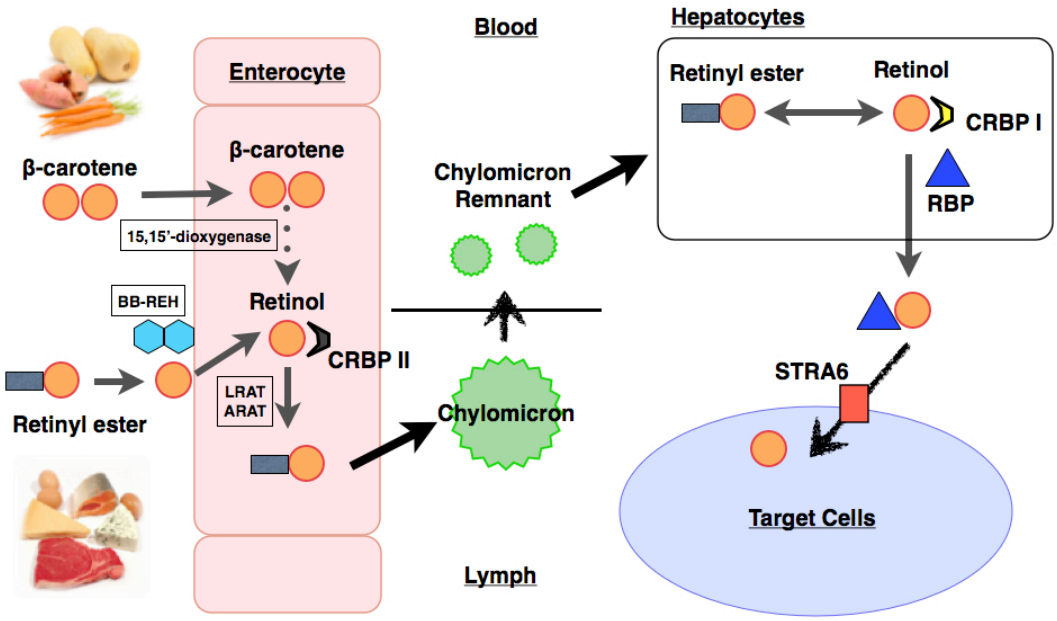

Figure 1-2: Schematic graph of the digestion, transport and absorption of molecules with vitamin A activity. Please see sections 5.1 through 5.4 for description. BB-REH, brush-border retinyl ester hydrolase; LRAT, lecithin:retinol acyltransferase; ARAT, acyl-CoA:retinol acyltransferase; CRBP, cellular-retinol binding protein; RBP, retinol binding protein; STRA6, stimulated by retinoic acid 6.

Under similar conditions, the absorption of preformed VA molecules is more efficient than that of provitamin A molecules. Experiments in rats show that more than 50% of provitamin A molecules could be passed into feces and subsequently lost [65]. Therefore, to obtain equal efficacy in treating VAD symptoms, it is suggested that twice the amount of provitamin A molecules is needed compared to that of retinol [49].

5.2 The uptake of VA molecules into enterocytes

Once in the lipid micelles (Figure 1-2), dietary REs are hydrolyzed into retinol and FAs by the brush-border retinyl ester hydrolase (BB-REH) in the intestinal lumen [66,67]. This enzyme is activated by bile salts and plays a central physiological role in converting RE into retinol *in vivo* [66]. Then retinol is taken up into the enterocytes (intestinal mucosal cells) by a transporter located at the brush border membrane [68]. This membrane-bound retinol transporter is specific to the all-*trans* isomer, and its function can be inhibited by the cysteine modification agent N-ethylmaleimide [68]. These results suggest that retinol is absorbed via facilitated diffusion. In comparison, carotenoids enter enterocytes via passive diffusion, which does not require transporter or energy [69,70]

Several studies also look at the absorption of supplemented retinol, retinal and RA drugs in experimental rodents. The results show that the majority of supplemented retinol and retinal are taken up by the enterocytes, and subsequently converted into RE [71]. In the contrary, 92~95% of supplemented RA is secreted into the bile [71]. Depending on the isomerization of the molecule, variable small amount of RA can be absorbed, and later, released into the portal vein as free RA [71,72].

5.3 The fate of retinol and β-carotene within enterocytes

The intracellular metabolism of carotenoids in the enterocytes is a key step to generate retinol in animals. Because of its relative abundance in food, β-carotene is the most studied carotenoid in terms of absorption and metabolism. In human the majority of β-carotene in the enterocytes will be symmetrically cleaved by 15,15'-dioxygenase to generate retinal [73]. Residual intact β-carotene can be delivered to the liver, where the same enzyme in the hepatocytes catalyzes the same cleavage reaction [70]. Even though 15,15'-dioxygenase was discovered about 50 years ago, the cloning of the corresponding gene was not successful until recently [74]. Functional analysis of the gene confirmed its primary expression in duodenal enterocytes and hepatocytes, consolidating its

predominant role in metabolizing β-carotene [75]. Aside from the symmetrical cleavage, β-carotene can also be asymmetrically cleaved at the 9',10' double bond by a specific enzyme in the enterocyte [76,77].

The resulting retinal from the cleavage of the β-carotene is readily reduced into retinol by a microsomal enzyme, retinal reductase [78]. Due to their limited solubility in the cytosol, both retinol and retinal need to bind to cellular-retinol binding protein II (CRBP II) to participate in this enzymatic reaction [79]. The generated retinol converges into the retinol repertoire that comes from the hydrolysis of dietary REs [78].

From this point on, the majority of retinol needs to be reesterified with FAs (usually palmitate). This key reaction converts retinol back into RE so that it can be incorporated into chylomicron for the transportation to the liver [78]. It is noteworthy that free retinol and RA can be directly secreted into portal circulation for transportation [78].

Two enzymes have been identified to possess the capability of reesterfying retinol *in vitro*: lecithin:retinol acyltransferase [80] (LRAT) and acyl-CoA:retinol acyltransferase [81] (ARAT). Both enzymes are associated with the microsomal fraction of the enterocytes, but only LRAT manifests substrate preference to CRBP II-bound retinol [60]. This suggests that LRAT plays a more important role in the reesterification of retinol in enterocytes [78].

5.4 The secretion, transportation and clearance of the RE containing chylomicrons

Chylomicrons formed in the enterocytes contain TGs, phospholipids, apolipoprotein B_{48} (Apo B_{48}), RE and other dietary lipophilic factors. Chylomicrons are secreted into lymph, which enter circulation through thoracic duct at the subclavian vein. The first experimental evidence for this phenomenon comes from ruminants and rats, in which the majority of postprandial VA molecules are observed in lymph instead of portal blood [82]. Additionally, pharmaceutical inhibition of chylomicron secretion by Pluronic L81 decreases RE secretion in Caco-2 cells [83]. In the same cell line, experiments show that only newly synthesized RE will be incorporated into the nascent chylomicrons. This demonstrates that RE synthesis and incorporation into the chylomicron are highly concerted and regulated [84].

In the circulation, chylomicrons interact with lipoprotein lipase (LPL) at the inner lining endothelial cells of the vascular system, which gradually hydrolyzes the TGs on

the chylomicrons. This process decreases the size of the chylomicrons and converts them into chylomicron remnants. Chylomicron remnants at the same time will take up apolipoprotein E (Apo E) from the plasma, which is an important factor assisting the hepatic clearance of the RE containing remnants [85]. In human and other animal species, plasma cholesteryl ester transfer protein (CETP) is able to transfer small amount of RE from chylomicron to low density lipoprotein (LDL) and HDL [86,87]. These transferred RE molecules will be cleared by the liver with its associated lipoproteins.

After entering the space of Disse, the RE containing chylomicron remnants are cleared by the hepatocytes via several parallel mechanisms [85]. The initial interaction of the RE containing chylomicron remnants with the hepatocytes is mediated by the heparan sulfate proteoglycans (HSPGs) located on the surface of the hepatocytes [88]. Then other cell surface receptors including LDL receptor (LDLr), LDL receptor related protein (LRP) and lipolysis-stimulated receptor (LSR) will bind to the Apo E on the chylomicron remnants, which in turn facilitate the endocytosis in the hepatocytes [85].

After the hepatocytes endocytose chylomicron remnants, the REs are hydrolyzed into retinol by the carboxylesterase ES-2 on the plasma membrane [89-91]. In the nascent endosomes, this enzyme is shown to colocalize with REs, and its activation did not require bile salts [92]. The formed retinol will then bind to cellular retinol binding protein I (CRBP I) for the subsequent metabolism in the hepatocytes [93].

5.5 The storage and metabolism of VA in the liver

Even though VA is fat soluble, white adipose tissue itself is not determinant player in the accumulation of VA [49]. In mammals, the liver is the primary storage site for REs, whereas minor storage can be found in the adipose tissue, lung and kidney [94]. In chow fed rats, 95~99% total hepatic retinol exists in the form of retinyl palmitate, and the total hepatic retinol concentration is estimated to be 2.6 nmol · mg protein^{-1} [93,95]. Histological studies show that hepatic RE reserve is in a dynamic equilibrium between stellate cells and hepatocytes (Figure 1-3). Depending on the VA status of the animal, 5~30% RE can be found in the hepatocytes, while the rest is stored in the stellate cells [93,95].

The formation of CRBP I bound retinol in the hepatocyte greatly facilitates the storage of retinol in the liver [90]. When dietary VA intake exceeds the physiological

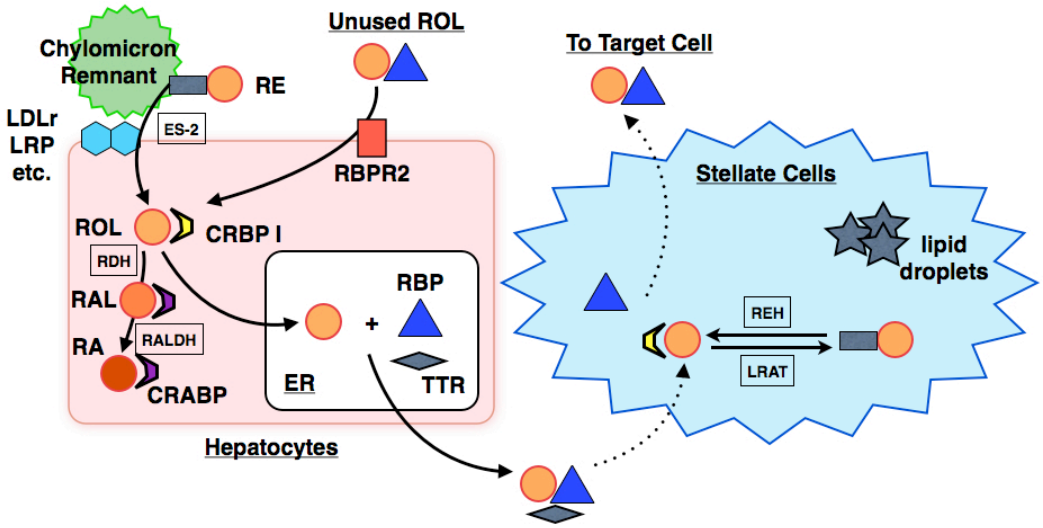

Figure 1-3: Schematic graph of the storage and metabolism of VA. Please see sections 5.5 through 5.7 for description. ROL, retinol; RAL, retinal; RA, retinoic acid; RE, retinyl ester; LDLr, low density lipoprotein receptor; LRP, LDL receptor related protein; ES-2, carboxylesterase; CRBP, cellular-retinol binding protein; CRABP, cellular retinoic acid binding protein; RDH, retinol dehydrogenase; RALDH, retinal dehydrogenase; ER, endoplasmic reticulum; RBP, retinol binding protein; TTR, transthyretin; RBPR2, retinol binding protein receptor 2; REH, retinyl ester hydrolase; LRAT, lecithin:retinol acyltransferase.

need, the holo-CRBP I in the cytoplasm is continuously delivered to the endoplasmic reticulum of the hepatocyte, where retinol binding protein 4 (RBP4) is actively synthesized [96]. Retinol will be transferred from CRBP I to RBP4 so that it can be secreted and transferred to the adjacent stellate cells. Within the stellate cells, LRAT esterifies retinol (also bound to CRBP I) back into RE, which is finally stored in the large cytoplasmic lipid droplets [94,97]. When the extrahepatic tissue is in need of VA, the RE reserve in the stellate cells can be mobilized by lysosomal REH, which produces free retinol [91,98]. The retinol will be bound to RBP4 and secreted into the circulation.

Compared with stellate cells, hepatocytes also maintain active metabolism of retinol. On one hand, small amount of retinol can be esterified by hepatic LRAT and stored in local lipid droplets [99]. On the other hand, hepatic retinol dehydrogenases (RDHs) and retinal dehydrogenases (RALDHs) can metabolize retinol into retinal and RA, which satisfies the local usage [94]. Depending on the physiological need in the body, it is postulated that CRBP I regulates the homeostasis between retinol esterification and metabolism [100]. Experiments in rodents show steady total CRBP I level in the liver regardless of the VA status in the animal [100]. It has been shown that Apo-CRBP I promotes RE hydrolysis and inhibits retinol esterification [101,102]. These evidence suggest that the ratio of holo-CRBP I/apo-CRBP I indicates the cellular retinol status and determines the route of its metabolism [100].

5.6 The delivery of retinol to extrahepatic tissues

The delivery of hydrophobic retinol to extrahepatic tissues is accomplished with the assistance of plasma transport proteins, RBP4 and transthyretin (TTR). RBP4 is a small protein expressed in a wide range of tissues and organs, including liver, adipose tissue, kidney and muscle [94]. The circulating level of RBP4 has been associated with insulin resistance in obese and diabetic individuals [103,104]. Its structure contains a hydrophobic pocket that binds to one molecule of retinol [105]. In the circulation, RBP4-retinol complex is associated with TTR, which blocks the exit site of retinol in RBP4 and presumably prevents the filtration loss of the vitamin in the kidney [94,106].

Once the RBP4- retinol-TTR ternary complex is delivered to the peripheral target cells, RBP4 is proposed to interact with the extrahepatic retinol transport protein STRA6 (Stimulated by retinoic acid 6) in the cell membrane. The interaction directly mediates

the uptake of retinol into the cell without RBP4 being endocytosed [107]. Further investigation shows that TTR does not affect the STRA6-mediated retinol uptake [107]. Additionally, the expression of STRA6 can be found in different embryonic development stages and in a variety of adult organs and tissues except the liver [107]. STRA6 expression can also be up-regulated by RA in certain cancer cell lines [108]. These data suggest that the uptake of retinol into target cells is not through passive diffusion, but through a highly controlled process [107].

However, more recent studies have argued against the necessity of STRA6 as a retinol transporter. Experiments with HepG2 and 3T3-L1 cells show that the transport of retinol from RBP4 to CRBP I by STRA6 is linked to the activation of Janus kinase (JAK)/Signal Transducer and Activator of Transcription (STAT) pathway within the cell [109]. Furthermore, TTR is shown to block the activation of JAK/STAT pathway via interfering with the RBP-STRA6 interaction [110]. These results suggest that STRA6 is not a necessary retinol transporter, but a sensor of holo-RBP in the circulation [110].

5.7 Re-uptake of VA into hepatocytes

Unused retinol by the peripheral tissues will be eventually brought back to the liver, where hepatocytes re-uptake retinol from the circulation. This process is mediated by the RBP4 receptor 2 (RBPR2), a specific liver retinol transporter sharing high homology with STRA6 [111]. Interestingly the expression of RBPR2 is suppressed by RA. Its expression is also negatively correlated to the hepatic VA storage [111]. These results suggest that the re-uptake of retinol in the liver plays a critical role in the overall VA homeostasis and metabolism.

6. VA Status assessment and VA dietary recommendation

6.1 VA status assessment in human

The assessment of VA status in human body is mainly focused on two major VA reserves: the RE reservoir in the liver and the circulating retinol in the plasma [49].

The hepatic RE content is considered the best indicator of VA status, since more than 90% of total VA molecules are stored in the liver [49]. By analyzing liver samples of healthy individuals who died from accidents, Moore determined the median VA reserve was 324 IU per gram of liver tissue. If the average weight of an adult liver is 1,500 grams,

the total liver VA reserve is estimated to be around 500,000 IU [49]. Despite the usefulness of the liver VA content in medicine, two obstacles hinder the application of the measurement: one being the difficulty in obtaining liver samples, and the other being the huge between-individual variance [112].

In early 1930s, a non-intrusive indirect procedure called dark adaptation test was devised to determine moderate degrees of VA deficiency [113]. This procedure measures how quickly a person adapts to darkness once the vision cells are light-bleached. In the event of VA deficiency, the adaptation time is significantly longer and the threshold of illumination used to illicit night vision is significantly higher [113]. Dark adaptation test is widely accepted in the clinics, but it is less successful to identify subclinical VA deficiency, which is believed to be more prevalent in the population [114].

As the high performance liquid chromatography (HPLC) tools become available in the clinical settings, measurements of the circulating retinol or RBP4 concentration have been used to determine the VA status in large populations [114]. According to the data collected in the Health and Nutrition Examination Surveys, vitamin A sufficiency is defined as the plasma retinol level above 1.05 μmol/L, whereas VA deficiency is defined as the plasma retinol level less than 0.7 μmol/L [115]. Despite its wide application, the plasma retinol level has its drawback in determining VA status. The reason is that serum retinol concentration is tightly controlled within a small physiological range, and it does not decrease until the liver storage is depleted [114,116]. Additionally, serum RBP4 level has been shown to decrease in light of acute infections [117]. These drawbacks suggest that serum retinol concentration is most useful in assessing VA status in those who chronically have low VA intake.

In the last two decades, a novel approach termed relative dose response test (RDR) has been developed to indirectly evaluate hepatic VA storage. This approach is based upon the fact that exogenous VA molecules are stored in the liver under VA sufficient (VAS) condition, but are mobilized into circulation under VAD condition [114,116]. In this approach, a large dose of retinol, retinyl palmitate or retinol derivative (e.g. 3,4-didehydroretinol) is given to the recipient, whose serum retinol concentration is measured before the drug administration. Five or six hours later, the recipient is subjected to another serum retinol concentration measurement. Then the percentage increase of serum

retinol concentration over baseline is determined ($(Retinol_{5h}\text{-}Retinol_{0h})/Retinol_{0h} \times 100\%$). A value greater than 20% indicates the suboptimal intake of VA [118]. Even though this approach does not measure the total hepatic RE storage, it is proven to be able to reflect the hepatic VA status with high fidelity [118].

6.2 VA deficiency and hypervitaminosis A

The lack of VA in the body is termed VA deficiency, which manifests itself in an array of clinical symptoms, including growth stunt, loss of appetite, weight loss, impaired immunity, night blindness, anemia and xerophthalmia [116]. These clinical consequences are defined as vitamin A deficiency disorders (VADD), which affect millions of children and adults around the globe [119,120]. Particularly in the developing world, VADD remain a big nutrition and public health problem despite the huge advances in the health care service in the past decades [119,121].

The primary cause of VA deficiency is the suboptimal intake of VA. However, many diseases may also cause VA deficiency by decreasing physiological utilization of the nutrients from the diet [116]. The development of VA deficiency is a chronic process. Early clinical signs start to show up when the liver VA concentration drops below 10 μg/(gram tissue) [122]. As the deficiency progresses, more severe symptoms will appear. Due to the barriers of obtaining the liver VA concentration, clinical characterization of VA deficiency is established as the plasma retinol level below 0.7 μmol/L [115], or a RDR value above 20% [118]. Once the deficiency is confirmed, large doses of VA supplementation over a few weeks is necessary to bring back the liver VA reserve and stop the progression of VA deficiency [123].

VA toxicity denotes the adverse effects caused by the excessive amount of VA *in vivo* [124]. The toxic effects can come from both acute and chronic overdose of the vitamin. Acute VA toxicity is a transient effect caused by doses of VA greater or equal to 150,000 μg over a short period. It is identified by nausea, vomiting, headache, vertigo, increased cerebrospinal fluid pressure and blurred vision [125]. In the contrary, chronic VA toxicity is caused by doses of VA greater or equal to 30,000 μg/day for months or years. It is associated with increased risk of developing bone fracture, which often occurs unnoticed [124]. Since serum retinol level is tightly controlled within a small range, it is particularly difficult to assess the VA status in people with VA subtoxicity or toxicity. Therefore, new

diagnostic methods are needed for the assessment of VA status in the well-nourished individuals.

6.3 Dietary recommendation of VA in human

Determining the recommended daily dietary VA intake in human is a challenging task, owing to many aspects of the vitamin in relation to food and human physiology [49]. First, dietary VA comes from both plant and animal sources. Depending on the presence of dietary fat, food processing method, food matrix and potential nutrient-nutrient interaction, dietary VA in different food items has different availabilities and absorption efficiencies [49]. Second, human liver VA storage differs greatly among well-nourished individuals. It is, therefore, difficult to decide a single liver storage value to deduce the recommended daily intake for the whole population [49]. Third, the daily requirement of VA is influenced by age, sex, diseases, pregnancy and lactation. The recommended daily intake should be adjusted for those factors in the practice [49].

In order to evaluate and compare the availability of VA from different sources, Institute of Medicine (2001) introduces retinol activity equivalent (RAE) to substitute the previous used international unit (IU). One RAE is defined equal to 1 μg retinol, or 2 μg supplemental β-carotene. If β-carotene is obtained from dietary sources, the equivalent dose is set at 12 μg. All other provitamin A carotenoids share an equivalent dose of 24 μg to 1 RAE. This standard makes it possible to determine the dietary VA intake from different individuals and establish the recommendation for the population.

Since it is difficult to decide daily VA intake recommendation based on the total hepatic VA reserve, Institute of Medicine utilized a computational method to derive the estimated average requirement (EAR) of VA, such that the amount maintains the adequate stores in the liver of well-nourished individuals. The mathematical formula and the corresponding values for the variables are listed in Table 1-2. This formula results in an EAR of 627 μg RAE per day for adult man and 503 μg RAE per day for adult woman. To account for individual variance and ensure 97% of the population ingest adequate amount of VA, recommended dietary allowance (RDA) for VA is set at 900 μg RAE per day for adult man and 700 μg RAE per day for adult woman.

Table 1-2: Calculation of EAR of vitamin A for adult*.

$$EAR \times F = A \times B \times C \times D \times E$$

Letters	Meaning	Value
A	Percent of vitamin A stores lost per day on vitamin A-free diet	0.5%
B	Minimum liver vitamin A reserve without adverse effects	20 μg/g tissue
C	The liver/body weight ratio	1:33
D	Reference weight	76kg for male 61kg for female
E	Total body vitamin A/liver vitamin A ratio	10:9
F	Efficiency of storage of ingested vitamin A	40%

* Adapted from IOM (2001)

7. VA, retinoid signaling pathway and gene transcription

7.1 Overview of the retinoid signaling pathway

The importance of VA is well recognized in the regulation of a myriad of biological events. The investigation of its pleiotropic effects in animals resulted in the discovery of the retinoid signaling pathway, by which VA exerts its function by modulating gene expression in target cells (Figure 1-4) [126,127]. In general, retinol is reversibly oxidized into retinal by RDHs, and then, retinal is further irreversibly oxidized into RA by RALDHs. RA molecules move to cell nucleus, where they interact with transcription factors to regulate the down-stream gene expressions. It has been generally believed that RA mainly binds to and activates two subfamilies of nuclear receptors (NRs), retinoid acid receptors (RARs) and retinoid X receptors (RXRs). Specifically, all-*trans*-RA is an exclusive ligand for RAR, whereas 9-*cis*-RA is a common ligand for both RAR and RXR [128]. RARs and RXRs can recognize short consensus DNA sequences, which are termed retinoic acid response elements (RAREs), located in the promoter region of RA responsive genes. Depending on the specific gene, RXRs can bind to RARE in a homodimer or a heterodimer with RARs or other NRs. In addition to RARs and RXRs, RA signals have been suggested to be mediated by other NRs, such as peroxisome proliferator-activated receptor (PPAR) β/δ, hepatocyte nuclear factor 4α and chicken ovalbumin up-stream transcription factor II [24]. The binding of the NR dimers by their ligands will help recruit corresponding transcriptional coactivators, dissociate transcriptional corepressors, and interact with the general transcription machinery, leading to the regulation of target gene expression.

7.2 Generation of retinoic acid in target cells

Given the importance of VA in different aspects of physiology and its hydrophobic property, the generation of RA is a highly regulated process involving complex retinoid binding proteins and metabolic enzymes [100].

RDHs catalyze the first step in the biosynthesis of RA, by which retinol is oxidized into retinal. This reversible reaction has a low V_{max} value, which makes it the rate limiting step in the generation of RA [129]. *In vitro* biochemical experiments have so far identified almost a dozen enzymes with retinol oxidation capabilities, but only RDH1, RDH10 and DHRS9 (dehydrogenase/reductase member 9) are verified and supported by

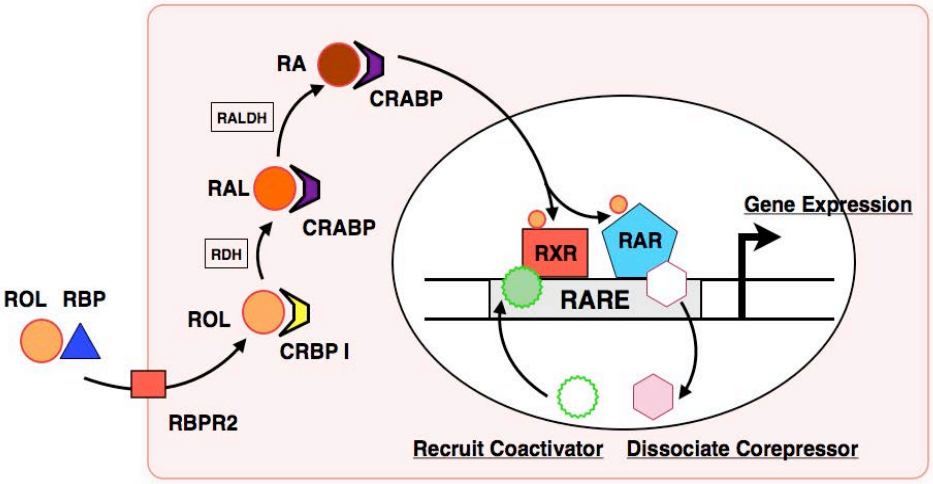

Figure 1-4: Schematic graph of the retinoid signaling pathway. Please see section 7.1 for description. ROL, retinol; RAL, retinal; RA, retinoic acid; RBP, retinol binding protein; RBPR2, retinol binding protein receptor 2; CRBP, cellular-retinol binding protein; CRABP, cellular retinoic acid binding protein; RDH, retinol dehydrogenase; RALDH, retinal dehydrogenase; RARE, retinoic acid responsive element; RXR, retinoic X receptor; RAR, retinoic acid receptor.

in vivo evidence (Table 1-3) [100]. Early cell fractionation data suggest that most retinal-generating capacity are associated with microsomes [130], showing the presence of RDHs in the ER of intact cell. This is confirmed by the discovery of a short signal sequence in the N-terminus of RDH, which can anchor the enzyme in the ER with the catalytic domain facing toward the cytoplasm [131]. The catalytic property of RDH does not require CRBP I, despite that the majority of retinol in the cell are bound to it [132]. One explanation is that CRBP I acts as a chaperone and facilitates the transfer of retinol to enzyme [132].

The irreversible conversion of retinal into RA is catalyzed by RALDHs. Currently, four RALDHs have been identified, which are expressed and regulated in a tissue specific manner (Table 1-4). RALDH1 is universally expressed in tissues and accounts for over 90% retinal oxidation capability in rat liver and kidney [133]. Despite its ubiquitous expression profile, RALDH1 knockout mice do not manifest developmental difference compared to their wild type counterparts [134]. However, functional defects in certain organs and tissues are observed in RALDH1 null mice. At 6 to 9 months of age RALDH1 null mice develops cataract, showing its critical role in the production of RA in the eye [135]. Additionally, RALDH1 suppresses PPARγ and RXR responses in rodent fat, which suggests that it is a key modulator of adipogenesis [136]. RALDH1 null mice are resistant against high-fat diet induced glucose intolerance and obesity [136,137]. Multiple studies in mouse hepatoma cells also provide evidence that RALDH1 expression can be down-regulated by all-*trans*-RA, suggesting the presence of a negative feedback loop in the generation of RA *in vivo* [138,139]. In contrast to RALDH1, RALDH2 knockout mice are embryonically lethal. This suggests that RALDH2 is responsible for the local production of RA during embryo development [140]. RALDH3 does not recognize 9-*cis*-retinal as a substrate, whereas RALDH4 only recognizes 9-*cis*-retinal as a substrate [141,142]. The selective recognition of substrates suggests the distinct functions of the two enzymes *in vivo*, however, more research is necessary to elucidate the underlying mechanisms [141,142].

The catabolic cytochrome P450 (CYP) family enzymes partially contribute to the RA homeostasis. These enzymes require NADPH and oxygen to convert RA into a myriad of end products, including 4-hydroxy-RA, 4-oxo-RA and 18-hydroxy-RA [143]. A

Table 1-3: List of physiological relevant RDHs*.

Mouse gene	Orthologs	Tissue Distribution	Functions	Mouse Models
RDH1	Rat: RDH7, RDH2 Human: RDH16	Widespread	• atRA generation • Metabolism • Immune function	• RDH1 null mouse on chow diet shows no developmental phenotype • RDH1 null mouse on vitamin A restricted diet has increased body weight and adiposity. • RDH1 mRNA is decreased in Tg26 (HIV-1) mouse.
RDH10	Rat: RDH10 Human: RDH10	RPE cell, Müller cell Dendritic cell Early embryo	• Vision cycle • Immune response • Embryogenesis	• RDH10 null mouse is embryonically lethal.
DHRS9	Rat: DHRS9 Human: DHRS9	Zebrafish embryo Human colon Human epidermis	• Embryogenesis • Suppress tumorigenesis	• No knockout available

* Adapted from Napoli (2012) and Kumar et al. (2012)

Table 1-4: List of physiological relevant RALDHs*.

Gene Name	Alternative Name	Tissue Distribution	Functions	Mouse Models
RALDH1	Aldh1A1	Widespread	• ~90% atRA generation • Vision • Metabolism	• RalDH1 null mouse develops normally, and is fertile. • RalDH1 null mouse develops cataract. • RalDH1 null mouse is resistant to high-fat diet induced glucose intolerance and obesity.
RALDH2	Aldh1A2	Widespread, enriched in testis	• Embryogenesis	• RalDH2 null mouse is embryonically lethal.
RALDH3	Aldh1A3	Widespread during embryogenesis	• Embryogenesis • Suppress tumorigenesis	• RalDH3 null mouse develops choanal atresia and is lethal at birth.
RALDH4	Aldh1A4	Early embryo, liver, kidney	• To be determined	• Not available

* Compiled from Napoli (2012), Kumar et al. (2012) and Lin et al. (2002)

representative member of the family, CYP26A1, is cloned and investigated for its role in the regulation of RA homeostasis in animals [144-146]. CYP26A1 level is low in VAD animals, but is substantially induced by RA or a VAS diet [145]. CYP26A1 null mice are embryonically lethal, showing the phenotypes similar to wild type mice with excessive RA [147]. These data show an autoregulatory mechanism by which CYP26A1 controls RA catabolism to maintain RA level *in vivo*.

Most naturally occurring VA molecules in the diet and their metabolites are the all-*trans* isomers. The discovery of 9-*cis*-RA as the preferred ligand for RXR raises the possibility of a 9-*cis*-RA metabolic pathway *in vivo*. However, the information on this subject thus far is still limited. First of all, the detection of endogenous 9-*cis*-RA in different tissues has been unconvincing except in pancreas, where 9-*cis*-RA acts as autacoid to attenuate glucose stimulated insulin secretion [148,149]. Second of all, there is no enzyme found to catalyze the isomerization of all-*trans* retinoids, except the system in the vision cycle to produce 11-*cis*-retinal. Despite these, many studies tried to provides explanations on how 9-*cis*-RA is formed *in vivo*. Urbach and Rando propose that the isomerization of all-*trans*-RA into 9-*cis*-RA is a non-enzymatic reaction, which requires sulfhydryl group in the microsome [150]. In contrast, many studies supported a possible separate enzymatic system for the generation of 9-*cis*-RA. 9-*cis*-β-carotene was shown to serve as a precursor for 9-*cis*-RA in a ferret model [151]. This is consolidated by the discovery that 9-*cis*-retinal is the preferred substrate for RALDH4 [142], showing that it is possible to generate 9-*cis*-RA *in vivo*.

7.3 RXRs and RARs

RARs and RXRs each have three subtype members, which are RARα, β, and γ, and RXRα, β, and γ, respectively. Each subtype is encoded by a separate gene in the human and rodent genomes. However, alternative splicing transcripts of one gene may generate different isoforms for a subtype [152]. RARs and RXRs belong to the NR superfamily, whose members share similar structural arrangements and functional domains (Figure 1-5). The A/B domain resides in the N-terminus of the receptors, and it contains the activation domain I (AF-1) [153]. The AF-1 domain is necessary for the full activation of the transcription activity of RARs and RXRs, but the activation process is autonomous and ligand-independent [153]. Following the A/B domain in the structure resides the

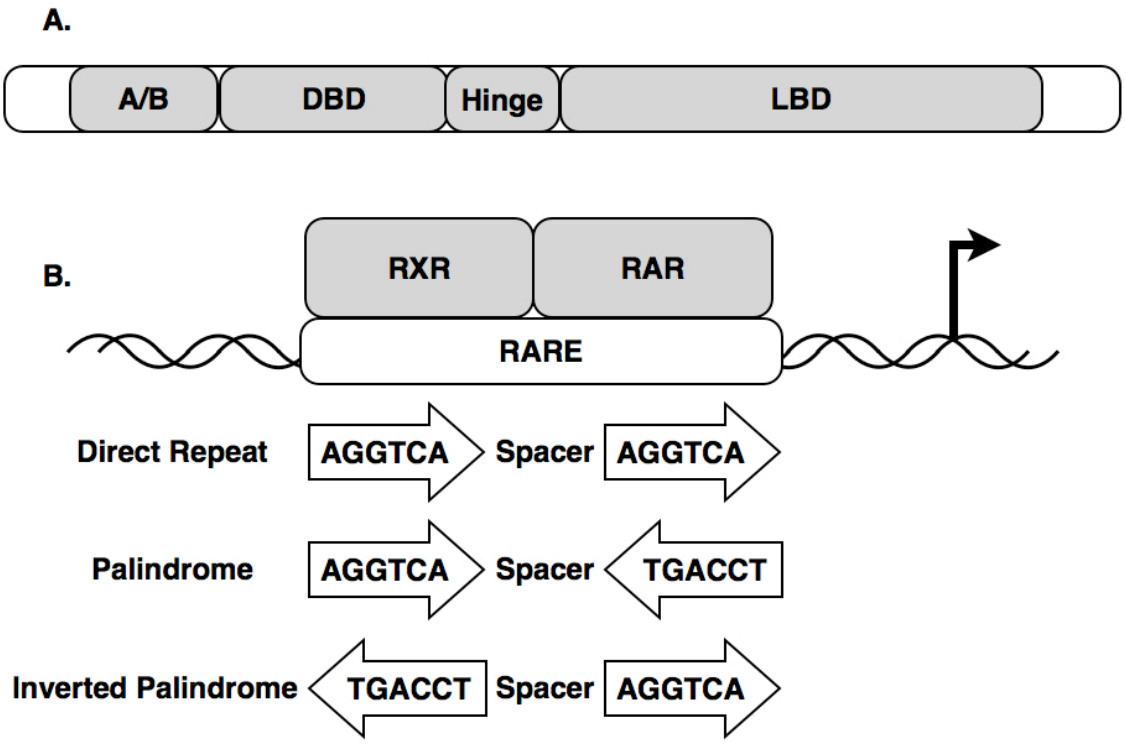

Figure 1-5: Schematic graph of (A) NR structures and (B)RARE in the promoter region.

DNA-binding domain (DBD). The amino acid sequence of DBD is highly homologous across the members of NRs. Two C4 zinc fingers organized into two α-helices interact with the target DNA [154]. Within the DBD, a short peptide of three amino acids in the P box differentiates and recognizes the RARE in the target DNA [155,156]. The ligand-binding domain (LBD) is linked to the DBD via a short hinge domain. The LBD is a multifunctional domain which not only binds to specific ligands, but also helps the dimerization of NRs and the binding to other transcriptional factors [127,157]. Notably, the dimerization of NRs and the binding of the NRs to the DNA are a ligand-independent process, whereas the binding of other transcriptional factors and achieving maximal transcriptional activity require ligand binding [127,153,158].

Both RXRs and RARs recognize and bind to the RARE located in the promoter region of a gene. Within RARE two consensus half sites (AGGTGA) are separated by a spacer in the arrangement of either direct repeats, or palindrome, or inverted palindrome (Figure 1-5) [159]. The RXR-RAR heterodimer can bind to those RARE arrangements with different efficiencies. Depending on the RARE in the promoter region of the target gene, the different binding efficiencies of the heterodimer confers a level of specificity in the gene expression regulation [94,159].

7.4 Coactivators and Corepressors

The LBD domains in the RXRs and RARs are involved in the recruitment of transcriptional coactivators and corepressors. Biochemical analysis of RXRs and RARs shows that the LBD domains of apo-RXRs and apo-RARs interact with a conserved motif (CoRNR) in the C terminus of corepressors [160]. Once the specific ligand binds to the ligand pocket in the LBD, it induces a conformational change in the LBD domain, where H12 α-helix forms a surface for coactivators to bind with other motifs [161]. Interestingly, this surface recognizes the LXXLL motifs in the structures of coactivators, which shares great homology with the CoRNR motif in the corepressors [127,160]. These results showed that the binding of coactivators and corepressors to the RXRs and RARs are mutually exclusive [160].

8. Major physiological functions of VA

8.1 VA and the vision

Thousands of years before Holm [162] and Yudkin [163] detected trace amount of VA in the retina of farm animals, ancient civilizations around the globe had learned to use VA enriched animal liver to treat night blindness by either ingestion or topical treatment [47]. However, the puzzle pieces for the molecular mechanism of the vision cycle were not found until 20th century (Figure 1-6). First, the trace amount of VA in the retina was proved to exist mainly in the aldehyde form [164-166]. Second, the visual pigment rhodopsin (also known as visual purple) was discovered [49]. Third and most important, through a series of experiments Wald elucidated the enzymatic systems required for the interconversion of *cis*- and *trans*- retinal and the formation of rhodopsin in the eye [167]. The information helped establish the current picture of the vision cycle involving retinal pigment epithelial (RPE) cells, photoreceptor cells (cone cells and rod cells), and Müller cells in the retina.

Photoreceptor cells are specialized neurons with lamellar membrane structures in the eye. These highly specialized structures contain transmembrane pigment rhodopsin and face toward the microvascular network [57]. The RPE cells are specialized epithelial cells, which separate the photoreceptor cells and the microvascular network. Their particular cell polarity ensures the directional movement of nutrients from the blood to the photoreceptor cells [57]. The Müller cells extend across photoreceptor cells, which function as glial cells in the specialized neuronal system. However, recent investigation suggests that they might as well participate the vision cycle in the cone cells [57].

The vision cycle starts with the rhodopsin located in the lamellar membranes of the photoreceptor cells. In its stable state, rhodopsin is the protein opsin bound to 11-*cis*-retinal via a Schiff base [57]. An exposure to light will isomerize the 11-*cis*-retinal to all-*trans*-retinal and give out the light neuronal signal. All-*trans*-retinal is subsequently released from rhodopsin into the cytosol of the photoreceptor cells due to the hydrolyzation of the Schiff base [57]. In vertebrate animals All-*trans*-retinal is reduced to 11-*trans*-retinol by RDH8 and RDH12 in the photoreceptor cells [168,169]. The latter, secreted and bound to interphotoreceptor RBP (IRBP), is taken up by RPE cells in a STRA6 mediated process [107]. All-*trans*-retinol in the RPE cells will bind to CRBP I so

that it can be esterified by LRAT [170]. The retinyl ester is the substrate for the isomerhyd retinol ase RPE65, which hydrolyzes the ester and produces 11-*cis*-retinol [171]. 11-*cis*-retinol is then bound to CRABP I so that it can be oxidized into 11-*cis*-retinal by 11-*cis*-retinol dehydrogenases (11-RDHs) in the presence of NAD(P)$^{+}$. The 11-*cis*-retinal will be transported back to the photoreceptor cells to form rhodopsin, thereby completing the visual cycle [57].

Apart from the participation in the visual cycle, VA is also critical for the normal morphology of the cornea. Severe VA deficiency causes xerophthalmia, which has affected people in the deprived areas and people having VA restricted diet in the world [172,173].

8.2 VA and immunity

VA was initially named the "anti-infective" vitamin in 1928 for the observation of impaired immunity in VAD animals and human beings [174]. Lung infection, epithelial abnormalities, and kidney stones are among the most common manifestations [174]. However, recent studies have otherwise showed that infection could cause VA deficiency [175]. Serum retinol level decreases in response to acute infection, whereas hepatic VA storage quickly depletes during acute viral infection [176]. The mechanism of infection-induced VA deficiency is postulated to be multifactorial [175]. Infection can (1) dramatically change appetite and nutrient intake [177-179]; (2) disturb digestive system and cause malabsorption [180,181]; (3) cause direct loss of nutrients via vomit, urine, sweat, stool and other body secretions [182]; (4) dramatically increase daily nutrient requirement by altering metabolism [175]; (5) dramatically decrease the cellular nutrient utilizations [175]. These points suggest that VA mainly helps the recovery from infection, rather than the prevention of infection in the first place [175].

VA deficiency compromises both innate immunity and adaptive immunity according to experiments in rodent and observations in human. The integrity of mucosa, the first defense in innate immunity, is poorly maintained in VAD individuals [183]. Additionally, RA, the active form of VA, has been used clinically to treat promyelocytic leukemia, which is a genetic disease characterized by defective neutrophil maturation [184]. In rodents VA deficiency has been shown to increase macrophage number and the secretion of proinflammatory cytokine IL12 [185]. In humans VA deficiency is associated with

lower phagocytotic activity of microphages against gram positive bacteria [186]. The evidence clearly shows that VA deficiency impairs multiple components of the innate immunity.

Adaptive immunity is a pathogen-specific defense that requires B and T lymphocytes. It is yet unclear how VA affects the functions of B lymphocytes, but sufficient evidence has shown that VA is critical in regulating the differentiation of T lymphocytes into Th1 and Th2 cells [175,187]. Low VA status pushes the fate of naive T lymphocytes into Th1 cells, whereas high VA status generally promotes differentiation toward Th2 cells [175,187]. The fine balance of Th1/Th2 cells in the body is postulated to affect autoimmunity, anti-/pro-inflammation and antibody recognition, underlining the critical role of VA in adaptive immunity [175,187].

8.3 VA and cell differentiation, proliferation and apoptosis.

In response to different hormonal and nutritional stimuli, cell differentiation, proliferation and apoptosis coordinate in a temporal-spatial manner to maintain tissue homeostasis, and to control growth and development [94]. Early documentation in animal husbandry has shown that VA affects animal growth and development [188,189]. With the discovery of the NRs, RA and other retinoids have been established as the effector molecules in the regulation of growth and development [94]. The regulation is postulated to occur at three different levels [94,190]: (1) the expression of hormones, cytokines and growth factors; (2) the expression of corresponding receptors and binding proteins for the hormones, cytokines and growth factors; (3) the expression of downstream genes in different signaling pathways that control growth and development. The detailed molecular mechanism by which RA regulates each specific gene expression may differ, but the NRs mediated RA signals and the binding of retinoids to them are central to the general mechanism of regulation [94,191].

In mammals, the dietary VA is required for the progression of spermatogenesis in testis. Due to the blood-testis barrier and low absorption rate, RA supplementation is unable to recover male sterility in VAD rats, suggesting the indispensable role of retinol in spermatozoa differentiation [192]. Furthermore, male sterility is also observed in strains of RARα, RARγ and RXRβ mutant mice, which manifest defects in different stages of the spermatozoa differentiation [193-195]. Besides spermatogenesis, another

well studied phenomenon is the effect of RA on the differentiation of myeloid leukemic cells, including HL-60, THP-1 and U-937 [196,197]. Experiments have shown that RA can specifically induce the differentiation of acute promyelocytic leukemic cells into granulocytes, which provides the basis for the clinical treatment of promyelocytic leukemia with RA [184].

RA affects the cell proliferation by modulating key regulators in the progression of the cell cycle. In different cancer cell lines, RA treatment can up-regulate cyclin-dependent kinase (CDK) inhibitors, whereas down-regulate CDK and c-myc expression [94]. This results in the accumulation of cells arrested at the G0/G1 phase in the cell cycle, which showcases the anti-proliferative properties of RA [198]. Correspondingly, NRs have also been implicated in the modulation of cell proliferation. For example, RARβ has been shown to mediate the growth inhibitory effects of retinoids in many cell lines, including fibroblasts [199], mammary epithelial cells [200] and neuroblastoma cells [201]. In mammary carcinoma RARβ also depends on RARα and estrogen receptor (ER) to confer the tumor suppressive effect [198], suggesting the crosstalk between signaling pathways in the regulation of cell proliferation.

Apoptosis is the critical counterbalance against cell differentiation and proliferation in the process of growth and development [202]. Even though the information is still limited, several studies have shown evidence that RA is able to promote or inhibit apoptosis depending on the system. In MCF-7 mammary carcinoma cells all-*trans*-RA is able to induce apoptosis preceded by G1 arrest in the cell cycle [198]. In keratinocytes all-*trans*-RA acts as an apoptosis sensitizer instead of an apoptosis inducer, in that it increases the expression of p53 and proapoptotic caspases [203]. On the contrary, in neuronal cells and retinal cells RA shows anti-apoptotic activities to maintain cell survival [202].

8.4 VA and growth

VA was first recognized as an essential factor for animal growth. Following the withdrawal of VA from the diet, growth retardation is the earliest and most reproducible sign of deficiency in many experimental animals [204]. Rats fed a VAD diet upon weaning (about three weeks old) manifest cessation of growth and significant weight loss later on [205,206]. The reduction of body mass can be prevented by RA supplementation. However, once RA is removed from those rats fed the VAD diet, the weight loss will

reappear in a couple of days [189,207]. These demonstrate that VA is important for the normal growth and development of animals.

In comparison to rats, mice are more resistant to the development of VA deficiency. Normal growth curve is usually observed in weaning mice with sufficient hepatic VA storage despite being sustained on a VAD diet [208,209]. In one study, significant weight loss was achieved in mice fed a VAD diet only when the VA storage was pre-depleted prior to weaning [208]. This suggests that mice might have special mechanisms to maintain VA homeostasis or they might use VA more efficiently. As a result, experiment conclusions obtained in mice cannot be directly extrapolated to rats or humans in terms of VA and its effects on growth and metabolism.

8.5 VA and appetite, taste and olfaction

VAD animals exhibit decreased appetite and food intake during the period of growth cessation [205,206]. The underlying molecular mechanisms by which VA regulate energy intake remain elusive. Since leptin, an adipocyte-derived peptide hormone, exerts its action in the brain to regulate appetite, energy expenditure and metabolism [210], some research investigated the effects of VA on the expression of leptin in rodents. The results showed that both RA treatment and VA supplementation were able to decrease leptin mRNA expression in adipocytes, which, in turn, decreased the serum leptin levels [211,212]. Interestingly, the energy intakes of these rodents did not change during the course of VA supplementation [213]. These data suggest that the VA-induced decrease in leptin levels does not correlate with the food intake in the animals [213].

VA has also been implicated in the normal functions of the taste and olfactory system. VA depletion causes the loss of both preference to sodium chloride and aversion to quinine in rats, and these abnormal responses could be restored by VA supplementation [214]. One study also shows that the response to sweetness in the VAD rats is impaired [215]. Furthermore, VA supplementation can improve the impairment of taste and olfaction in patients with cirrhosis [216]. Despite these many observations, the mechanism is not clear. Keratin infiltration into the taste buds is proposed as a mechanism by which VA deficiency affects the taste in rats [214]. But the physical change could not be confirmed in all VAD rodent models [215].

9. VA and metabolism

9.1 VA and plasma parameters: clinical evidence

The association between VA and metabolism was discovered from the clinical observations in human subjects with type 2 diabetes. Biopsies of the liver of diabetic patients showed that the hepatic VA content was twice as much as that in healthy individuals [112]. Independent studies carried out more than eighty years ago also found that, about 85% of adult patients with type 2 diabetes had elevated carotene levels in the plasma, and more than 10% of them were clinically diagnosed with xanthosis [217,218]. Similar results were obtained in a lesser degree in type 2 diabetic children, but their plasma VA levels were found to be subnormal [219]. More recently, retinol binding protein 4 (RBP4), a serum retinol transporter, was shown to be elevated in insulin resistant and type 2 diabetic subjects [104]. Interestingly, reduction of serum retinol and RBP levels was found in type 1 diabetic patients [220]. These data suggest that VA plays important roles in the metabolic homeostasis.

The association between VA and plasma lipid metabolism was also observed in patients taking retinoid drugs. Medical administration of isotretinoin (13-*cis*-RA) results in hypertriglyceridemia in human subjects with acne [221]. Treatment of acute promyelocytic leukemia with all-*trans*-RA leads to weight gain, and elevation of plasma TG and cholesterol levels [222,223]. It is postulated that the dysregulated plasma lipid levels are caused by the RA-induced apolipoprotein CIII expression [224]. Apolipoprotein CIII is regarded as an inhibitor of LPL activity [225]. In the contrary, long-term administration of fenretinide, a synthetic retinoid drug currently under phase II clinical trial, could prevent diet-induced obesity, insulin resistance and hepatosteatosis [226,227]. As more and more retinoid drugs are synthesized and tested, it would be interesting to see how they affect human metabolism in any given health condition.

9.2 VA and metabolism in the liver

9.2.1 VA and the hepatic carbohydrate metabolism

The liver plays a leading role in the regulation of carbohydrate metabolism in response to the feeding and fasting statuses. Experiments in rodents show that both hypervitaminosis A and hypovitaminosis A affect carbohydrate metabolism in the liver [42].

Glycogen is a crucial polysaccharide, in which intracellular glucose is stored. Hepatic glycogen synthesis and degradation contribute to the plasma glucose homeostasis. In VAD rats, the liver glycogen content is abolished due to decreased glycogenesis from acetate, lactate and glycerol, rather than directly from glucose [228,229]. The decreased glycogenesis can be recovered by the administration of glucocorticoid hormone [229]. Since VAD animals have lower adrenal steroid production, it is possible that VA deficiency partially affects glycogen metabolism via decreasing glucocorticoid hormone synthesis [229]. In hypervitaminotic A rats, the liver glycogen deposition in the fed state is almost the same or slightly lower than that in rats fed a chow diet [230,231]. However, the liver glycogenesis of hypervitaminotic A rats after 18 to 20 hours of fasting is significantly higher than that in rats fed chow [231]. This suggests that excessive VA intake for a short-term can prevent the hepatic glycogenolysis under the fasting condition. Additionally, excessive VA can also enhance the hepatic glycogenesis from glucose after refeeding in normal rats, but not in adrenalectomized rats [232]. This suggests that adrenal hormones are involved in the VA-regulated hepatic glycogen metabolism [232].

Glycolysis is a series of enzymatic reactions, which break down glucose to produce pyruvate and generate ATP and NADH. This important carbohydrate metabolic pathway is influenced by VA status. In VAD hamster, the hepatic generation of glucose-6-phosphate was decreased by up to 90% due to the reduced glucokinase (gene *Gck*) activity [233]. Similarly, the generation of mannose-6-phosphate was also decreased due to the impaired hexokinase activity [233]. In the contrary, hypervitaminosis A does not affect the enzymatic activities of hepatic glucokinase and hexokinase [234]. Instead, the excessive VA can decrease the enzymatic activities of phosphofructokinase and pyruvate kinase [234]. Additionally, the *Gck* mRNA levels in the liver of the VAD rats are lower than that of the VA sufficient counterparts [206]. Retinoids not only increases the hepatic *Gck* expression in rats, but also synergize with insulin to induce *Gck* expression in primary rat hepatocytes [235]. These observations suggest that VA is an important regulator of hepatic glycolytic enzymes.

Gluconeogenesis is a series of enzymatic reactions, which utilize non-carbohydrate substrates (e.g. lactate, pyruvate, amino acid) to generate glucose. This metabolic pathway is very important in maintaining the fasting blood glucose level in animals.

Experiments with VAD rats show that the enzymatic activities of glucose-6-phosphatase and fructose-1,6-bisphosphatase were decreased in the liver, showing an inhibition of hepatic gluconeogenesis [236]. Comparably, hypervitaminotic A rats have elevated enzymatic activities of hepatic phosphoenolpyruvate carboxykinase (PEPCK, gene *Pck1*), glucose-6-phosphatase and fructose-1,6-bisphosphatase [237,238]. In addition, the VA-mediated increase in gluconeogenesis is abolished in adrenalectomized rats [239], showing the requirement of adrenal hormones in the process. The regulation of gluconeogenesis by VA can also occur at the transcription level of *Pck1* expression in the liver. RA not only induces the *Pck1* expression in primary rat hepatocytes, but also attenuates the insulin-suppressed *Pck1* expression [240]. In fact, insulin can inhibit the RA-activated RXRs, but not RARs in the *Pck1* promoter. This mechanism underlies the production of *Pck1* mRNAs in the presence of RA despite in an insulin-suppressed state [240]. Additionally, a *Pck1* transgenic mice model shows that all-*trans*-RAs and 9-*cis*-RAs differentially regulate the hepatic *Pck1* expression in the periportal region of the liver acinus [241]. This retinoid regulated *Pck1* expression is purportedly mediated by different RAREs and NRs at its promoter [241,242].

9.2.2 VA and the hepatic protein metabolism

Ever since the increased nitrogenous metabolism was first described in the VAD rats [243], many animal models were used to investigate the effects of VA on protein metabolism. In young male rats on a VAD diet, urinary nitrogen excretion is increased with concurrent negative nitrogen balance [244]. It is in line with the observation of increased plasma urea in the VAD adult rats [245]. Interestingly, these physiological changes cannot be obtained in VAD female rats, indicating a sex difference in the effects of VA on protein metabolism [246]. Additionally, VA deficiency increases both the mRNA levels and the enzyme activities of most urea cycle enzymes in the rat liver [245]. These data suggest that VA deficiency increases protein catabolism by upregulating the enzymes of the urea cycle in both the liver and kidney.

The effect of VA deficiency on protein anabolism is controversial. The analysis of the incorporation rate of ^{14}C-leucine into proteins in both VAD and chow-fed rats shows that VA deficiency does not adversely affect protein synthesis [247]. However, in vitro protein synthesis assay using isolated rat liver ribosomes shows the opposite effect. Cell

precipitates from the pH 5.1 fraction of the VAD rat liver homogenate exhibits enhanced protein synthesis capability [248]. The reason for these conflicting results is not known.

Very few studies looked at the effects of hypervitaminosis A on protein metabolism in animals. It is proposed in one study that 400 times of normal dose of VA causes the toxicity-induced weight loss and negative nitrogen balance [249]. However, the molecular mechanism by which the VA toxicity offsets nitrogen balance in vivo is unknown.

9.2.3 VA and the hepatic lipid metabolism

Dysregulation in the metabolism of either VA or lipid could negatively affect the metabolism of the other. On one hand, long-term retinoid drug users and people who take excessive amount of VA supplements exhibit symptoms of hypercholesterolemia, hypertriglyceridemia and high serum low density lipoprotein levels [250-252]. On the other hand, patients with severe hypertriglyceridemia associated with type V hyperlipoproteinemia have increased risk for developing hypervitaminosis A [253]. The mechanisms underlying these phenomena have been actively investigated in rodent models. Oral administration of large doses of retinol leads to the accumulation of lipid droplets in the rat liver [254]. Overdose of retinol or retinyl palmitate also causes the elevation of hepatic cholesterol, FA, and TG contents in different strains of rats [255-257].

It has been shown that hypervitaminotic A rats have increased rates of hepatic FA oxidation and ketogenesis [257]. On the other hand, the hepatic TG synthesis rate is greatly enhanced in the hypervitaminotic A rats. This is due to the increased incorporation rate of palmitate into TGs and the formation of glycerophosphate from glucose [256,257]. Interestingly, the rate of hepatic TG secretion is not changed in hypervitaminotic A rats [258]. These data suggest that VA increases hepatic lipid synthesis to an extent much greater than it elevates hepatic lipid oxidation. The net result is the accumulation of lipid in the liver. Further investigation shows that the hyperlipidemic effect of excessive intake of VA can not be observed in adrenalectomized rats, showing the involvement of adrenal hormones [256].

In the contrary to the hyperlipidemic effect of hypervitaminosis A, VA deficiency causes a partial hypolipidemic effect in rodents. In general, VAD rats have decreased

hepatic phospholipid content and decreased serum levels of TG, cholesterol and HDL [206,259]. Interestingly, these rats manifest unaltered hepatic contents of TG and cholesterol [257,260-262]. Depending on the severity of VA deficiency in the animals, not all the above-mentioned symptoms can be observed. The partial hypolipidemic effect of VA deficiency in rodent may be caused by decreased FA synthesis activity in the liver and impaired cholesterol synthesis from mevalonate [259,262]. However, it is worth mentioning that the VA deficiency-induced body mass loss and food intake drop may also contribute to the hypolipidemic symptoms. Evidence shows that the decrease in total percentage of body fat is similar between the VAD rats and their counterparts pair-fed a VA sufficient diet [263]. All the data suggest that the dyslipidemia in VAD and hypervitaminotic A animals is a multicausal effect.

The hepatic FA synthesis is governed by an allotment of lipogenic genes, including acetyl-CoA carboxylase (ACC, gene *Acc*) and FA synthase (FAS, gene *Fas*). The transcription of hepatic *Acc* and *Fas* is controlled by a transcriptional factor termed sterol-responsive element binding protein 1c (SREBP-1c, gene *Srebp-1c*) [264]. In primary rat hepatocytes, insulin induces the *Srebp-1c* expression through transcription factors associated to the liver X receptor elements in the *Srebp-1c* gene promoter [265]. Interestingly, the corresponding liver X receptor elements in the *Srebp-1c* promoter are also identified as RAREs [266]. This finding provides a possible mechanism, by which RA synergizes with insulin to induce the hepatic *Srebp-1c* expression [266]. It also showcases how nutritional and hormonal converge at the transcription level to regulate *de novo* FA synthesis in the liver.

9.2.4 VA and mitochondrial functions in hepatocytes

Mitochondrion is the powerhouse of an eukaryotic cell, within which tricarboxylic acid cycle (TCA cycle) and coupled-oxidative phosphorylation together generate ATP for physiological events. TCA cycle is a series of enzymatic reactions that generates reducing equivalents (NADH and FADH2) by utilizing acetyl-CoA derived from monosaccharide, amino acid and FA. The reducing agents ultimately provide electrons, which are consumed in the coupled oxidative phosphorylation process to reduce O2 and generate ATP and water.

In the rodent liver, both hypo- and hypervitaminosis A are implicated in the uncoupled oxidative phosphorylation in the mitochondria [267-269]. On one hand, the oxygen consumption by liver homogenates of hypo- and hypervitaminotic A rats is significantly increased upon the supply of some TCA intermediates [267,268]. On the other hand, the capacity for the oxidative phosphorylation is severely impaired in the liver mitochondria of hypo- and hypervitaminotic A rats without affecting the ATPase activity [269]. These data suggest that deficient or excessive VA status may increase basal energy metabolism in the liver.

9.3 VA and islets of Langerhans in the pancreas

Islet of Langerhans, which account for less than 2% of the total pancreas mass, produces and secrets peptide hormones from five different types of specialized cells, including α-, β-, polypeptide (PP-), δ-, and ε-cells [270,271]. Among all the hormones produced by islets, glucagon from α-cells and insulin from β-cells are of great clinical interest due to their concerted roles in the regulation of blood glucose and lipid levels. Glucagon promotes hepatic glucose production, glycogenolysis and ketone production in response to hypoglycemia, whereas insulin promotes glucose disposal, glycogenesis and lipogenesis in response to the increase of plasma glucose level [272].

The secretion of glucagon is controlled by autonomous nervous system, direct actions of glucose on α-cells, and indirect effects of paracrine factors from non-α-cells on α-cells [273]. On the other hand, the secretion of insulin is mainly stimulated by the influx of glucose into β-cells. Glucose metabolism in β-cells leads to the elevated ATP/ADP ratio, which in turn, inhibits the ATP-sensitive potassium channels on the cell membrane. The inhibition depolarizes the plasma membrane, which results in the secretion of insulin. In addition to glucose, amino acid and neural stimuli can also stimulate insulin secretion [274].

It has been shown that VA and its metabolites can affect the secretion of glucagon. In the VAD rats, the impaired glucagon secretion occurs from early stage of the deficiency, and the impairment cannot be rescued by RA replenishment [275]. This demonstrates a critical physiologic role of VA in the normal function of α-cells. Interestingly, in the isolated intact rat islets and glucagon secreting cell lines, both retinol and RA inhibit the glucagon secretion in a dose-dependent manner [276]. This result suggests that the acute

effects of VA on glucagon secretion in vitro do not correlate with its physiological effects in vivo.

VA deficiency has been shown to decrease β-cell functions in rat in two ways. First, it reduces the β-cell mass in fetal islets by reducing the fetal β-cell replication [277]. Second, it impairs the glucose-stimulated insulin secretion (GSIS) from β-cells [278]. In comparison, the effects of VA and its metabolites on isolated islets and insulin secreting cells are both chemical- and dosage-dependent. For example, retinol at 10^{-7}M stimulates GSIS from isolated rat islets, which is in opposition to the inhibitory effect of retinol at $10^{-4} \sim {}^{-5}$M [279]. Additionally, all-*trans*-RA potentiates GSIS [280-282], whereas 9-*cis*-RA inhibits GSIS [148] from rodent islets and INS-1 cells. CRBP I knockout mice exhibits increased level of 9-*cis*-RA in the pancreas and reduced GSIS [283]. It is also observed that all-*trans*-RA induces the *Gck* mRNA level and enzyme activity of glucokinase [282], whereas 9-*cis*-RA treatment is associated with decreased GLUT2 and glucokinase activities in rodent islets [148]. Given the fact that retinoid receptors require preferential ligands to exert full function, these results suggest that the production and balance of RA and its metabolites are critical for the normal functions of β-cells.

9.4 VA and metabolism in adipose tissues

9.4.1 VA and metabolism in white adipose tissue

White adipose tissues not only store excessive energy as TGs, but also secrete important adipocyte-derived hormones and cytokines to regulate whole body energy metabolism. VA and its metabolites have determinant effects on the metabolic homeostasis in white adipose tissue.

Firstly, VA status has been shown to affect adiposity in animals. In VAD rats, the loss of body fat deposit mass is reflected in the decreased total body mass [244]. Since the VAD rats have significantly lower body mass compared to their counterparts pair-fed the VAS diet, it suggests that the reduction of fat mass in the VAD rats cannot be fully attributed to the VA deficiency associated with the reduction of food intake [244]. In Zucker lean rats, VA deficiency decreases the epididymal fat mass and its fat mass/body mass ratio [206]. In Zucker fatty rats, a genetic rat model of obesity, VA deficiency retards the development of obesity [206]. Additionally, hypervitaminotic A rats have decreased release of FAs from white adipocytes, whereas VAD rats exhibit increased rate

of lipolysis in white adipose tissue [284]. Despite these findings supporting VA's role in maintaining adiposity, other studies have reported different observations. Mice on a VAD diet for 10 weeks show increased adiposity [285]. More importantly in humans, low plasma VA status has been associated with overweight and obesity [286,287]. These divergent data warrant further research into the relationship between VA status and adiposity in animals.

Secondly, it has been reported that RA treatment induces lipolysis and depletes lipid storage in mature white adipocytes, which leads to weight loss in diet-induced obese mice [288]. All-*trans*-RA treatment also decreases white adipose tissue mass in healthy lean mice [289]. The anti-obesogenic effect of all-*trans*-RA may be mediated through the activation of PPARβ/δ and RAR, which are important factors in the upregulation of energy dissipation [288]. It is also hypothesized that all-*trans*-RA promotes the acquisition of brown adipose tissue-like properties in white adipocytes [289]. Indeed, all-*trans*-RA induces the expression of uncoupling protein 1 (UCP1), an mediator of adipose thermogenesis, in mouse white adipocytes, possibly via the activation of RARs [290]. However, all-*trans*-RA has no effect, or even inhibits, the expression of *UCP1* in human white adipocytes [290]. These conflicting results suggest that other retinoids besides RA may regulate energy metabolism in white adipose tissue. Interestingly, *Raldh1* deficiency has been shown to induce brown adipose tissue-like transcriptional program in white adipose tissue [291]. Furthermore, retinal can induce the expression of *Ucp1* mRNA and protein in white adipose tissue by activating RAR [291]. These data show that both retinal and RALDH1 are regulators of adaptive thermogenesis in white adipose tissue.

Thirdly, RA has distinct influences on different stages of adipocyte differentiation. In several mouse preadipocyte cell lines and 3T3-L1 cells, RA can block the preadipocyte differentiation through inhibiting the induction of PPARγ and CCAAT-enhancer-binding protein α (C/EBPα) [292]. It has been shown that cellular retinoic-acid binding protein II (CRABP II) mediates the effect of RA [293]. Interestingly, the inhibitory effect of RA on differentiation cannot be observed in the late stage of adipocyte differentiation due to the reduced RAR expression level [294]. Additionally, low doses of all-*trans*-RA potentiated the differentiation of Ob17 mouse pre-adipocytes [295].

9.4.2 VA and metabolism in brown adipose tissue

Brown adipose tissue, with the landmark expression of *UCP1*, is engaged in thermogenesis in mammals [296]. Feeding a VAD diet in mice reduced the expression of *Ucp* genes in their brown adipose tissue [297]. In contrast, retinol supplementation induced the *Ucp1* mRNA in rat brown adipocytes [211]. Additionally, in both cultured brown adipocytes and rodent brown adipose tissue, RA treatment stimulated thermogenesis by upregulating the expression of *Ucp1* [297-299]. This regulation is mediated through the RARE in the promoter of *Ucp1* gene [300]. It has been shown that all-*trans*-RA treatment also reduces the RARα and RXRα protein levels in mouse brown adipose tissue [301]. Collectively, these data provide an interesting mechanism by which VA and its metabolites regulate brown adipose tissue thermogenesis.

9.5 VA and metabolism in the skeletal muscle

The skeletal muscle is the largest organ in the body, which plays a critical role in the regulation of energy metabolism [302]. However, very limited research has been performed to investigate the effects of VA on the carbohydrate and protein metabolism in the skeletal muscle. In avian species, VA deficiency depletes the glycogen content in the pectoralis major muscle [303]. On the other hand, RA treatment of mouse myoblast C2C12 cells leads to increased glucose uptake possibly through the activation of AMP-activated protein kinase [304]. In addition, VA deficiency rats have lowered protein synthesis rate and increased proteolysis rate in the skeletal muscle [245,305]. This change in protein metabolism partly contributes to the body mass loss in the VA deficiency animals. Interestingly, the acute VA toxicity accelerates the myofibrillar protein breakdown without affecting the rate of protein synthesis, which may also lead to muscle wasting [306]. These data, though sparing, collectively demonstrate the involvement of VA in the regulation of glucose and protein metabolism in the skeletal muscle.

In terms of the lipid metabolism, VAD rats do not show significant change in the FA oxidation capacity in the skeletal muscle [257]. In contrast, RA treatment of mouse skeletal muscle dose-dependently increases the transcripts of genes that are involved in FA oxidation and thermogenesis [307]. Indeed, RA treatment and retinyl palmitate supplementation induce the expression of UCP3 in the mouse skeletal muscle [213,288].

Despite the different results observed between rats and mice, these data suggest that VA may increase the energy dissipation in the skeletal muscle.

10.Conclusion

VA is a crucial regulator of carbohydrate, protein and lipid metabolism in all of the major metabolic active organs. The manifold of the VA effects may be attributed to the roles of RA (or other VA metabolites) in regulating the expression of critical genes in different metabolic pathways. A lot of efforts and progresses have been made for the understanding of the actions of VA (RA) in different organs. We think that further investigations are warranted in the following areas: (1) the molecular mechanisms by which VA regulates the transcription of critical metabolic genes, such as *Gck*, *Pck1* and *Srebp-1c*, in different organs and tissues; (2) the interplay between VA and other hormones in the regulation of metabolic homeostasis; (3) the roles of VA in the regulation of macronutrients metabolism in the disease states, especially obesity, type 2 diabetes and other metabolic diseases. The findings in the abovementioned areas will not only help understand the effects of micronutrients on energy metabolism, but also help create new pharmaceutical strategies to combat metabolic diseases.

CHAPTER II. VITAMIN A AND FEEDING STATUSES MODULATE THE INSULIN-REGULATED GENE EXPRESSION IN PRIMARY RAT HEPATOCYTES

Abstract

Unattended hepatic insulin resistance predisposes individuals to dyslipidemia, type 2 diabetes and many other metabolic complications. The mechanism of hepatic insulin resistance at the gene expression level remains unrevealed. To examine the effects of vitamin A (VA), total energy intake and feeding conditions on the insulin-regulated gene expression in primary hepatocytes of Zucker lean (ZL) and fatty (ZF) rats, we analyze the expression levels of hepatic model genes in response to the treatments of insulin and retinoic acid (RA). We report that the insulin- and RA-regulated glucokinase, sterol regulatory element-binding protein-1c and cytosolic form of phosphoenolpyruvate carboxykinase expressions are impaired in hepatocytes of ZF rats fed chow or a VA sufficient (VAS) diet ad libitum. The impairments are partially corrected when ZF rats are fed a VA deficient (VAD) diet ad libitum or pair-fed a VAS diet to the intake of their VAD counterparts in non-fasting conditions. Interestingly in the pair-fed ZL and ZF rats, transient overeating on the last day of pair-feeding regimen changes the expression levels of some VA catabolic genes, and impairs the insulin- and RA-regulated gene expression in hepatocytes. These results demonstrate that VA and feeding statuses modulate the hepatic insulin sensitivity at the gene expression level.

1. Introduction

The liver is critical for glucose and lipid homeostasis, which is achieved partially through the regulation of hepatic genes expression in response to hormonal and nutritional stimuli [24,37]. The disturbance of these responses may lead to the development of metabolic diseases, including obesity and type 2 diabetes [24]. Even though the pathogenesis of these diseases has not been fully elucidated, insulin resistance is established as the key risk factor [308]. Current theory postulates that overnutrition triggers system inflammation, dysregulates lipid metabolism, and alters gastrointestinal microbiota, all of which may interplay and lead to impaired insulin action in the body [38].

The insulin-regulated hepatic metabolism is partially attributed to the regulation of hepatic genes expression. For instance, in primary rat hepatocytes, insulin induces the glucokinase (GCK, gene *Gck*) expression to promote glycolysis and suppresses the phosphoenolpyruvate carboxykinase (PEPCK-C, gene *Pck1*) expression to reduce gluconeogenesis [309,310]. Insulin also promotes hepatic lipogenesis via inducing sterol regulatory element-binding protein 1c (SREBP-1c, gene *Srebp-1c*) expression. SREBP-1c induces the expression of hepatic lipogenic genes, such as acetyl-coenzyme A carboxylase and fatty acid synthase [311]. In insulin resistant liver, insulin is unable to suppress the expression of gluconeogenic genes. But it is able to concurrently induce the expression of lipogenic genes [37]. This phenomenon demonstrates the coexistence of hyperglycemia and hyperlipidemia in the type 2 diabetic.

As an essential lipophilic micronutrient, vitamin A (VA, retinol) is implicated in the regulation of glucose and lipid metabolism [24]. Two stepwise cytosolic enzymatic reactions convert retinol into retinoic acid (RA, all-*trans* RA or 9-*cis* RA), which then enters the nucleus and modules gene expression through the activation of retinoid acid receptors and retinoid X receptors [127]. Recent reports by our group show that RA synergizes with insulin to induce the *Gck* and *Srebp-1c* expressions in primary rat hepatocytes [235,266]. RA attenuates the insulin-suppressed *Pck1* expression in the same cells [240]. These data suggest that micronutrient status can affect hepatic insulin sensitivity at the gene expression level. However, the roles of caloric intake and

micronutrient composition in the hepatic insulin resistance at the gene expression level have not been investigated.

Here, we chose Zucker lean (ZL) and ZF rats as insulin sensitive and resistant models, respectively, to investigate the effects of energy intake and VA status on the hepatic insulin sensitivity at the gene expression level. We demonstrate that VA deficiency partially corrects the impaired insulin-regulated gene expression in ZF primary hepatocytes. More importantly, transient overeating in ZL and ZF rats causes the impairment of insulin-regulated gene expression in their primary hepatocytes.

2. Materials and methods

2.1 Animals and rodent diets

Zucker rats (Harlan Laboratories) were bred and housed on a 12 hr light-dark cycle under constant temperature and humidity in the animal facility at University of Tennessee at Knoxville. Breeding pairs were kept on Teklad rodent chow (#8640, Harlan Laboratories, Indianapolis, IN). Weaned male ZL (fa/+ or +/+) and ZF (fa/fa) rats (21 days old) were fed experimental diets for 8 weeks before primary hepatocyte isolation. Synthetic VA sufficient (VAS, #5755, 22.1 IU/g VA) and VA deficient (VAD, #5822, 0 IU/g VA) diets were isocaloric diets from TestDiet (Richmond, VA). All procedures (Protocol #1256, #1863) were approved by the Institutional Animal Care and Use Committee at UTK.

2.2 Pair-feeding study.

Male ZL or ZF rats (VAD-AD group, and VAD ad libitum, 5 rats per group) had free access to the VAD diet and water for 56 days. The body mass and food intake were recorded every 2 days. Primary hepatocytes were isolated on Day 56. Two pair-feeding groups were set up to circumvent a potential caveat on the last day of pair-feeding. Since VAD animals consume significantly less diet than their VAS counterparts in ad libitum feeding condition [206], the VAS pair-fed rats would conceivably consume the last day's ration rapidly. This caveat would result in a fasting status in these rats and affect the analysis of insulin-regulated hepatic gene expression. Therefore, 10 rats with matching genotypes were paired up with rats in VAD-AD group according to weaning body mass. They were pair-fed the VAS diet for 55 days to the intakes of their VAD-AD

counterparts. During the course of pair-feeding, unfinished food pellets were rolled over to ensure that equal total calories were provided. The body mass and food intake of these rats were recorded daily. On Day 56, one group, VAS-PF-AD (VAS pair-feeding last day ad libitum), was allowed to have free access to the VAS diet to prevent fasting energy status. The other group, VAS-PF-4M (VAS pair-feeding last day 4 meals), was fed the VAS diet to the amount consumed by the VAD-AD group. One fourth of the ration was provided to VAS-PF-4M rats every 6 hrs, so that they remained non-fasted energy status till the end of the study. Before primary hepatocyte isolation, the tail tip whole blood glucose was measured using a LifeScan OneTouch® Ultramini glucometer (Milpitas, CA).

2.3 Primary hepatocyte isolation.

The primary hepatocytes were isolated according to previously described protocol [312]. The rat was euthanized by primary carbon dioxide asphyxiation, and then secondary cervical dislocation according to the protocol. A peristaltic pump with the flow rate of 10ml/min was set up to infuse about 120 ml liver perfusion buffer and 120 ml liver digestion buffer. A catheter connected to the pump was inserted into the portal vein. The inferior vena cava was punctured to allow the outflow of blood and buffers. The liver was then excised and put into a cell culture dish containing liver digestion buffer to remove connective tissues. The released hepatocytes were filtered through a 100 μm cell strainer and collected by 50×g centrifugation for 3 min. The hepatocytes were washed twice with high glucose DMEM containing 8% fetal bovine serum, 1% penicillin/streptomycin. Isolated hepatocytes were seeded on 60-mm collagen type I coated dishes at 2×10^6 cells per dish and incubated in high glucose DMEM containing 8% fetal bovine serum, 1% penicillin/streptomycin at 37˚C and 5% CO_2 for 3 hrs. The attached hepatocytes were washed once with PBS and pretreated in medium A (Medium 199 with 100 nM dexamethasone, 100 nM 3,3',5-triiodo-L-thyronine (T3), and 1% penicillin/streptomycin) containing 1 nM insulin at 37˚C and 5% CO_2 for 14-16 hrs.

2.4 Insulin and RA treatments, RNA extraction and real-time PCR.

The pretreated hepatocytes were washed once with PBS, and then treated for 6 hrs at 37˚C and 5% CO_2 with medium A containing indicated concentrations of insulin (0 nM to 100 nM) with or without 5 μM RA. The methods for total RNA extraction and cDNA

synthesis were described elsewhere [313]. The gene expression level was determined by real-time PCR with respective primer sets, and normalized to the mRNA level of ribosomal gene 36B4. The data were presented as either minus Δ cycle threshold (Ct) or the induction fold (ΔΔCt) for which the control treatment group was arbitrarily set as 1.

2.5 Statistical Analysis.

Statistical analyses were performed using SPSS 19.0 software. Student t-test was used to compare the means between two treatments. One-way ANOVA with LSD post-hoc test was used to compare the means of three or more treatments. Two-way ANOVA with Bonferroni's post-hoc test was used to determine the effects of diets and genotypes on hepatic gene expression. Data were presented as means ± SEM. The number of experiments indicates hepatocyte isolations from different animals. A p value less than 0.05 is considered statistically significant.

3. Results

3.1 The insulin- and RA-regulated *Gck, Pck1*, and *Srebp-1c* expressions were impaired in the primary hepatocytes from ZF rats fed chow ad libitum compared with ZL rats.

We compared the insulin-regulated gene expression in primary hepatocytes from ZL and ZF rats fed chow ad libitum. Insulin dose-dependently induced the *Gck* and *Srebp-1c* expressions (Figure 2-1A and C), and suppressed the *Pck1* expression (Figure 2-1B) in ZL hepatocytes. RA (5 μM) synergized with insulin to induce the *Gck* and *Srebp-1c* expressions (Figure 2-1A and C). The elevated *Pck1* level in the presence of RA was still lowered by insulin at 1 nM or higher (Figure 2-1B). Comparably in ZF hepatocytes, the fold inductions of *Gck* by insulin (marked by *) and RA + insulin (marked by #) at the corresponding concentrations were significantly lower than that in ZL hepatocytes (Figure 2-1A). The inductions of *Srebp-1c* by insulin (0.1 nM to 100 nM) and RA + insulin (0.1 nM to 100 nM) were abolished in ZF hepatocytes (Figure 2-1C). Additionally, the insulin-mediated suppression of *Pck1* was less profound in ZF hepatocytes compared with that in ZL hepatocytes (Figure 2-1B, marked by * and #). Furthermore, the expressions of liver type pyruvate kinase gene (*Pklr)* in primary hepatocytes from either ZL or ZF rats were not affected by insulin and RA treatments (Figure 2-1D). These data

Figure 2-1. Impaired insulin-regulated gene expression in primary hepatocytes isolated from ZF, but not ZL, rats fed chow ad libitum. ZL and ZF rats were fed standard chow for eight weeks before primary hepatocytes were harvested. The primary hepatocytes were incubated in medium A with increasing concentrations of insulin (0 nM to 100 nM) in the absence or presence of RA (5 μM) for 6 hrs. Total RNA was extracted, synthesized into cDNA, and then subjected to real-time PCR analysis for the expression levels of *Gck* (A), *Pck1* (B), *Srebp-1c* (C), and *Pklr* (D). The expression level of each gene transcript in ZL or ZF hepatocytes treated with vehicle control was arbitrarily set to 1. The data were expressed as fold induction. All $p<0.05$; for (A), a'<b'<c', a<b<c, d'<e', d<e; for (B), f'>g'>h', f>g>h, i'>j', i>k; for (C), l'<m'<n', m<o, p'<q', r<s using one-way ANOVA; * or # for comparing ZL or ZF at corresponding treatments using Student's t-test, respectively.

(A) ***Gck***

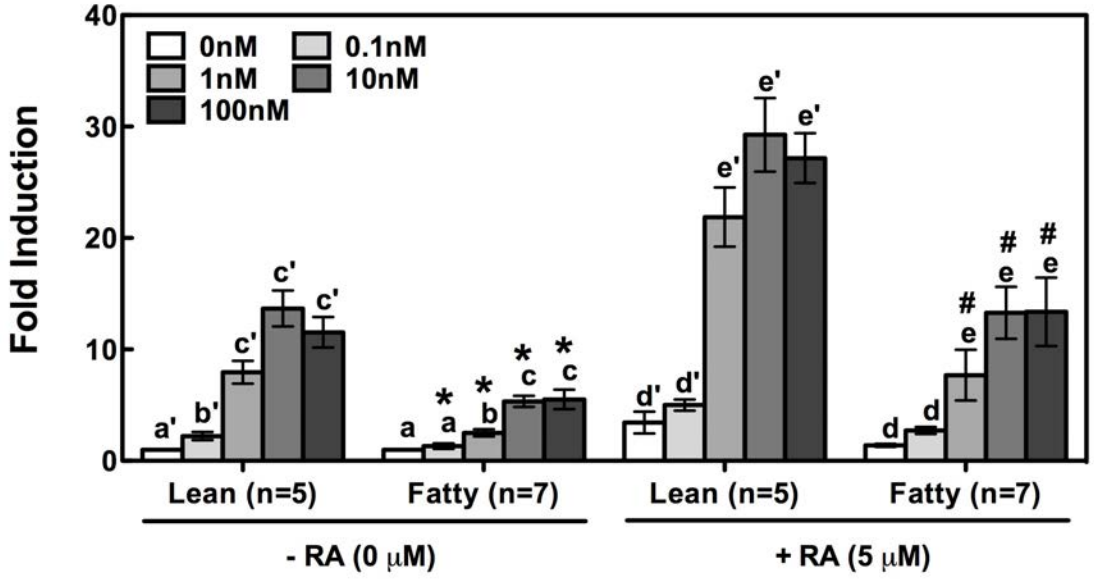

(B) ***Pck1***

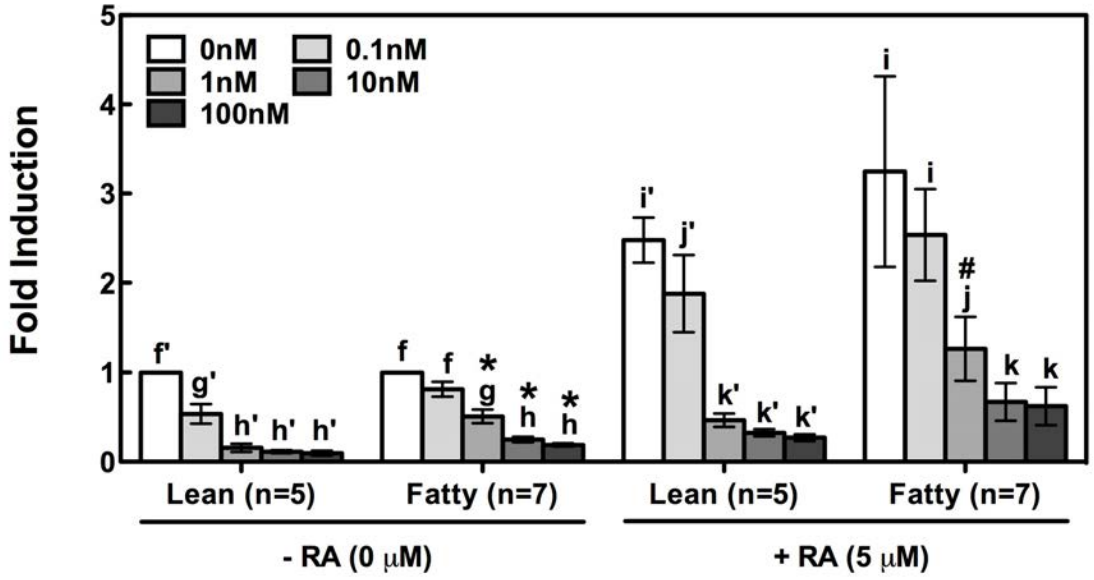

Figure 2-1

(C) ***Srebp-1c***

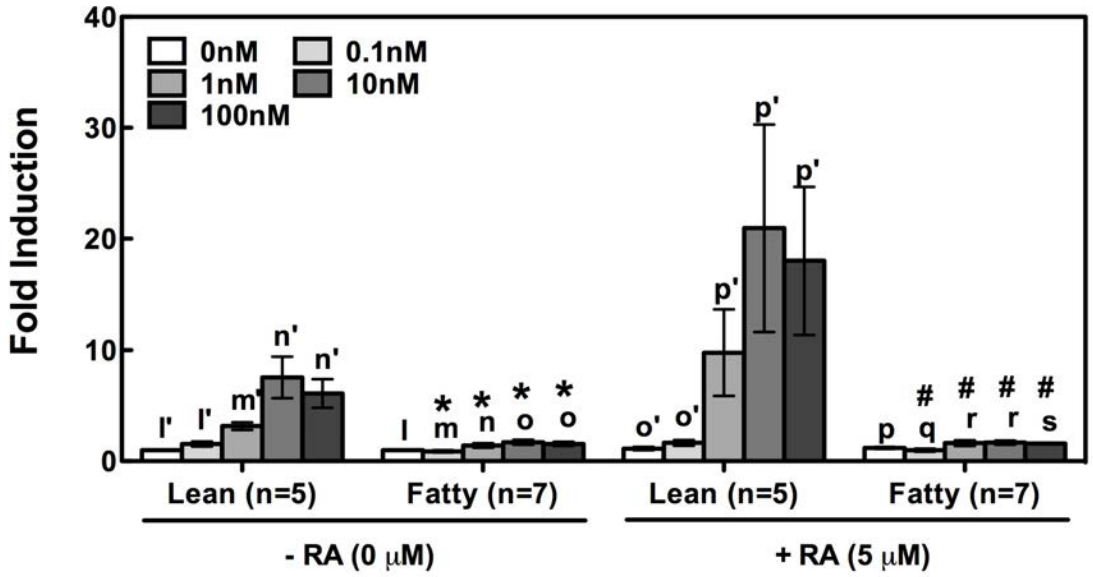

(D) ***Pklr***

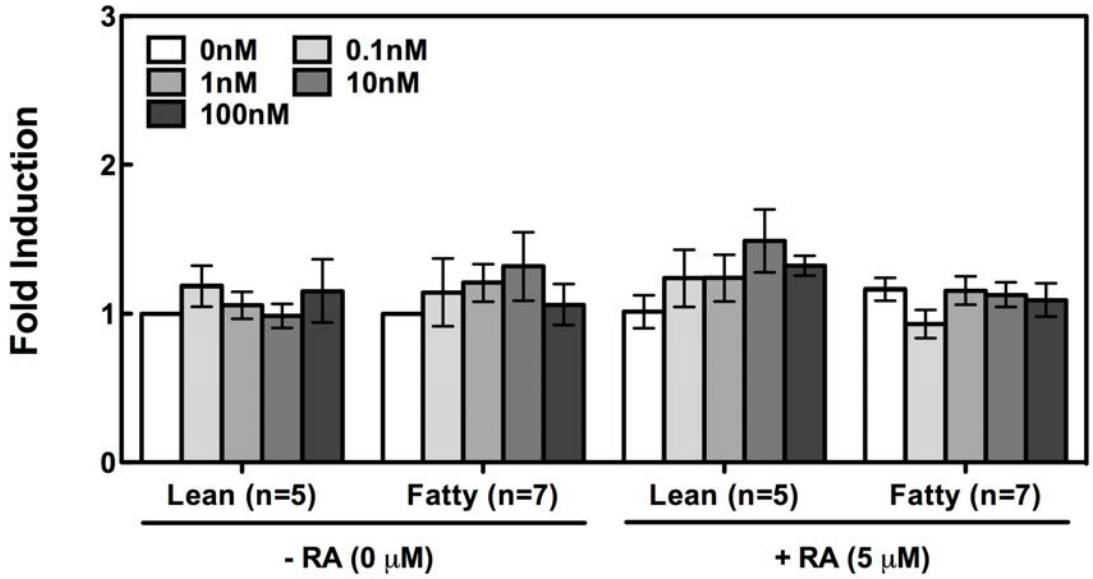

Figure 2-1 Continued

demonstrated the hepatic insulin resistance at the gene expression level in ZF rats fed chow ad libitum.

3.2 The insulin- and RA-regulated *Gck, Pck1* and *Srebp-1c* expressions were partially recovered in the primary hepatocytes from ZF rats fed a VAD diet ad libitum.

VA deficiency reduced food intake, body mass, plasma insulin and triglyceride levels in Zucker rats [312]. Hence, it may attenuate the impairment of the insulin-regulated gene expression in ZF rat hepatocytes. Figure 2-2A (left panel) showed that, in both VAD and VAS ZL primary hepatocytes, insulin dose-dependently induced the *Gck* expression (first and second column clusters), and RA synergized with insulin to induce its expression (third and fourth column clusters). The fold inductions of *Gck* expression by insulin (marked by *) or by RA + insulin (marked by #) in the VAS ZL hepatocytes were significantly higher than that in VAD ZL hepatocytes at the corresponding insulin concentrations. In comparison, the insulin-induced *Gck* expression was impaired in both VAD and VAS ZF hepatocytes regardless of RA (Figure 2-2A, right panel).

Insulin dose-dependently suppressed the *Pck1* expression in both VAD and VAS ZL hepatocytes (Figure 2-2B, left panel, first and second column clusters). RA induced the *Pck1* expression. Insulin at 1 nM to 100 nM suppressed the *Pck1* expression by over 90% in both VAD and VAS ZL hepatocytes (third and fourth column clusters). The net *Pck1* mRNA levels in the presence of RA were higher than that in the absence of RA. On the other hand, the insulin-suppressed *Pck1* expression was impaired in VAS ZF hepatocytes. Insulin at 0.1 nM or 1 nM only suppressed 10% or 40% of the *Pck1* expression level, respectively. However, in VAD ZF hepatocytes, the suppression of *Pck1* expression by 0.1 nM or 1 nM insulin was 40% or 60%, respectively, suggesting improved regulation by insulin (Figure 2-2B, right panel, first and second column clusters). RA induced the *Pck1* expression in VAD and VAS ZF hepatocytes (right panel, third and fourth column clusters). Insulin at 0.1 nM or 1 nM respectively suppressed the *Pck1* expression by 50% or 70% in VAD ZF hepatocytes, which was greater than 20% or 50% in VAS ZF hepatocytes.

Insulin dose-dependently induced the *Srebp-1c* expression, and RA synergized with insulin to induce its expression in both VAD and VAS ZL hepatocytes (Figure 2-2C, left

Figure 2-2. The impaired insulin-regulated gene expression in primary hepatocytes from ZF rats was partially recovered in rats fed a VAD diet for 8 weeks. ZL and ZF rats were fed either a VAS or VAD diet for 8 weeks. Primary hepatocytes were isolated from rats in ad libitum. Cells were incubated in medium A with increasing concentrations of insulin (0 nM to 100 nM) in the absence or presence of RA (5 μM) for 6 hrs. Total RNA was extracted, synthesized into cDNA, and then subjected to real-time PCR analysis for the expression levels of *Gck* (A), *Pck1* (B), and *Srebp-1c* (C). The data were expressed as fold induction. The gene transcript levels from the no treatment group (0 nM insulin, no RA) for both ZL and ZF were arbitrarily set to 1. All $p<0.05$; for (A), a<b<c, d<e<f, g<h<i, j<k<l, m<o, p<r/s/t, q<s/t, r<t, x<y; for (B), a'>b'>c', d'>e'>f', g'>h'>i, j'>k'>l', m'>n', o'>q'/r', p'>r', s'>t'>u', v'>x'/y', w'>y'; for (C), a"<b"<c", d"<e"<f", h"<i"<j", k"<m", n"<p", q"<s", using one-way ANOVA. * or # for comparing ZL and ZF at corresponding treatments using Student's t-test, respectively.

(A) *Gck* - ZL

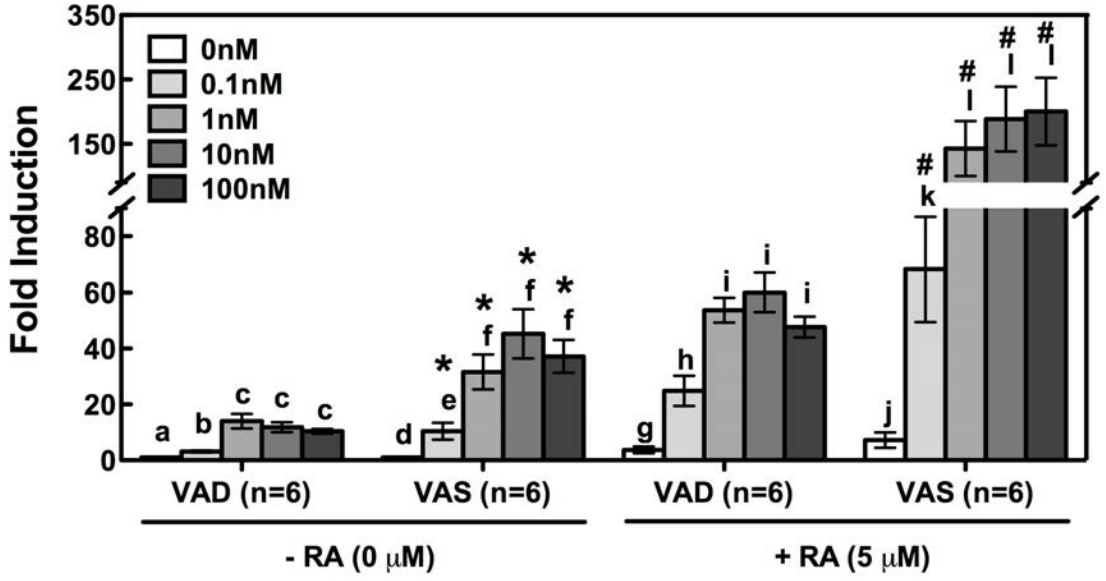

ZF

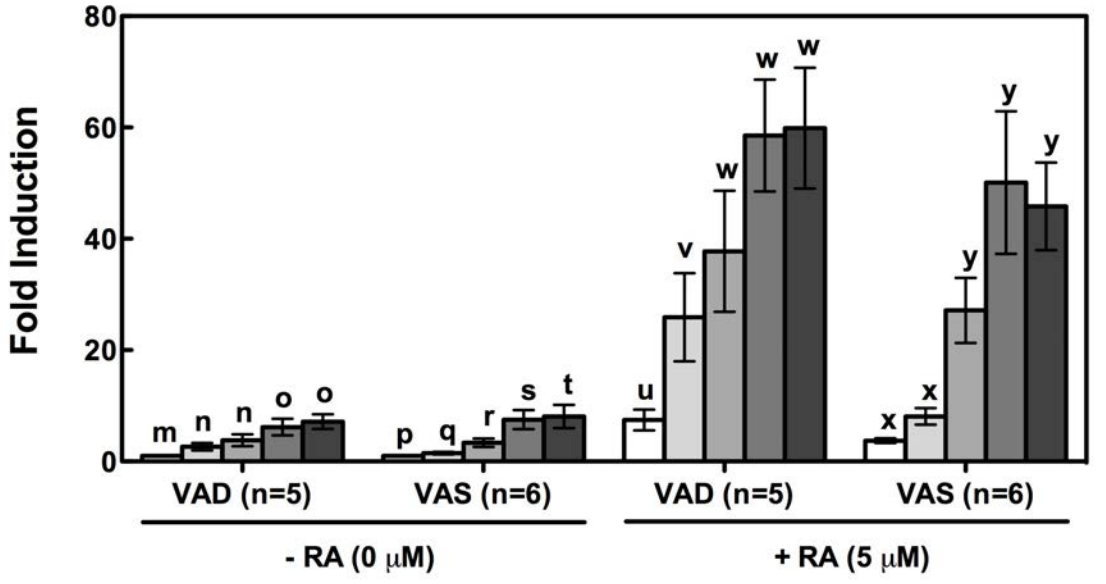

Figure 2-2

(B) *Pck1* - ZL

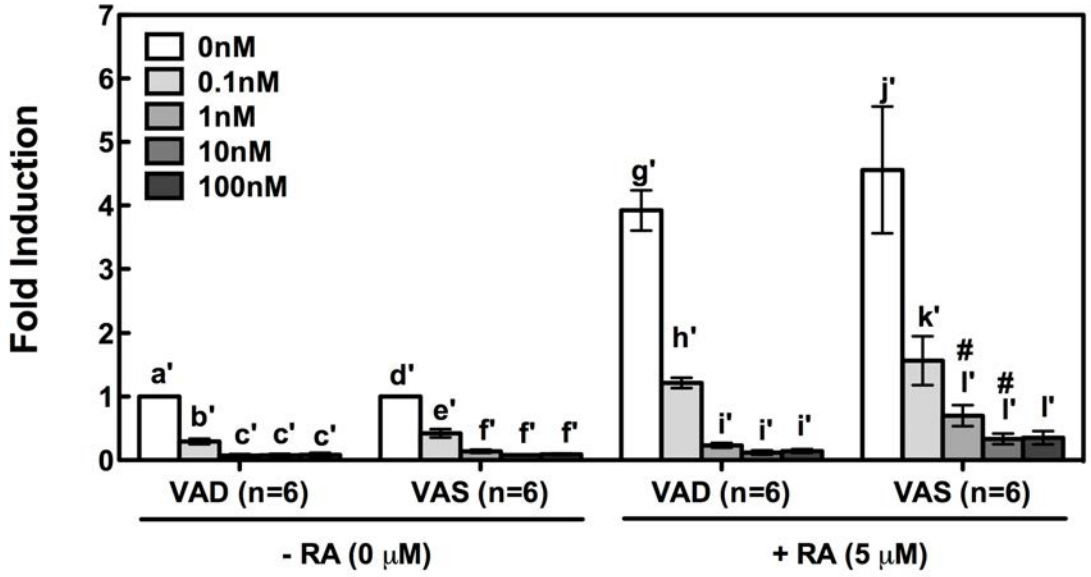

ZF

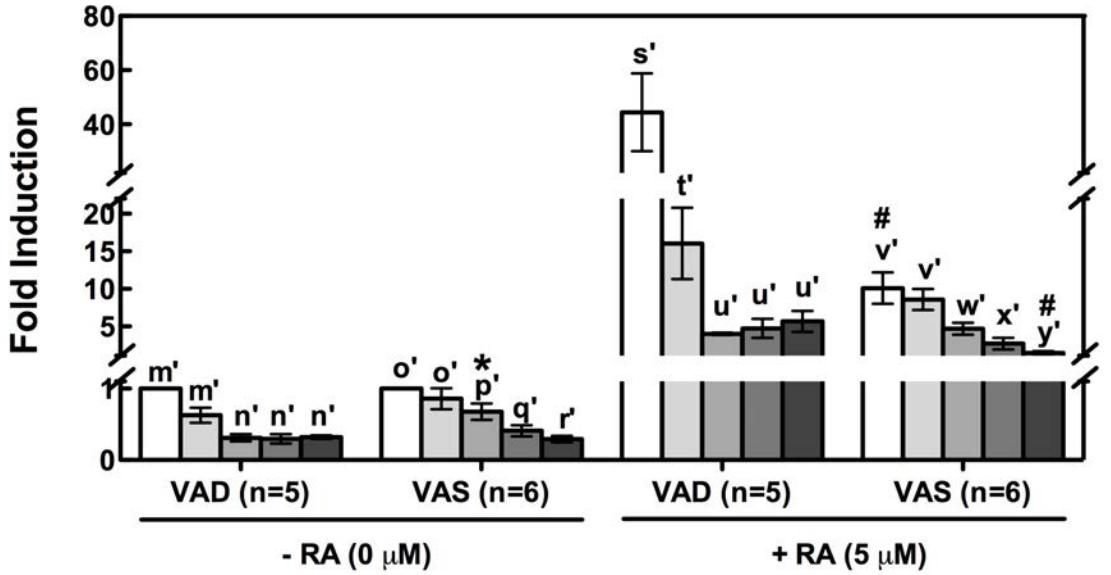

Figure 2-2 Continued

(C) *Srebp-1c* - ZL

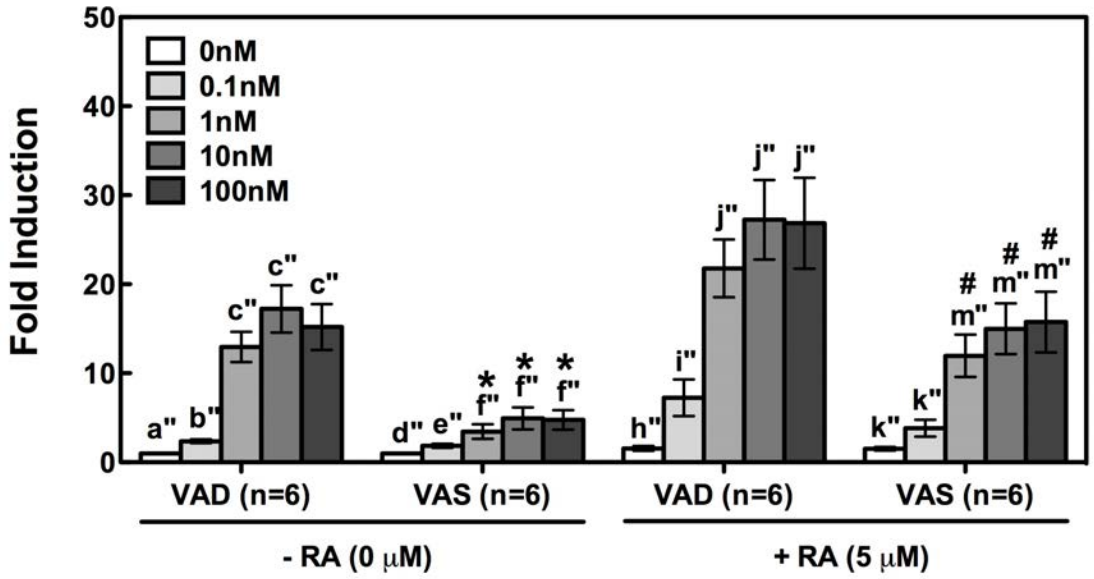

ZF

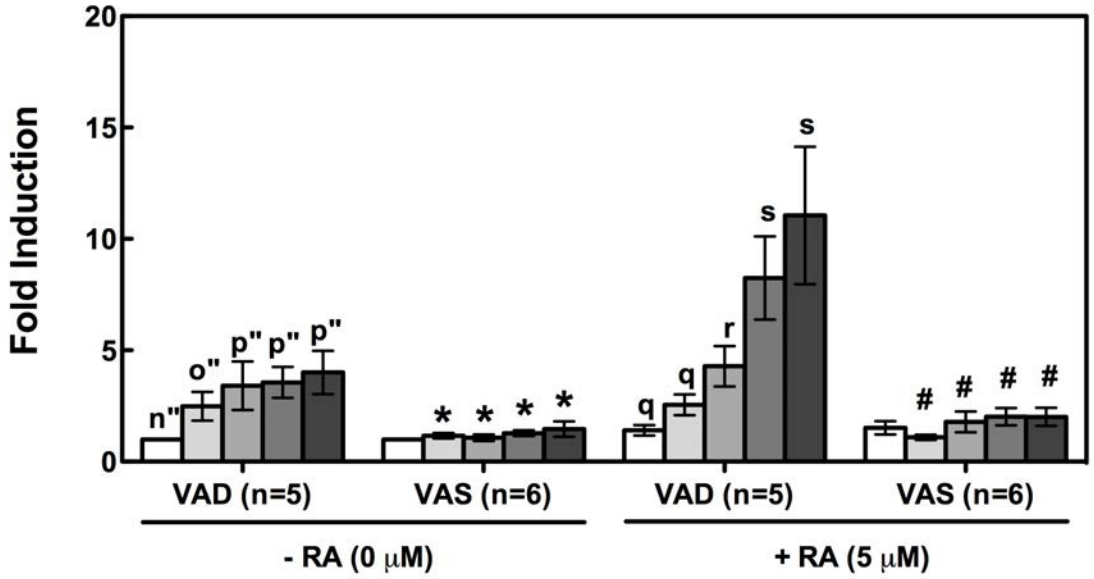

Figure 2-2 Continued

panel). The fold inductions of *Srebp-1c* expression by insulin (marked by *) or by insulin and RA (marked by #) in VAS ZL hepatocytes were significantly lower than that in VAD ZL hepatocytes. In VAS ZF hepatocytes, the insulin-induced *Srebp-1c* expression in the absence or presence of RA was abolished (Figure 2-2C, right panel). Interestingly in VAD ZF hepatocytes, insulin (1 nM to 100 nM) partially regained the ability to induce the *Srebp-1c* expression, showing improved regulation (first and third cluster).

3.3 ZL or ZF rats pair-fed the VAS diet tended to overeat when sufficient amount of diet was provided.

Rats on the VAD diet reduced food intakes at around 5 weeks after weaning [206]. To determine how total and acute food intakes affect insulin-regulated hepatic gene expression, an 8-week pair-feeding experiment was designed. Rats were divided into three groups, VAD-AD, VAS-PF-AD and VAS-PF-4M (Figure 2-3A, see Materials and Methods for detail). Figure 2-3B shows that VAS-PF-AD ZL and ZF rats ingested 54% and 112% more food on the last day than VAD-AD ZL and ZF rats did, respectively, demonstrating the overeating of VAS-PF-AD rats. The overeating of VAS-PF-AD rats did not significantly increase the total caloric intake over the entire pair-feeding period compared to VAD-AD and VAS-PF-4M counterparts (Figure 2-3C). Correspondingly, VAS-PF-AD ZL and ZF rats gained 4% and 6% of body mass on the last day, respectively (Figure 2-3D). Before sacrifice, the tail tip whole blood glucose levels of VAS-PF-AD ZF rats were significantly higher than those of VAD-AD and VAS-PF-4M rats (Figure 2-3E).

3.4 ZL and ZF rats pair-fed the VAS diet had higher body mass and feed efficiency than their VAD fed counterparts after the reduction of food intake.

During the 56-day pair-feeding regimen, the two-day food intake of VAD-AD ZL rats gradually increased from ~10 g initially to ~40 g on days 33-34, and kept relatively stable until days 41-42 (Figure 2-4A, left panel). As anticipated, the food intake then started to decline until the end of the dietary manipulation. The two-day food intake of VAD-AD ZF rats quickly rose from ~10 g initially to ~60 g on days 17-18, leveled off between days 20 to 34, started to decline on days 35-36, reached ~30 g on days 47-48, and leveled off again until the end of the dietary manipulation (right panel). During the same period, all VAS pair-fed ZL and ZF rats received the same amount of the isocaloric VAS diet to

Figure 2-3. VAS-PF-AD ZL and ZF overate on the last day when sufficient VAS diet was provided. (A) The schematic graph of the setup for the pair-feeding regime. VAD ad libitum (VAD-AD, n=5), VAS pair-feeding last day ad libitum (VAS-PF-AD, n=5), VAS pair-feeding last day 4 meals (VAS-PF-4M, n=5) (B) Tail tip whole blood glucose from ZL and ZF rats before sacrifice. Each circle represents a value from an individual animal. The bars represent mean ± S.E.M. * Indicates $p<0.05$ using one-way ANOVA with LSD post-hoc test. (C) The accumulative food intake for ZL and ZF rats over 56 days of pair-feeding regime. (D) The food intake and (E) body mass change for ZL and ZF rats on day 56 of the pair-feeding regime. * Indicates $p<0.05$ using one-way ANOVA with LSD post-hoc test.

(A)

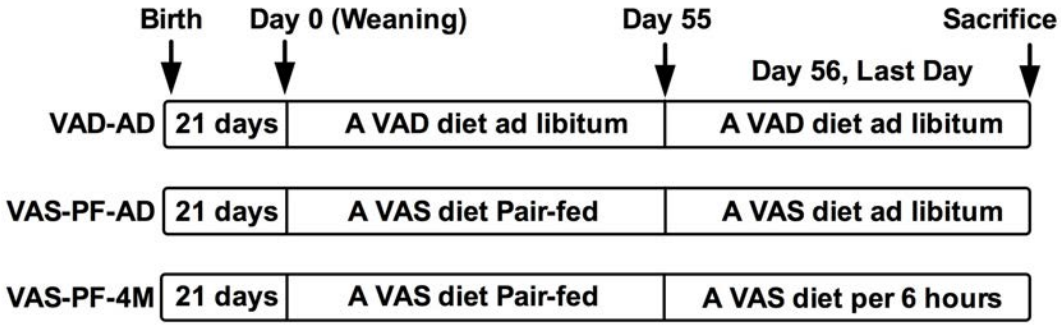

(B)

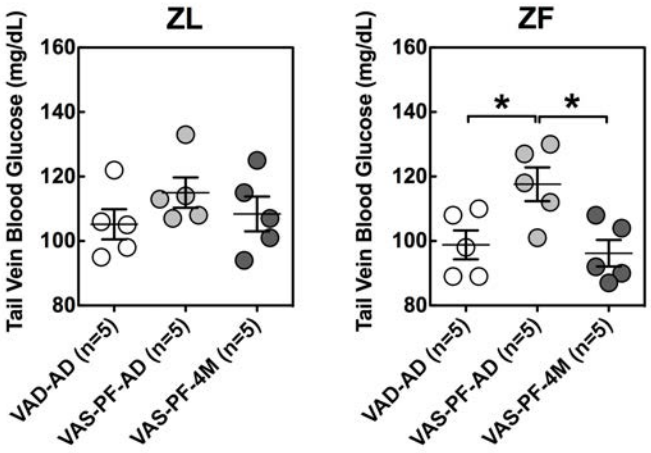

(C)

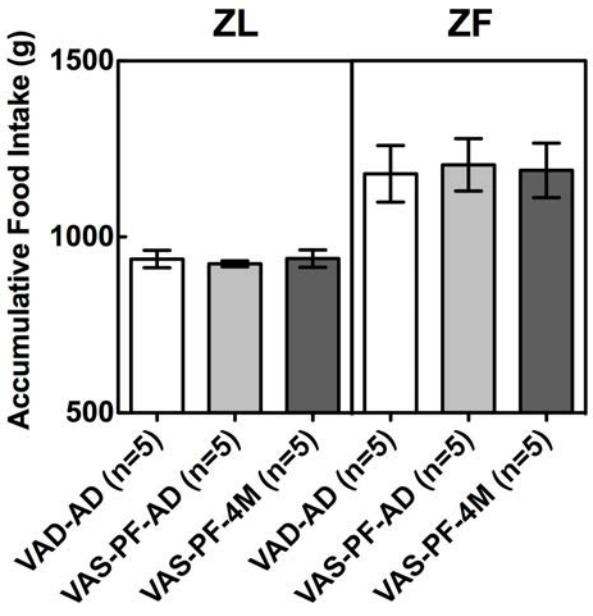

Figure 2-3

(D)

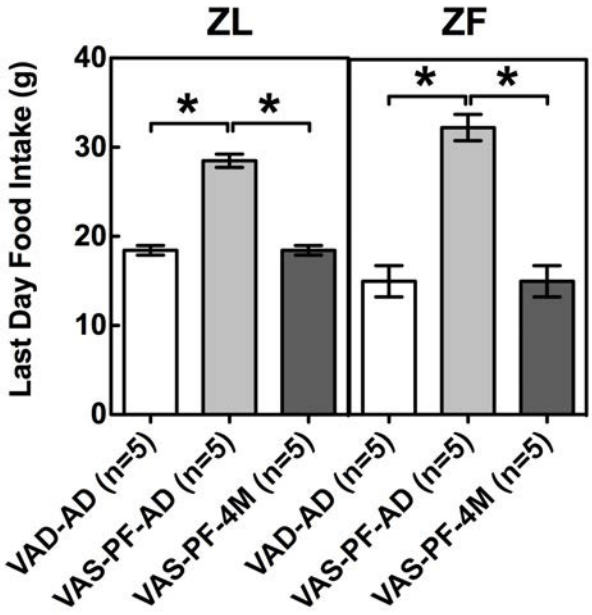

(E)

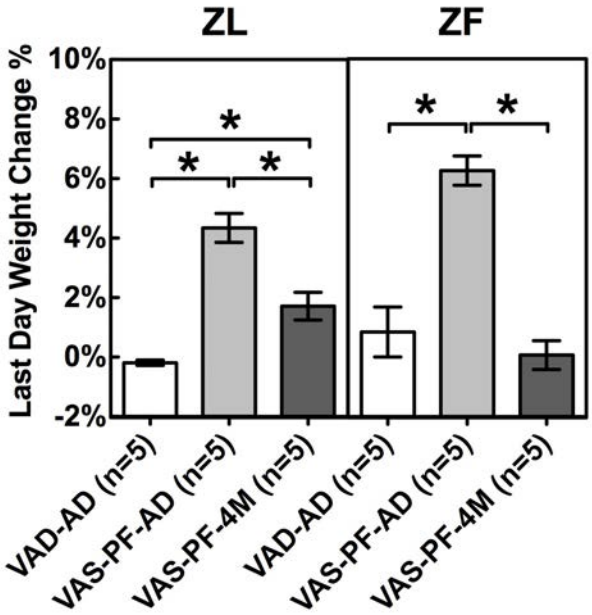

Figure 2-3 Continued

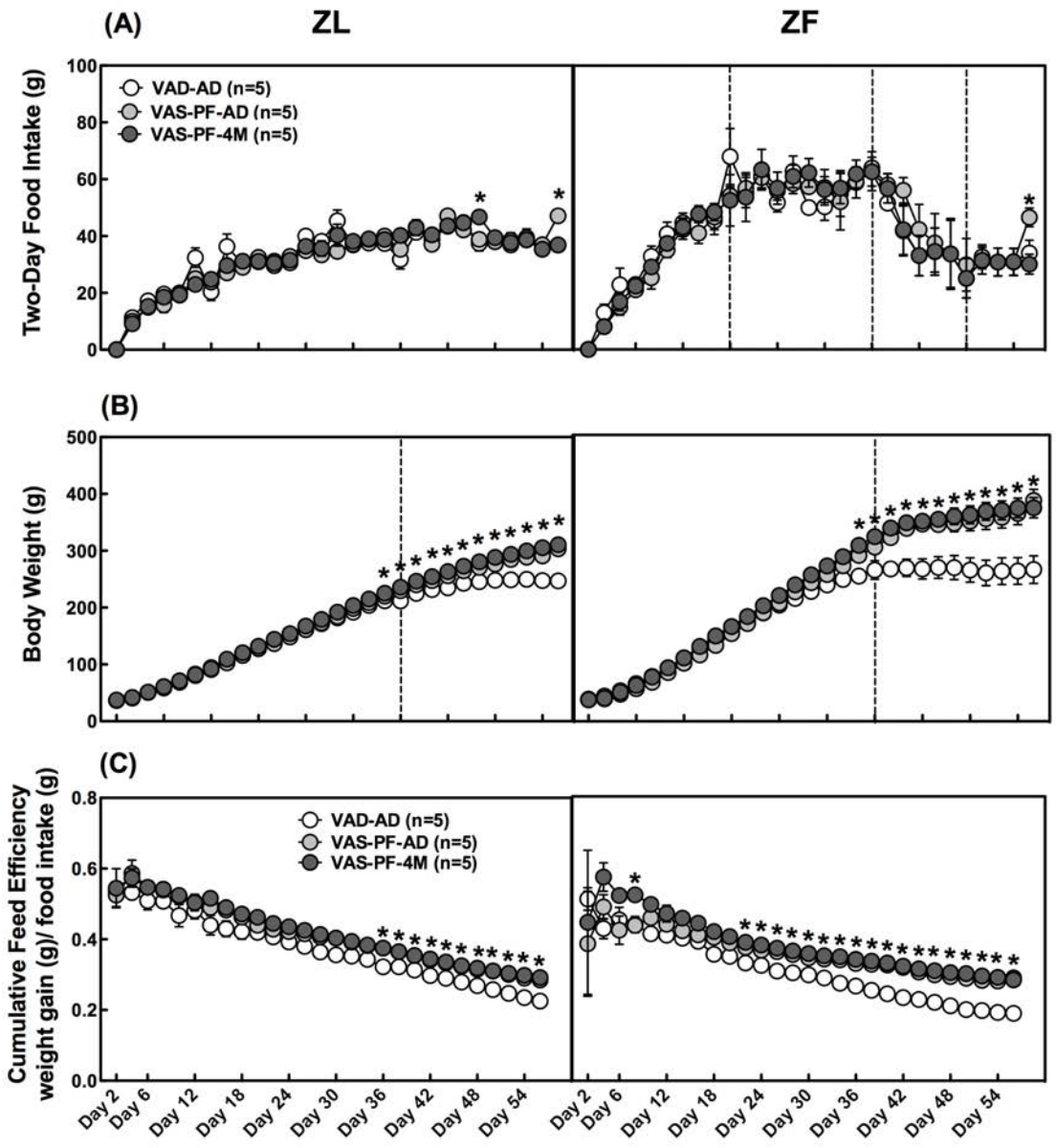

Figure 2-4. The food intake, body mass and cumulative feed efficiency over 56 days of dietary manipulation. (A) Two-day food intake of ZL and ZF on VAD ad libitum (VAD-AD, n=5), VAS-Pair-feeding Last Day ad libitum (VAS-PF-AD, n=5), VAS-Pair-feeding Last Day 4 meals (VAS-PF-4M, n=5) (B) Body mass of ZL and ZF on VAD AD, VAS-PF AD and VAS-PF 4M. (C) Cumulative feed efficiency (unit weight gain per unit diet consumed) of ZL and ZF on VAD-AD, VAS-PF-AD and VAS-PF-4M. * Indicates $p<0.05$ using one-way ANOVA with LSD post-hoc test.

match the energy intake of VAD-AD rats. The body mass of VAD-AD ZL and ZF rats ceased to increase after 36 days of dietary manipulation (Figure 2-4B). From day 34, the body mass of VAD-AD ZL or ZF rats was significantly lower than that of VAS-PF ZL or ZF rats, respectively (marked by *). Furthermore, the cumulative feed efficiency of all three groups decreased over time. However, VAS-PF ZL or ZF rats had significantly higher feed efficiency than VAD-AD ZL or ZF rats after 36 or 22 days, respectively (Figure 2-4C).

3.5 Transient overeating impaired the insulin-induced *Gck* expression in the primary hepatocytes of VAS-PF-AD ZL and ZF rats.

In ZL hepatocytes, insulin dose-dependently induced the *Gck* expression (Figure 2-5A). Without or with RA, the fold inductions by insulin in VAS-PF-AD ZL hepatocytes were significantly lower than that in VAD-AD hepatocytes (marked by *) and VAS-PF-4M ZL hepatocytes (marked by $), suggesting an impaired insulin regulation. Additionally, the fold inductions by insulin in VAD-AD ZL hepatocytes were lower than that of VAS-PF-4M ZL hepatocytes without or with RA (marked by #). These results match the data shown in Figure 2-2A and indicate that VA status of ZL rats affects the insulin-stimulated *Gck* expression in their hepatocytes.

In ZF hepatocytes, insulin dose-dependently induced the *Gck* expression regardless of RA (Figure 2-5B). Without RA, the fold inductions by insulin (1 and 10 nM) in VAS-PF-AD ZF hepatocytes were significantly lower than that in VAS-PF-4M ZF hepatocytes (Figure 2-5B, left panel, marked by $). With RA (Figure 2-5B, right panel), the fold inductions by insulin in VAS-PF-AD ZF hepatocytes were significantly lower than that in VAD-AD (0.1 nM to 100 nM, marked by *) and VAS-PF-4M (1 nM to 100 nM, marked by $) ZF hepatocytes. These data demonstrate the impairment of the insulin-induced *Gck* expression in VAS-PF-AD ZF hepatocytes.

3.6 The insulin-suppressed *Pck1* expression was partially impaired in primary hepatocytes of VAS-PF-AD ZL rats compared with VAD-AD and VAS-PF-4M ZL rats.

In VAD-AD and VAS-PF-4M ZL hepatocytes, insulin at 0.1 nM suppressed *Pck1* expression of by 60% and 70%, respectively (Figure 2-6A). The insulin-mediated suppression reached over 90% at 1 nM to 100 nM (left panel). In VAS-PF-AD ZL

Figure 2-5. Insulin-induced *Gck* expression was attenuated in hepatocytes from VAS-PF-AD, but not VAS-PF-4M rats. The primary hepatocytes were treated by insulin (0 nM to 100 nM) with or without RA (5 μM) in medium A for 6 hrs. The expression levels of *Gck* in ZL hepatocytes (A) and ZF hepatocytes (B) were determined by real-time PCR analysis, and the data were expressed as fold inductions. The gene transcript levels from the no treatment group (0 nM insulin, no RA) for both ZL and ZF were arbitrarily set to 1. All $p<0.05$; for (A), a<b<c, a'<b'<c', a"<b"<c", d<e<f, d'<f'/g', e'<g', d"< e"<f"; for (B), h<i<j, h'<i', h"<i"<j", k<l<m, j'<k'<l', k"<i"<m", using one way ANOVA. *, #, and $ for comparing the effects of dietary manipulations at any treatment using one way ANOVA

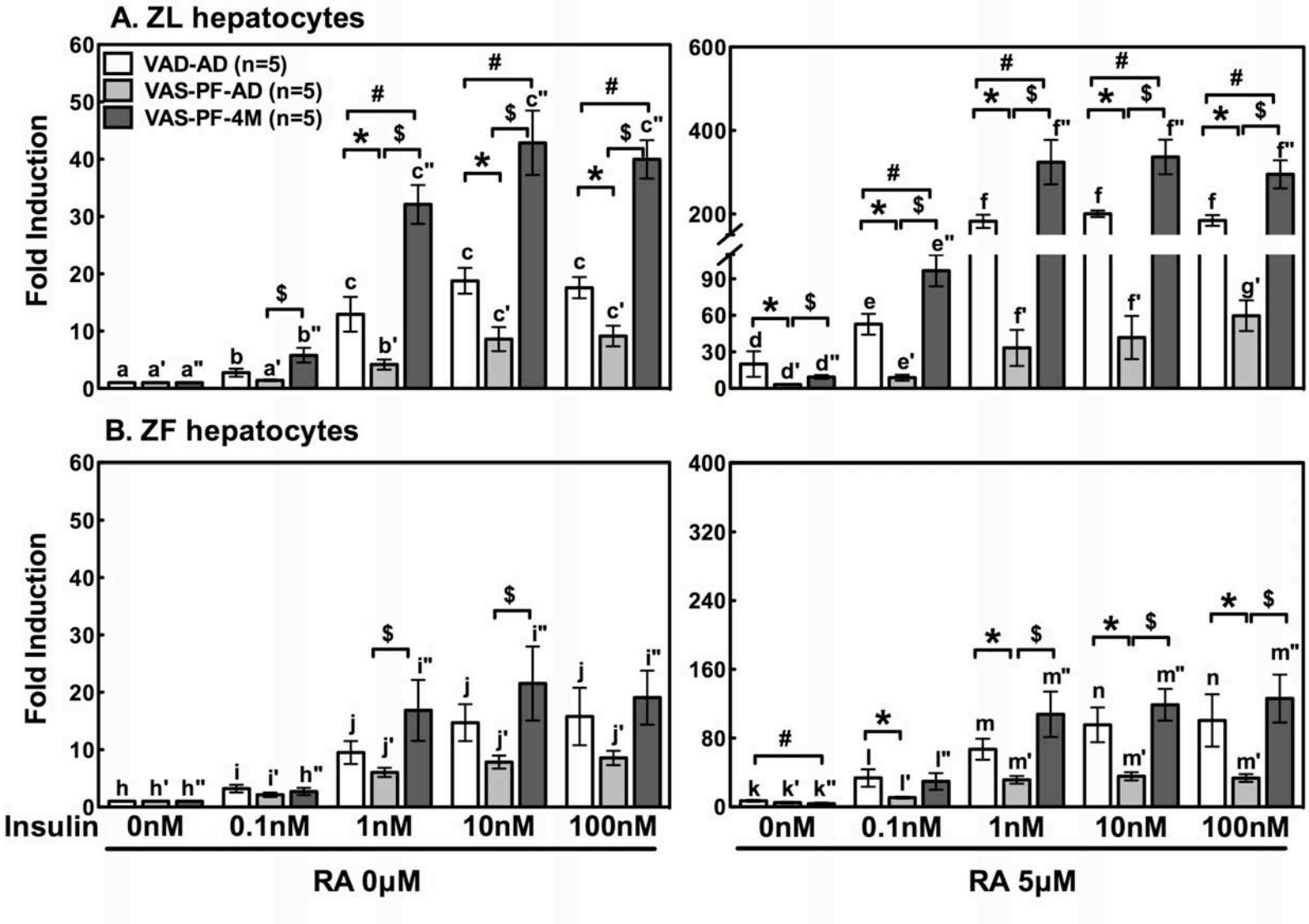
A. ZL hepatocytes
VAD-AD (n=5)
VAS-PF-AD (n=5)
VAS-PF-4M (n=5)
Fold Induction
B. ZF hepatocytes
Fold Induction
Insulin
0nM
0.1nM
1nM
10nM
100nM
RA 0μM
RA 5μM

Figure 2-6. Transient overfeeding of VAS diet impaired insulin-suppressed *Pck1* expression in hepatocytes of VAS-PF-AD ZL, but not ZF, rats. The primary hepatocytes were treated by insulin (0 nM to 100 nM) with or without RA (5 μM) in medium A for 6 hrs. The expression levels of *Pck1* in ZL hepatocytes (A) and ZF hepatocytes (B) were determined by real-time PCR analysis, and the data were expressed as fold inductions. The gene transcript levels from the no treatment group (0 nM insulin, no RA) for both ZL and ZF were arbitrarily set to 1. All $p<0.05$; for (A), a>b>c, a'>c', a">b">c", d>e>g, d>f, d'>f'/g', e'>g', d">e">f">g"; for (B), h>i, h'>i'>j', h">i">j", k>l, k'>l'>m', k">l", using one way ANOVA. *, #, and $ for comparing the effects of dietary manipulations at any treatment using one way ANOVA.

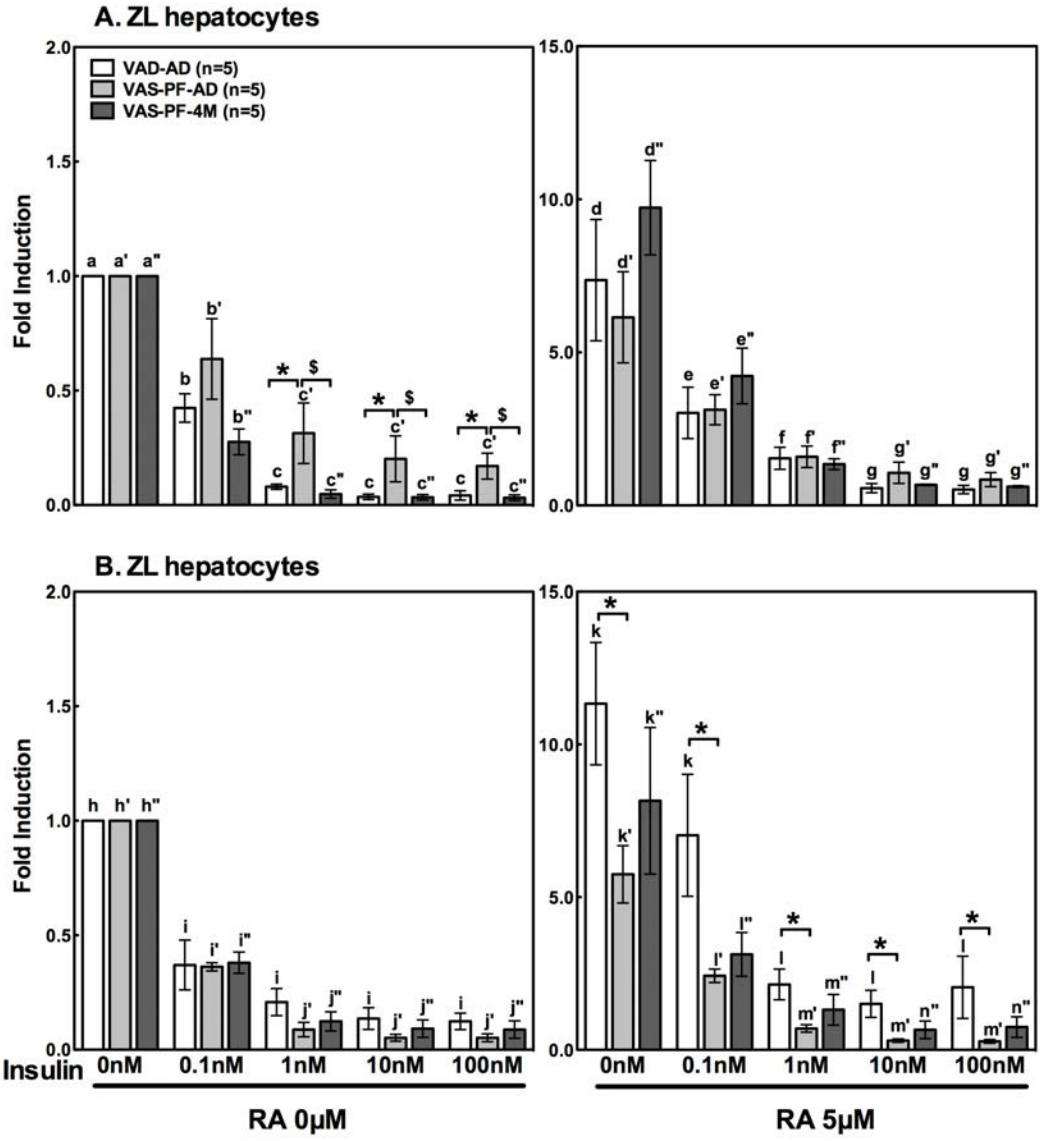
A. ZL hepatocytes
VAD-AD (n=5)
VAS-PF-AD (n=5)
VAS-PF-4M (n=5)
Fold Induction
B. ZL hepatocytes
Fold Induction
Insulin
0nM
0.1nM
1nM
10nM
100nM
RA 0μM
RA 5μM

hepatocytes, the *Pck1* expression levels in the presence of 1 nM to 100 nM insulin were significantly higher than that in VAD-AD and VAS-PF-4M ZL hepatocytes (marked by * and $, respectively). In the presence of RA, insulin at 0.1 nM to 100 nM reduced the elevated *Pck1* mRNA levels in all three groups of ZL hepatocytes (Figure 2-6A, right panel).

For ZF hepatocytes, insulin at 0.1 nM to 100 nM significantly suppressed the *Pck1* expression in VAD-AD, VAS-PF-AD and VAS-PF-4M groups (Figure 2-6B, left panel). With RA, insulin reduced the elevated *Pck1* mRNA levels in VAS-PF-AD (0.1 nM to 100 nM), VAD-AD (1 nM to 100 nM) and VAS-PF-4M (1 nM to 100 nM) ZF hepatocytes (right panel). Interestingly, the *Pck1* expression levels in VAS-PF-AD ZF hepatocytes were significantly lower than those in VAD-AD ZF hepatocytes at every concentration (marked by *).

3.7 The insulin-induced *Srebp-1c* expression was impaired by transient overeating in hepatocytes of VAS-PF-AD ZL and ZF rats.

In VAD-AD and VAS-PF-4M ZL hepatocytes, insulin at 0.1 nM to 100 nM induced the *Srebp-1c* expression with or without RA (Figure 2-7A). The fold inductions of *Srebp-1c* by insulin (1 nM to 100 nM) and insulin + RA (10 nM to 100 nM) in VAS-PF-AD ZL hepatocytes were significantly lower than that in VAD-AD (marked by *) and VAS-PF-4M ZL (marked by $) ZL hepatocytes at the corresponding treatments.

In VAD-AD and VAS-PF-4M ZF hepatocytes, insulin at 1 nM to 100 nM induced the *Srebp-1c* expression with or without RA (Figure 2-7B). In contrast, the insulin-mediated inductions of *Srebp-1c* expression were abolished in VAS-PF-AD ZF hepatocytes regardless of RA. As a result, the fold inductions in VAS-PF-AD ZF hepatocytes were significantly lower than that in VAD-AD (marked by *) and VAS-PF-4M ZF (marked by $) hepatocytes. These data demonstrate that the transient overeating of VAS-PF-AD rats impairs the insulin-induced *Srebp-1c* expression in their hepatocytes.

3.8 Dietary manipulation and VA status regulated the expression levels of genes for VA metabolism in hepatocytes from ZL and ZF rats.

To understand the impact of transient overeating on the hepatic VA metabolism, we analyzed the expression levels of key enzymes for VA metabolism and RA responses in all three groups of ZL and ZF hepatocytes. As shown in Figure 2-8A, the expression level

Figure 2-7. Transient overfeeding of VAS diet impaired insulin-induced *Srebp-1c* expression in hepatocytes of VAS-PF-AD ZL and ZF rats. The primary hepatocytes were treated by insulin (0 nM to 100 nM) with or without RA (5 μM) in medium A for 6 hrs. The expression levels of *Srebp-1c* in ZL hepatocytes (A) and ZF hepatocytes (B) was determined by real-time PCR analysis, and the data was expressed as fold induction. The gene transcript levels from the no treatment group (0 nM insulin, no RA) for both ZL and ZF were arbitrarily set to 1. All $p<0.05$; for (A), a<b<c<d, a'<b', a"<b"<c", e<f, c'<g'/f', d'<f', d"<e"<f"; for (B), g<h, g"<i"/j", h"<j", i<k/l, j<l, h'<l', k"<l", using one way ANOVA. *, #, and $ for comparing the effects of dietary manipulations at any treatment using one way ANOVA.

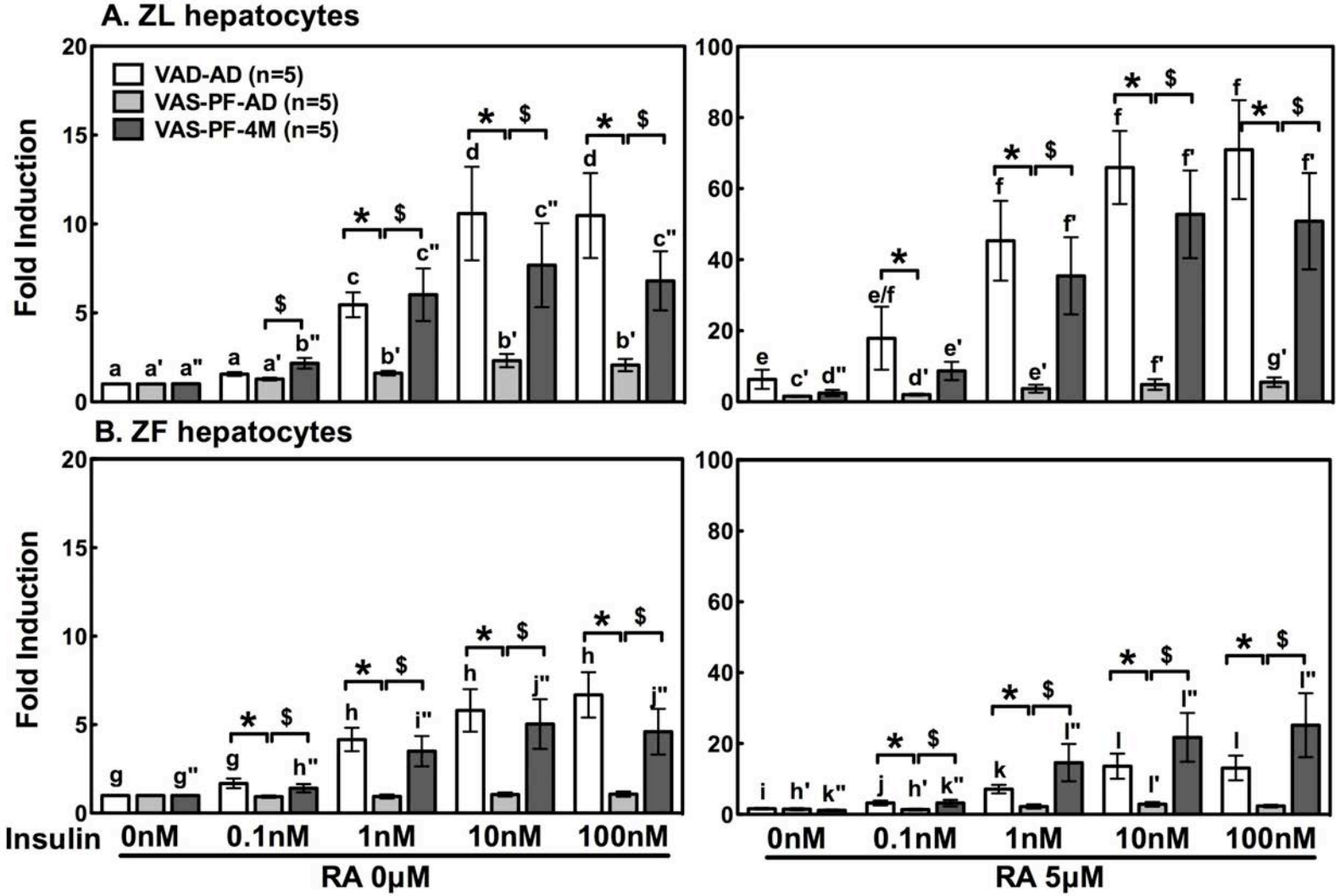
A. ZL hepatocytes
VAD-AD (n=5)
VAS-PF-AD (n=5)
VAS-PF-4M (n=5)
Fold Induction
B. ZF hepatocytes
Fold Induction
Insulin
0nM
0.1nM
1nM
10nM
100nM
RA 0μM
RA 5μM

Figure 2-8. Differential expression levels of indicated transcripts for vitamin A metabolism in the primary hepatocytes of ZL and ZF rats. The expression levels of *Rbpr2* (A), *Rdh2* (B), *Raldh1* (C), *Raldh4* (D), *Cyp26a1* (E), and *Rarb* (F) were determined by real-time PCR in the cultured primary hepatocytes receiving no treatment. The data were expressed as -ΔCt (36B4-interest gene). All $p<0.05$; *, #, and $ for comparing the effects of dietary manipulation variables on gene transcript levels using two-way ANOVA with Bonferroni's post-hoc test; a>b, and c>d, using Student's t-test to compare ZL with ZF with the corresponding dietary manipulation.

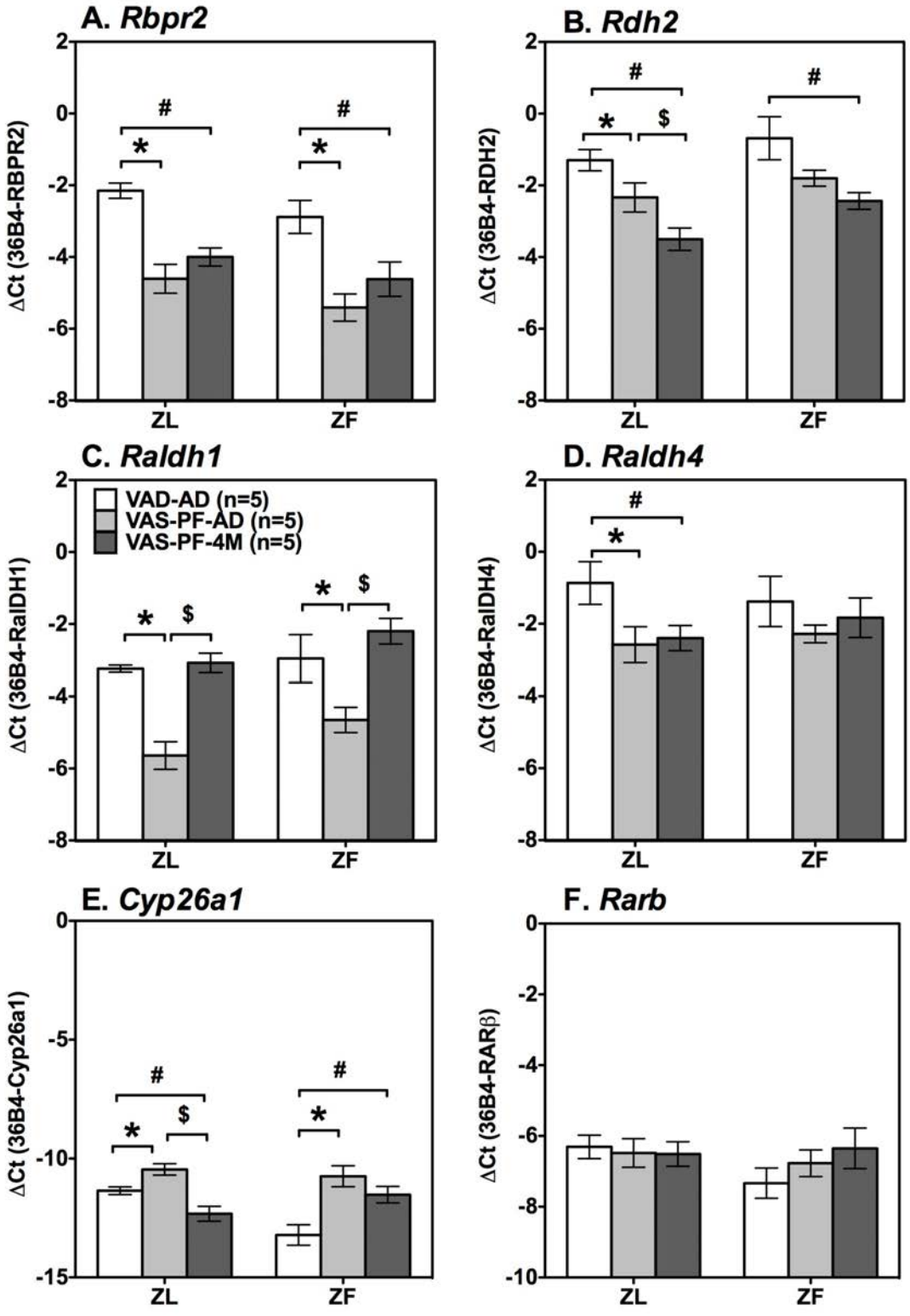
A. Rbpr2
ΔCt (36B4-RBPR2)
B. Rdh2
ΔCt (36B4-RDH2)
C. Raldh1
ΔCt (36B4-RalDH1)
VAD-AD (n=5)
VAS-PF-AD (n=5)
VAS-PF-4M (n=5)
D. Raldh4
ΔCt (36B4-RalDH4)
E. Cyp26a1
ΔCt (36B4-Cyp26a1)
F. Rarb
ΔCt (36B4-RARβ)
ZL
ZF

of RBP4 receptor 2 (*Rbpr2*), a proposed liver-specific retinol transporter [111], was higher in VAD-AD hepatocytes than that in VAS-PF-AD and VAS-PF-4M hepatocytes (both ZL and ZF). RDH2 catalyzes the reversible conversion between retinol and retinal[100]. In Figure 2-8B, the expression level of *Rdh2* in VAD-AD ZL or ZF hepatocytes was higher than that in VAS-PF-4M ZL or ZF hepatocytes, respectively. The expression level of *Rdh2* in VAS-PF-AD ZL hepatocytes was higher than that in VAS-PF-4M, but lower than that in VAD-AD ZL hepatocytes.

Both RALDH1 and RALDH4 are involved in the irreversible conversion of retinal into RA [100]. The *Raldh1* expression level in VAS-PF-AD ZL or ZF hepatocytes was significantly lower than that in VAD-AD and VAS-PF-4M ZL or ZF hepatocytes, respectively (Figure 2-8C). The *Raldh4* expression level in VAD-AD ZL hepatocytes was higher than that in VAS-PF-AD and VAS-PF-4M groups (Figure 2-8D), suggesting the alteration of VA metabolism in the liver. However, the *Raldh4* expression levels in all groups of ZF hepatocytes were similar.

Additionally, the expression level of *Cyp26a1* (Figure 2-8E), a RA catabolic gene [145,313], in VAD-AD ZL hepatocytes was significantly lower than that in VAS-PF-AD, but higher than that in VAS-PF-4M ZL hepatocytes. The *Cyp26a1* expression level in VAD-AD ZF hepatocyte was lower than that in VAS-PF-AD and VAS-PF-4M ZF groups. The *Rarb* expression levels were not different among VAD-AD, VAS-PF-AD, and VAS-PF-4M groups (Figure 2-8F).

Two-way ANOVA analysis showed that dietary manipulations accounted for the majority of overall variance observed in the expression levels of *Rbpr2* (F=23.04, 61% variance explained), *Rdh2* (F=13.14, 47%), *Raldh1* (F=23.27, 61%), and *Raldh4* (F=3.56, 22%). This suggests that dietary manipulation can potentially change the availability of RA in primary hepatocytes by changing the expression levels of VA metabolic genes. Aside from the genes described above, we also checked *Stra6*, *Rdh10*, *Raldh2* and *Raldh3*, whose transcript levels in primary hepatocytes were too low to be determined by real-time PCR analysis.

4. Discussion

Elucidating the molecular mechanisms resulting in hepatic insulin resistance is of great clinical importance. It helps understand the development and progression of metabolic diseases. We investigated the effects of food intake and VA status on the insulin-regulated gene expression in ZL and ZF primary rat hepatocytes. ZF rat, which bears a loss-of-function leptin receptor gene, develops obesity, dyslipidemia and insulin resistance due to hyperphagia [314]. We found that the insulin-regulated *Gck*, *Pck1* and *Srebp-1c* expressions were impaired in the primary hepatocytes of ZF rats fed chow diet ad libitum (Figure 2-1), confirming our previous observation [312]. VA deficiency partially corrected the impairment (Figure 2-2). We have reported that retinoids affect the expression levels of several insulin-regulated genes in primary hepatocytes previously. These observations are somewhat anticipated and in line with our hypothesis that both hyperinsulinemia and RA overproduction may take part in the regulation of the expression of genes for glucose and lipid metabolism, and contribute to hepatic insulin resistance at the gene expression level [24].

Compared to ZL rats, ZF rats are hyperinsulinemic. Previous research showed that the insulin binding capacity of the isolated liver plasma membrane of ZF rats was not different from that of ZL rats [315]. In addition, the insulin-induced phosphorylation of AKT at Ser473 and Thr308 were similar in the primary hepatocytes of ZL and ZF rats [312]. These data indicate that the impairment of insulin-regulated gene expression in ZF hepatocytes is likely to be caused by alterations downstream of AKT activation in the insulin signaling cascade. Indeed, VA and insulin operate through separated pathways to regulate hepatic gene expression. RA, as a metabolite of VA catabolism, moves to the nucleus and activates the nuclear receptors (e.g. retinoic acid receptor, retinoid X receptor, peroxisome proliferator-activated receptor β/δ, hepatocyte nuclear factor 4α, and chicken ovalbumin up-stream transcription factor II) that are located in the promoters of the target genes [24]. How these two pathways interact with each other in normal or disease states deserves further investigation.

We also found that the degree of the impairment of *Srebp-1c* expression was more profound than that of *Gck* and *Pck1* in ZF hepatocytes (Figure 2-1). It suggests that branching points may exist in the downstream of insulin signaling pathway, below which

the expressions of *Gck*, *Pck1* and *Srebp-1c* are differentially regulated by nutritional and hormonal stimuli. This is in accordance with other studies. For example, a bifurcation point at mTORC1 in the insulin signaling pathway separated the insulin-induced *Srebp-1c* expression and the insulin-suppressed *Pck1* expression [316]. The knockout of SREBP cleaving-activating protein gene in *ob/ob* mice resulted in the amelioration of hepatic lipogenesis without the improvement of hepatic gluconeogenesis [317]. Additionally in primary rat hepatocytes treated with insulin, the *Gck* expression reached the peak level 6 hrs earlier than did the *Srebp-1c* expression [235]. Further studies are needed to dissect these branching points and discover any change of regulation in insulin resistance.

The negative effects of the short-term overfeeding on the hepatic insulin sensitivity have been observed in both rodents and humans. However, the underlying mechanisms are not revealed. The pair-feeding study indicates that the transient overeating of the VAS diet (VAS-PF-AD groups) caused the impairment of insulin-regulated *Gck*, *Pck1* and *Srebp-1c* expressions in the primary hepatocytes of ZL and ZF rats compared (Figure 2-5, 2-6, 2-7). In contrast, VAS-PF-4M ZL rats showed normal insulin-regulated gene expression. This suggests that, in the livers of so called insulin-sensitive ZL rats, insulin sensitivity at gene expression level can be acutely impaired after excessive food intake, and then restored overtime. Indeed, in young human subjects, a 7-day overfeeding increased circulating adiponectin and glucagon-like peptide 1 levels, which are proposed to act against the hepatic insulin resistance [321,322]. On the other hand, transient overeating of the VAS diet caused worsened impairment of insulin-regulated *Gck* and *Srebp-1c* expressions in the primary hepatocytes of ZF rats (Figure 2-5, 2-7). ZF rats persist in overeating state due to deficient leptin signaling. This may hamper the restoration of insulin sensitivity after food intake. As a result, ZF rats fed VAS or chow ad libitum manifest the hepatic insulin resistance at the gene expression level.

Long term VA deficiency decreased the insulin-regulated expression of *Gck*, but not *Pck1* and *Srebp-1c*. In VAS-PF-AD ZL rats, the insulin-induced *Gck* expression was significantly lower than that in VAS-PF-4M ZL rats (Figure 2-5), showing that adequate VA status is instrumental to the insulin-regulated *Gck* expression in insulin-sensitive ZL primary hepatocytes. This observation demonstrates that VA status differentially affects

the hepatic insulin-regulated gene expression, suggesting complex interactions of VA and insulin signaling systems.

The impairment of insulin-induced *Gck* (Figure 2-5) and insulin-suppressed *Pck1* expressions (Figure 2-6) in VAS-PF-AD hepatocytes suggests an elevation of plasma glucose level and an acute loss of insulin-sensitivity in over-eating state. This is supported by the elevated tail tip whole blood glucose level observed in these animals (Figure 2-3E), and may explain the elevated hepatic glucose production in human subjects who are overfed for short terms [318,319]. The dysregulation of insulin-induced hepatic *Srebp-1c* expression after the transient overeating (Figure 2-7) suggests increased de novo lipogenesis, which may explain the increased hepatic fat content observed in short-term overfed humans [320]. More importantly, the impairment was observed in both ZL and ZF rats after transient overeating. These data suggest the existence of a mechanism that may dynamically regulate hepatic insulin sensitivity at the gene expression level in response to feeding status.

Short-term overeating provides excessive intake of not only calories but also micronutrients. We showed transient overeating for one day greatly affected the expression levels of genes involved in VA metabolism in the ZL and ZF rat hepatocytes (Figure 2-8). VAD-AD rats exhibited high hepatic levels of *Rbpr2*, *Rdh2*, *Raldh1* and *Raldh4* transcripts, showing compensatory upregulation of the VA metabolic genes. In contrast, VAS-PF-4M rats exhibited low hepatic transcript levels of *Rbpr2*, *Rdh2* and *Raldh4*. These suggest that the hepatic VA metabolic gene expression is greatly influenced by the availability of dietary VA.

VAS-PF-AD rats had lowered hepatic levels of *Rbpr2* and *Raldh1* transcripts. Indeed, the *Rbpr2* expression is inversely related to the liver retinol stores, and RA reduces the *Rbpr2* mRNA level in HepG2 cells [111]. Additionally, the elevated RA controls its biosynthesis by down-regulating RALDH1 through the modulation of retinoic acid receptor α and CCAAT/enhancer binding protein β [138,139].These suggest that the expression levels of VA metabolic genes are modulated in VAS-PF-AD rats to prevent the RA overproduction in response to the transient influx of the dietary VA. Despite the negative feedback regulation, excessive RA may have been produced. This is supported by the increased expression level of *Cyp26a1* [145], a RA-responsive gene, in VAS-PF-

AD hepatocytes (Figure 2-8E). The excessive RA may affect the expression of hepatic metabolic genes, and promote the hepatic insulin resistance at the gene expression level [24]. It is interesting to note that the VA status does not seem to affect the expression levels of *Raldh1* gene in primary hepatocytes as its expression levels are similar in VAD-AD and VAS-PF-4M groups. The underlying mechanism deserves further investigation.

In summary, we have demonstrated that both VA and feeding statuses affected the hepatic insulin sensitivity at the gene expression level. This finding provides insight into the development of the hepatic insulin resistance, and helps find solutions to combat metabolic diseases.

CHAPTER III. OVEREXPRESSION OF ATYPICAL PROTEIN KINASE Cζ (PKCζ) OR ι/λ (PKCι/λ) ATTENUATES INSULIN-REGULATED GENE EXPRESSION IN PRIMARY RAT HEPATOCYTES

Abstract

Results demonstrated in the previous chapter and publications from our lab have shown that the insulin-regulated gene expression is impaired in primary hepatocytes from Zucker fatty (ZF), but not Zucker lean (ZL) rats fed ad libitum. We have systemically compared the hepatic expression levels and activation statuses of the critical components in signaling pathway between ZL and ZF rats. The preliminary data indicate that the expression levels of atypical protein kinase Cζ (PKCζ), member of PKC family, are higher in hepatocytes and liver of ZF than that of ZL rats. In individuals with type 2 diabetes, hepatic aPKC levels are elevated. It is postulated that increased activation of aPKC are associated with dysregulated glucose and lipid metabolism. aPKC inhibitors can partially correct the increased levels of hepatic lipogenic and gluconeogenic enzymes in rodent and human hepatocytes. In order to investigate the roles of aPKC in the impairment of the insulin-regulated gene expression, PKCζ and PKCι/λ were overexpressed in primary hepatocytes from ZL rats using recombinant adenoviruses. The insulin-regulated expressions of these genes were attenuated upon overexpression of PKCζ or PKCι/λ. Interestingly, PKCζ or PKCι/λ overexpression increased the basal transcript levels of glucokinase, sterol regulatory element-binding protein-1c and cytosolic form of phosphoenolpyruvate carboxykinase. PKCζ and PKCι/λ overexpression in primary hepatocytes from ZL rats significantly reduces the protein level of insulin receptor substrate 1 (IRS1), and the phosphorylation of protein kinase B (PKB/AKT) at Ser473, Thr308, and Thr450 in response to insulin treatment. These data demonstrate the effects of PKCζ and PKCι/λ on the regulation of insulin signal transduction, and their critical roles in the regulation of the insulin-regulated expressions of genes for glucose and lipid metabolism in hepatocytes.

1. Introduction

The liver is a crucial organ for the maintenance of whole body glucose and lipid homeostasis. Normal physiological responses to the anabolic hormone insulin stimulation result in increased glycolysis, decreased gluconeogenesis and increased lipogenesis in the liver [309,310]. In individuals with obesity or type 2 diabetes, normal amount of insulin is unable to suppress hepatic glucose production, but able to promote hepatic lipid synthesis [37]. The paradoxical coexistence of elevated gluconeogenesis and lipogenesis in the liver is a characteristic of hepatic insulin resistance, which exacerbates hyperinsulinemia and contributes to systemic insulin resistance [37,38]. This abnormality will create a vicious cycle and eventually lead to the onset of overt diabetes. At present, the knowledge about the molecular mechanisms underlying hepatic insulin resistance is limited. The elucidation of these mechanisms will help understand the pathogenesis of an array of metabolic diseases, including obesity, cardiovascular disease, type 2 diabetes and non-alcoholic fatty liver disease.

In hepatic parenchymal cells, insulin initiates its signaling cascade upon binding to its receptor on the cell membrane, which is followed by the activation of insulin receptor substrates (IRSs) [10]. Tyrosine phosphorylation of IRS1/2 leads to the association and activation of the phosphatidylinositol 3-kinase (PI3K). PI3K catalyzes the conversion of phosphatidylinositol-4,5-bisphosphate into phosphatidylinositol-3,4,5-triphosphate. The latter is a lipid messenger that anchors the downstream effector proteins, e.g. phosphoinositide dependent protein kinase-1, protein kinase B (PKB, also known as AKT) and atypical protein kinase C (aPKC), to the cell membrane [10]. The activations of AKT and aPKC differentially regulate the transcription of hepatic genes for glucose and lipid metabolism [25,32,323]. For example, insulin induces the expression of glucokinase (GCK, gene *Gck*) to promote glycolysis, and suppresses the expression of cytosolic form of phosphoenolpyruvate carboxykinase (PEPCK, gene *Pck1*) to reduce gluconeogenesis in association with the activation of AKT [25,324]. On the other hand, the induction of sterol-responsive element binding protein 1c (SREBP-1c, gene *Srebp-1c*) by insulin to promote lipogenesis is mediated not only by the activation of AKT [324], but also by the activation of aPKC [30,33].

Members of PKC family include classical PKC, novel PKC, and aPKC. Unlike the other two types of PKC, aPKC does not require diacylglycerol or Ca^{2+} for activation. PKCζ and PKCι/λ (genes *Prkcz* and *Prkci*) are two current members of aPKC. PKCζ shares 70% homology in amino acid sequence with PKCι/λ (PKCι in human; PKCλ in mouse) [25]. The tissue expression profiles of PKCζ and PKCι/λ depend on the species. In rat muscle and adipocytes, PKCζ is more abundant than PKCι/λ. Comparably in human muscle, adipocytes and liver, PKCι is the predominant isoform [25]. Both PKCζ and PKCι/λ mediate a variety of physiological events, such as cell polarity establishment, cell motility, immune response and metabolism [20,25].

Activations of PKCζ or PKCι/λ have been associated with increased lipogenesis and insulin resistance in multiple tissues and organs [25,325]. Currently in the mouse liver, the activation of aPKC isoforms seems to play a role in the *Srebp-1c* transcription and lipogenesis. For example, in liver-specific PKCλ knockout mice, the basal transcript level of hepatic *Srebp-1c*, but not *Gck* or *Pck1*, declined by 50% [30]. In a mouse model within which the regulatory subunit of PI3K was ablated in the liver, decreased PKCζ/λ activity was observed in association with the reduction of *Srebp-1c* expression [32]. On the other hand, the insulin-induced activation of aPKC and subsequent *Srebp-1c* expression were retained in the liver of diabetic mice [31,34]. PKCζ/λ is also activated in the livers of mice on a high fat diet, which increased the expression of hepatic *Srebp-1c* [33]. This effect could be negated by the overexpression of kinase-inactive form PKCζ [33].

In the hepatocytes isolated from type 2 diabetic individuals, the activation of PKCι was elevated at the basal level and after insulin treatment [35,36]. Treatment of these hepatocytes with PKCι inhibitors lowered the levels of lipogenic, proinflammatory and gluconeogenic enzymes [35,36]. Moreover, metformin treatment was shown to induce aPKC activities, and increase lipogenic and gluconeogenic enzyme levels in non-obese human hepatocytes [326]. These data collectively suggest that aPKC isoforms are important players in the pathogenesis of obesity and type 2 diabetes. However, the molecular mechanisms by which aPKC activations or expressions impact insulin-regulated gene expression in the liver are still unclear.

Zucker fatty (ZF) rat is a genetic model of obesity, hypertriglyceridemia and hepatic insulin resistance [327]. We previously showed that primary hepatocytes from ZF rats fed

chow ad libitum exhibited impairment of the insulin-regulated gene expression [312]. Interestingly, the induced-phosphorylation of AKT at Ser473 and Thr 308 in ZF rat primary hepatocytes was not significantly different from that in Zucker lean (ZL) rat primary hepatocytes [312]. In this study, we observed the differential expression levels of PKCζ in the livers of ZF and ZL rats, and investigated the roles of PKCζ and PKCι/λ in the insulin-regulated gene expression in primary rat hepatocytes. We demonstrated that overexpression of PKCζ and PKCι/λ in ZL primary hepatocytes impaired the insulin-regulated gene expression.

2. Materials and methods

2.1 Reagents

The reagents for primary hepatocyte isolation and culture including Medium 199 (#11150059), Dulbecco's Modification of Eagle Medium (DMEM, #11995065), liver perfusion buffer (#17701038) and liver digest buffer (#17703034) were obtained from Invitrogen (Carlsbad, CA). RNA STAT-60 was purchased from TEL-TEST (Friendswood, TX). Restriction enzymes were from New England BioLabs (Ipswich, MA). The reagents for cDNA synthesis and real-time PCR were obtained from Applied Biosystems (Foster city, CA). All real-time PCR primer sets were synthesized by Sigma-Aldrich (St. Louis, MO). Antibodies against β-actin (#4967), PKCζ (#9368), PKCι (#2998), p-PKCζ/λ Thr410/403 (#9378), AKT (#9272), p-AKT Ser473 (#9271), p-AKT Thr308 (#9275), p-AKT Thr450 (#9267), IRS1 (#2382), FAS (#3189), ACC (#3662), p-ACC Ser79 (#3661) used in this study were purchased from Cell Signaling Technology (Danvers, MA). All other reagents and materials were purchased from Fisher Scientific (Pittsburgh, PA) unless described otherwise.

2.2 Animals and diets

Zucker rats were bred and housed under constant temperature and humidity in the animal facility at the University of Tennessee at Knoxville on a 12-hr light-dark cycle. Male lean (ZL, fa/+ or +/+) or fatty (ZF, fa/fa) rats at weaning (3 weeks old) were kept on Teklad rodent chow (#8640, Harlan Laboratories, Indianapolis, IN) for 8 weeks before liver tissue collection and primary hepatocyte isolation. All procedures were approved by

the Institutional Animal Care and Use Committee at the University of Tennessee at Knoxville (Protocols #1256, 1642 and 1863).

2.3 Liver tissue collection, total protein preparation and total RNA extraction

The rat was euthanized by primary carbon dioxide asphyxiation, and then secondary cervical dislocation according to regulations. A 10 ml syringe with a 21G × 1½" hypodermic needle was used to drain blood from the liver via the inferior vena cava. The liver was excised, sliced, snap-frozen in liquid nitrogen, and stored at -80˚C before further analysis. A small portion of the liver tissue was homogenized in 10 volumes of cold whole-cell lysis buffer (1% Triton X-100, 10% glycerol, 1% IGEPAL CA-630, 50 mM Hepes, 100 mM NaF, 10 mM EDTA, 1 mM sodium molybdate, 1 mM sodium β-glycerophsphate, 5 mM sodium orthovanadate, 1.9 mg/ml aprotinin, 5 mg/ml leupeptin, 1 mM benzamide, 2.5 mM PMSF, pH 8.0) for 1 min. The homogenized tissue suspension was centrifuged at 16,873×g (Eppendorf 5418 desktop centrifuge, FA-45-18-11 rotor at 14,000×rpm) and 4˚C for 20 min to remove insoluble matters. The protein concentration of the supernatant was determined with PIERCE BCA protein assay kit (Rockford, IL). For liver tissue total RNA extraction, a small portion of the liver tissue was homogenized in 10 volumes of cold STAT-60 for 1 min. Total RNA was extracted according to the instructions of the manufacturer.

2.4 Cultures of primary hepatocytes and 293 HEK cells

The primary hepatocytes were isolated according to previously described protocol [265]. After the euthanasia of the rat, a catheter connected to a peristaltic pump was inserted into the portal vein. The pump was set up to infuse 120 ml liver perfusion buffer and 120 ml liver digestion buffer at the flow rate of 10 ml/min. The inferior vena cava was punctured to allow the outflow of blood and buffers. After digestion, the liver was then excised and put into a cell culture dish containing liver digestion buffer to remove connective tissues and allow further digestion. The released hepatocytes were filtered through a 100 μm cell strainer and collected by 50×g centrifugation for 3 min. The hepatocytes were washed twice with DMEM containing 4.5 g/L glucose, 8% fetal bovine serum, 1% penicillin/streptomycin. Isolated hepatocytes were seeded on 60-mm collagen type I coated dishes at 2×10^6 cells per dish and incubated in the same medium at 37˚C and 5% CO_2 for at least 3 hrs to allow cell attachment. The attached primary hepatocytes

were washed once with PBS and pretreated in medium A (Medium 199 with 100 nM dexamethasone, 100 nM 3,3',5-triiodo-L-thyronine (T3), 1 nM insulin, and 1% penicillin/streptomycin) at 37˚C and 5% CO_2 for 16-18 hrs.

HEK 293 cells were seeded and kept in DMEM containing 4.5 g/L glucose, 4% fetal bovine serum, 1% penicillin/streptomycin at 37˚C and 5% CO_2.

2.5 Cloning of the rat *Prkci* cDNA and subcloning of the rat *Prkcz* cDNA.

Based upon the rat *Prkci* mRNA sequence (GenBank: EU517502.1), sense 5'-ATC CCC TCA GCC TCC AGC GG-3' and antisense 5'-ACT GTG ACC GGG CTA ACG GT-3' primers were designed using Primer-BLAST tools from the National Center Biotechnology Information. For cloning of the complete coding sequence of rat *Prkci* cDNA, PCR was carried out using cDNA derived from total RNA of ZL primary hepatocyte as the template. For subcloning of rat *Prkcz*, pEYFP-N1 vector containing its complete coding sequence was generously provided by Dr. Ralf Kubitz of Heinrich-Heine-Universität. The vector was used as the template for the PCR amplification of *Prkcz* using sense primer 5'-ACC TCG AGA TGC CCA GCA GGA CCG AC-3' and antisense primer 5'- GTG AAT TCA CAC GGA CTC CTC AGC AGA C-3'. The amplicons containing the complete coding sequences of *Prkci* and *Prkcz* cDNA sequences were ligated into pCR®2.1 vector through TA Cloning® Kit (Invitrogen) according to the manufacture's protocol. The cloned *Prkci* and subcloned *Prkcz* cDNA sequences were verified by DNA sequencing.

2.6 Generation of Ad-Prkcz and Ad-Prkci recombinant adenoviruses

pCR®2.1-Prkcz and pACCMV5 were digested by EcoRI to generate the insert containing complete coding sequence of *Prkcz* cDNA and EcoRI-cut pACCMV5 vector, respectively. pCR®2.1-Prkci and pACCMV5 were digested by HindIII/XbaI to generate the insert containing complete coding sequence of *Prkci* cDNA and HindIII/XbaI double-cut pACCMV5 vector, respectively. Desired fragments were separated in 0.9% agarose gels and purified using QIAquick Gel Extraction Kit (QIAGEN, Valencia, CA). The inserts containing the complete coding sequences of *Prkcz* and *Prkci* were ligated into their corresponding pACCMV5 vectors to make pACCMV5-Prkcz and pACCMV5-Prkci respectively. To generate Ad-Prkcz and Ad-Prkci recombinant adenoviruses, pACCMV5

plasmid containing the complete coding sequence of atypical *Prkc* sequences (0.8µg each) was co-transfected with JM17 (0.2µg) into HEK293 cells in 35mm plate using FuGENE®6 Transfection Reagent (Roche Applied Science, Indianapolis, IN) at 3:1 or 6:1 ratio (reagent: DNA). Transfected HEK293 cells were incubated in DMEM containing 2% FBS at 37˚C and 5% CO_2 until the formation of the viral plaques. The crude lysate was collected and stored at -80˚C.

100µl crude lysate of Ad-Prkcz and Ad-Prkci recombinant adenoviruses were incubated in boiling water for 10 min, and subsequently treated with proteinase K at 56˚C for 30 min. The total viral genome was isolated from the crude lysate by phenol chloroform extraction and dissolved in 50µl water. The presence of atypical *Prkc* sequences in the viral DNA was then confirmed by PCR using specific primers.

2.7 Generation and purification of recombinant adenoviruses

HEK 293 cells were cultured in 100mm tissue culture plates until 80% confluence in DMEM containing 4.5 g/L glucose, 2% FBS at 37˚C and 5% CO_2. Ad-Prkcz and Ad-Prkci recombinant adenoviral crude lysates were added into the medium respectively (lysate:medium ratio 1 to 10). The infected cells were incubated at 37˚C and 5% CO_2 for 48 to 72 hrs to allow maximal cell lysis to occur. Crude lysates from 10 culture plates were collected and combined for each recombinant adenovirus purification. NP-40 was added into the crude lysate to reach the final concentration of 0.5% v/v. The mixture was shaken gently at room temperature for 30 min and centrifuged at 6,000×g and 4˚C for 15 min to remove cell debris. The supernatant was transferred to a clean bottle, and 0.5 × volume of 20% PEG8000/2.5 M NaCl was added. The mixture was gently shaken at 4˚C overnight, and subsequently centrifuged at 15,000×g and 4˚C for 15 min. The precipitated pellet was re-suspended in 2–3 ml PBS. The re-suspension was spun at 6,000×g and 4˚C for 10 min to remove insoluble matter. The supernatant was transferred into a clean tube, and CsCl was added to reach a final density of 1.34 g/ml. The mixture was spun at 437,004×g (Beckman Optima Max-XP Ultracentrifuge, TLA 100.3 rotor at 90,000×rpm) and 25˚C for 4 hrs. The pure viral particles was collected and desalted with the PD-10 column Sephadex™ G-25M (Amersham Pharmacia Biotech AB, Sweden). Desalted viral particle suspension was supplemented with 0.2% w/v bovine serum

albumin and 10% v/v glycerol. The optical density (OD) at 260 nm of the suspension was determined by Spectronic® GENESYS™ 5 Spectrophotometer (Thermo Scientific) to estimate the plaque forming units (pfu) of the purified recombinant adenoviruses. We used that 1 OD equals to 1×10^{12} pfu/ml. The purified virus was frozen and stored at -80˚C until being used.

2.8 Infection of recombinant adenoviruses and treatments of primary hepatocytes

The attached primary hepatocytes were washed once with PBS and pretreated in medium A for pretreatment. In experiments using recombinant adenoviruses, purified Ad-Prkcz and Ad-Prkci were also added in the medium A to allow the overexpression of PKCζ and PKCι/λ in the primary rat hepatocytes during the pretreatment period, respectively. The pretreated hepatocytes were then washed once with PBS, and treated with medium A containing indicated concentrations of insulin (0 nM to 100 nM) for 6 hrs before total RNA extraction, or for 15 min before whole cell lysate preparation.

2.9 RNA extraction and real-time PCR analysis.

The methods for total RNA extraction and cDNA synthesis were described elsewhere [312]. In essence, total RNA was extracted from the treated hepatocytes with RNA STAT-60 according to the manufacture's protocol. The contaminated DNA in RNA samples was removed using the DNA-free™ kit. First strand cDNA was synthesized from 2μg total RNA by cDNA synthesis kit. The gene expression level was determined by real-time PCR with respective primer sets, and normalized to the mRNA level of ribosomal gene 36B4. The data were presented as either minus Δ cycle threshold (Ct) or the induction fold (ΔΔCt) for which the control treatment group was arbitrarily set as 1.

2.10 Whole cell lysate preparation

Treated primary hepatocytes were placed on ice and washed once with ice-cold proteinase inhibitors supplemented PBS (100 mM NaF, 1 mM sodium molybdate, 1 mM sodium b-glycerophsphate, 5 mM sodium orthovanadate, 1.9 mg/ml aprotinin, 5 mg/ml leupeptin, 1 mM benzamide, and 2.5 mM PMSF). The cells were lysed in 400μl ice cold whole-cell lysis buffer with proteinase inhibitors, and subsequently scraped into clean 1.5 ml centrifugation tubes. The lysates were vigorously vortexed and placed on ice for at least 20 min. Insoluble matter was removed by centrifugation at 16,873×g and 4˚C for 20

min. The protein concentration in the supernatant was determined with PIERCE BCA protein assay kit.

2.11 Immunoblot analysis of protein

Proteins samples (40μg) in the whole cell lysates of primary hepatocytes or liver tissues were separated by 8% sodium dodecyl sulfate polyacrylamide gel, and then transferred to BIO-RAD Immuno-Blot PVDF membrane (Hercules, CA). Membranes were blocked by incubation in a solution of 8% non-fat milk in TBST for 1h at room temperature, and then probed with specific antibodies diluted 1/1000 in 5% BSA in TBST overnight at 4˚C. After three times of 5 min gentle wash with TBST, membranes were incubated with goat anti-rabbit IgG conjugated with horseradish peroxidase (1/5000 dilution in 8% non-fat milk in TBST) for 1 hr at room temperature. After three times of 5 min gentle wash with TBST, detection of antigen-bound antibody was carried out using chemiluminescence (ECL Western Blotting Substrate, Thermo Scientific), and subsequently exposure to X-ray films (Phenix Research Products, Candler, NC). The films were scanned at 300dpi using a HP ScanJet 2200 Scanner. The images were stored for the analysis of densitometry using ImageJ software (National Institute of Health, MD). Densitometry data for each protein was normalized to β-actin levels in each sample.

2.12 Statistical Analysis.

Statistical analyses were performed using SPSS 19.0 software. Student t-test was used to compare the means between two treatments. One-way ANOVA with LSD post-hoc test was used to compare the means of three or more treatments. Two-way ANOVA with Bonferroni's post-hoc test was used to determine the effects of insulin treatments and genotypes on hepatic gene expression. Data were presented as means ± S.E.M. The number of experiments indicates hepatocyte isolations from different animals. A p value less than 0.05 is considered statistically significant.

3. Result

3.1 PKCζ expression was elevated in the liver of ZF rats compared with ZL rats.

To understand the underlying signaling mechanism for the hepatic insulin resistance at gene expression level in the liver of ZF rats, we analyzed the expression levels and activation status of critical components in the insulin signaling pathways. Despite the

well-reported hepatic insulin resistance, ZF rats had higher phosphorylation of AKT at Ser473 and Thr450 in liver tissues than ZL rats (Figure 3-1A). However, the phosphorylation of AKT at Thr308 could not be detected in the current experimental condition. This observation shows that the insulin-induced AKT phosphorylation in ZF rat liver tissue is unimpaired, indicating the consequences of hyperinsulinemia. In addition, ZF rat liver showed higher protein level of FAS, which is an indicator of increased hepatic lipogenesis (Figure 3-1A).

In ZF liver tissue, the protein level of PKCζ, but not PKCι/λ, were elevated compared to that in ZL liver tissue (Figure 3-1). Interestingly, the level of phospho-PKCζ/λ Thr410/403, which indicated the phosphorylation of both PKCζ, and PKC ι/λ, were similar between ZL and ZF rat liver tissues (Figure 3-1A). The mRNA level of *Prkcz*, but not that of *Prkci*, was also elevated in the ZF liver (Figure 3-1B). These data collectively suggest that aPKCs seem to be involved in the development of hepatic insulin resistance in the ZF liver.

3.2 Acute insulin treatment did not alter protein levels of total and phospho-aPKCs in primary rat hepatocytes.

To investigate whether insulin treatment changes total and phosphorylation states of AKT and aPKC protein levels, we examined the immunoblot of whole-cell lysates from ZL and ZF primary hepatocytes treated by insulin (0-100 nM) for 15 min. As expected, the protein levels of FAS, ACC and phospho-ACC Ser79 were substantially increased in ZF hepatocytes irrespective of insulin treatments (Figure 3-2). This result indicates that the increased hepatic lipogenic capability remains in the cultured primary hepatocytes isolated from ZF rats more than 20 hrs ago. Insulin treatment dose-dependently induced the phosphorylation of AKT at Ser473 and Thr308 in ZL and ZF primary hepatocytes, but no significant difference between ZL and ZF were observed in the phosphorylation of both sites (Figure 3-2). In contrast, the phosphorylation of AKT at Thr450 in ZL and ZF hepatocytes was insulin-independent. The level of phospho-AKT at Thr450 was higher in ZF hepatocytes than in ZL hepatocytes (Figure 3-2). These data suggest that the insulin-induced AKT phosphorylation is not impaired in ZF rat hepatocytes. The impaired insulin-regulated gene expression in ZF hepatocytes may be caused by other components in insulin signaling pathway. On the other hand, insulin treatment for 15 min did not

Figure 3-1: ZF rats on chow ad lib had elevated expression levels of PKCζ mRNA and protein in the liver. ZL (n=4) and ZF (n=4) rats were kept on chow ad lib for 8 weeks before sacrifice. Total proteins were obtained from the liver tissues of these rats, and subjected to immunoblot analysis. Total mRNA was extracted from the liver tissues, synthesized into cDNA, and then subjected to real time PCR analysis. (A) Immunoblot analysis of total liver proteins of ZL and ZF rats. (B) The mRNA levels of *Prkcz* and *Prcki* in the livers of ZL and ZF rats. The data were presented as minus Δ cycle threshold (Ct). * indicates $p<0.05$ for comparing ZL and ZF using Student's t-test.

A.

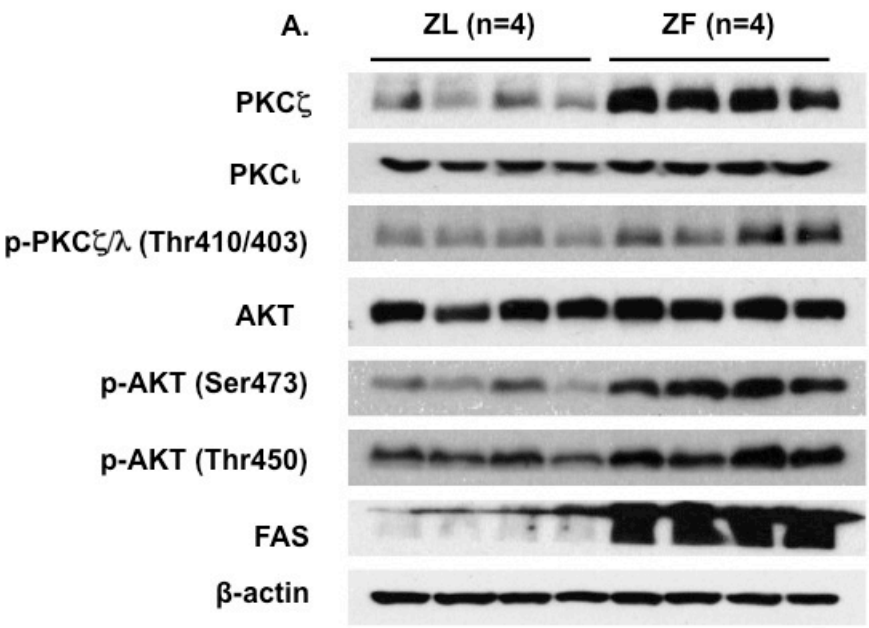
A.
ZL (n=4)
ZF (n=4)
PKCζ
PKCι
p-PKCζ/λ (Thr410/403)
AKT
p-AKT (Ser473)
p-AKT (Thr450)
FAS
β-actin

B.

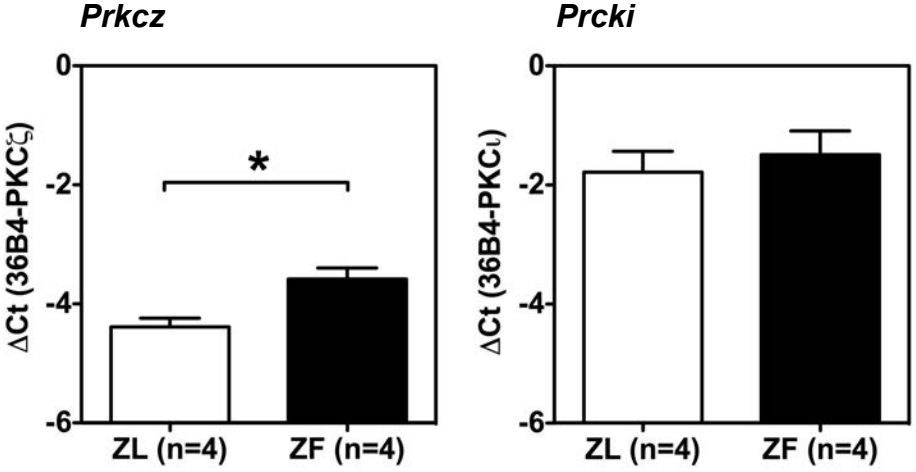
Prkcz
Prcki
ΔCt (36B4-PKCζ)
ΔCt (36B4-PKCι)
0
-2
-4
-6
*
ZL (n=4)
ZF (n=4)

Figure 3-1

Figure 3-2: Acute insulin treatment did not alter protein levels of total and phospho-aPKCs in primary rat hepatocytes. ZL and ZF rats were fed standard chow for eight weeks before primary hepatocytes were harvested. The primary hepatocytes were incubated in fresh medium A with increasing concentrations of insulin (0 nM to 100 nM) for 15 min after pretreatment. Control primary hepatocytes (indicated by C) were not replenished with fresh medium A after pretreatment. The whole cell lysates of these hepatocytes were obtained and subjected to immunoblot analysis with antibodies indicated in the figure (A). The figure shows the representative result of three parallel experiments obtained from three sets of animals. (B) Densitometry analyses of the immunoblot results. Data are arbitrary intensity units expressed as mean ± SEM. All $p<0.05$; a<b, a'<b'<c', d<e, d'<e' using one way ANOVA. * for comparing the difference between ZL and ZF using two way ANOVA.

(A)

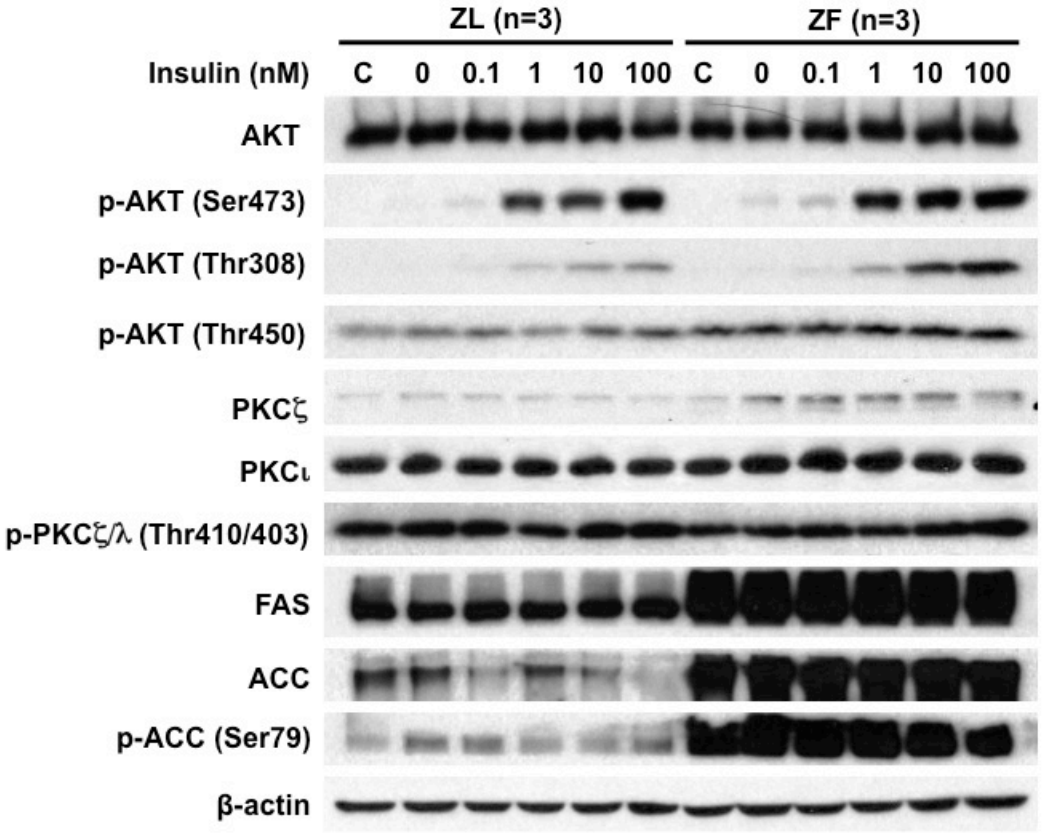
ZL (n=3)
ZF (n=3)
Insulin (nM)
C 0 0.1 1 10 100 C 0 0.1 1 10 100
AKT
p-AKT (Ser473)
p-AKT (Thr308)
p-AKT (Thr450)
PKCζ
PKCι
p-PKCζ/λ (Thr410/403)
FAS
ACC
p-ACC (Ser79)
β-actin

Figure 3-2

(B)

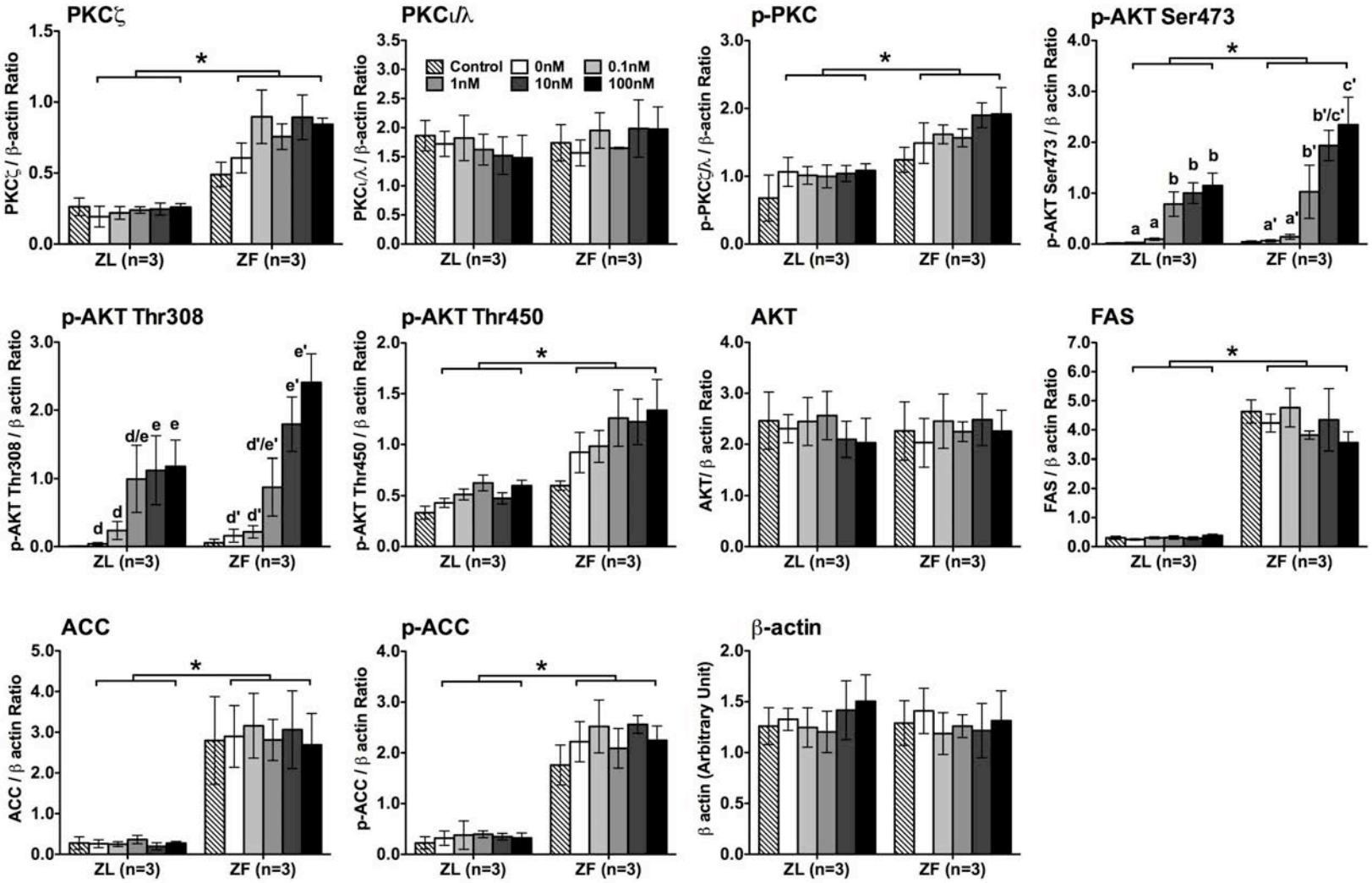

Figure 3-2 Continued

significantly induce or suppress the protein levels of PKCζ and PKCι/λ and the phosphorylation of PKCζ/λ at Thr410/403 in ZL and ZF primary hepatocytes (Figure 3-2). There was a slight induction of the total PKCζ when fresh M199 was added. However, ZF primary hepatocytes had higher level of PKCζ than ZL primary hepatocytes (Figure 3-2), which was in line with the finding from rat liver tissues (Figure 3-1).

3.3 Overexpression of PKCζ and PKCι/λ in ZL primary hepatocytes.

To investigate whether elevated aPKC protein levels contribute to hepatic insulin resistance, we infected ZL primary rat hepatocytes with recombinant adenoviruses Ad-Prkcz or Ad-Prkci, respectively. Compared to hepatocytes infected with Ad-β-gal, Ad-Prkcz infected hepatocytes had ~2000 fold overexpression of *Prkcz* mRNA, and Ad-Prkci infected hepatocytes had ~250 fold overexpression of *Prkci* mRNA (Figure 3-3A and B, *). Interestingly in the hepatocytes overexpressing PKCι/λ, 0.1-100 nM insulin treatments significantly suppressed the expression of *Prkcz* by 40-60% (Figure 3-3A). On the other hand, in the hepatocytes overexpressing PKCζ, the expression levels of *Prkci* at 1-100 nM insulin treatments were significantly lower than that at the corresponding treatments in hepatocytes overexpressing β-GAL (Figure 3-3B, #).

The immunoblot of total cell lysate from Ad-Prkcz infected primary rat hepatocytes showed ~9.3 fold overexpression of PKCζ, but not PKCι/λ, compared to Ad-β-gal infected cells (Figure 3-4). Overexpression of PKCζ did not lead to significant increase in phospho-PKCζ/λ Thr410/403 level. The immunoblot of total cell lysate from Ad-Prkci infected primary rat hepatocytes manifested ~4.0 fold overexpression of PKCι/λ and increased phosphorylation of PKCζ/λ at Thr410/403, compared to Ad-β-gal infected cells (Figure 3-5).

3.4 Overexpression of PKCζ and PKCι/λ attenuated the insulin signaling cascade in ZL primary rat hepatocytes.

Compared to Ad-β-gal infected primary hepatocytes, Ad-Prkcz infected hepatocytes showed similar level of total AKT, but the insulin-induced phosphorylation of AKT at Ser473 and Thr308, and insulin-independent phosphorylation of AKT at Thr450 were attenuated in these cells (Figure 3-4). Ad-Prkcz infected hepatocytes also had lower

(A) ***Prkcz*** **(B)** ***Prkci***

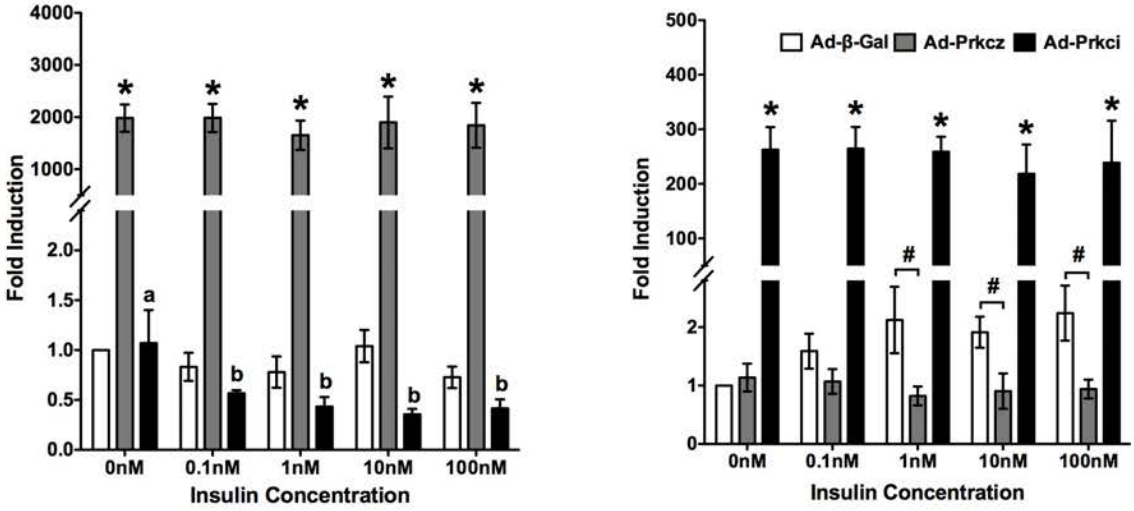

Figure 3-3: Overexpression of PKCζ and PKCι/λ attenuated the insulin signaling cascade in ZL primary rat hepatocytes. ZL rats were fed standard chow for eight weeks before primary hepatocytes were harvested. Purified Ad-Prkcz and Ad-Prkci were added in the medium A during the pretreatment period to allow the overexpression of PKCζ and PKCι/λ. Purified Ad-β-gal was used as a control recombinant adenovirus. The primary hepatocytes were then incubated in fresh medium A with increasing concentrations of insulin (0 nM to 100 nM) for 6 hrs before total RNA extraction Total mRNA was extracted, synthesized into cDNA, and then subjected to real time PCR analysis. The data were expressed as fold induction. The gene transcript levels from Ad-β-gal infected primary hepatocytes with 0 nM insulin treatment were arbitrarily set to 1. (A) The mRNA levels of *Prkcz* in the ZL primary hepatocytes (n=4) overexpressing β-GAL, PKCζ and PKCι/λ in response to insulin gradient treatments. All $p<0.05$; a>b using one way ANOVA. * for comparing fold inductions at corresponding treatments using one way ANOVA. (B) The mRNA levels of *Prkci* in the ZL primary hepatocytes (n=4) overexpressing β-GAL, PKCζ and PKCι/λ in response to insulin gradient treatments. All $p<0.05$; * and # for comparing fold inductions at corresponding treatments using one way ANOVA.

Figure 3-4: Overexpression of PKCζ attenuated the insulin signaling cascade in ZL primary rat hepatocytes. ZL rats were fed standard chow for eight weeks before primary hepatocytes were harvested. Purified Ad-Prkcz was added in the medium A during the pretreatment period to allow the overexpression of PKCζ. Purified Ad-β-gal was used as a control recombinant adenovirus. The primary hepatocytes were then incubated in fresh medium A with increasing concentrations of insulin (0 nM to 100 nM) for 15 min before whole cell lysate preparation. The whole cell lysates were subjected to immunoblot analysis with antibodies indicated in the figure. The figure shows the representative result of three parallel experiments obtained from three sets of animals. (A) Immunoblot analysis of Ad-Prkcz infected ZL primary hepatocytes treated with increasing concentrations of insulin for 15 min. (B) Densitometry analyses of the immunoblot results. Data are arbitrary intensity units expressed as mean ± SEM. All $p<0.05$; a<b, c<d<e using one way ANOVA. * for comparing the difference between ZL and ZF using two way ANOVA.

(A)

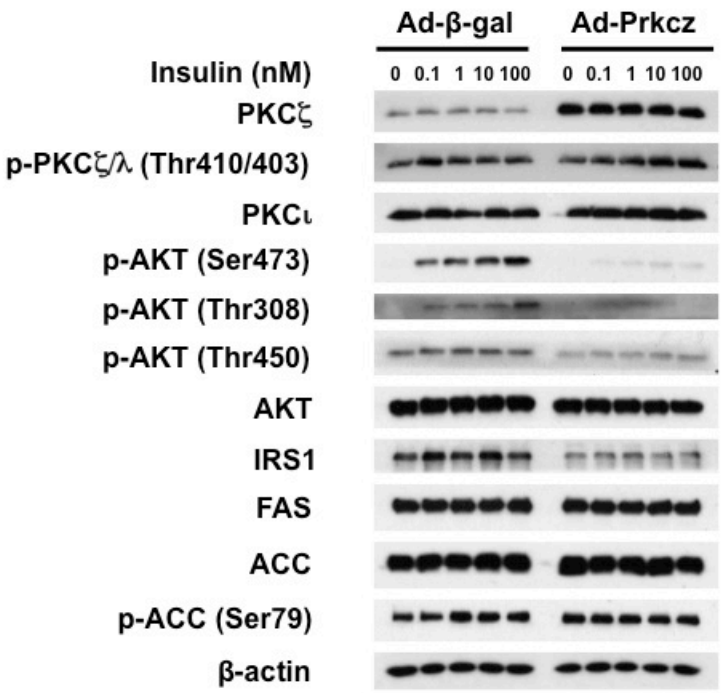
Ad-β-gal
Ad-Prkcz
Insulin (nM)
0 0.1 1 10 100
0 0.1 1 10 100
PKCζ
p-PKCζ/λ (Thr410/403)
PKCι
p-AKT (Ser473)
p-AKT (Thr308)
p-AKT (Thr450)
AKT
IRS1
FAS
ACC
p-ACC (Ser79)
β-actin

Figure 3-4

(B)

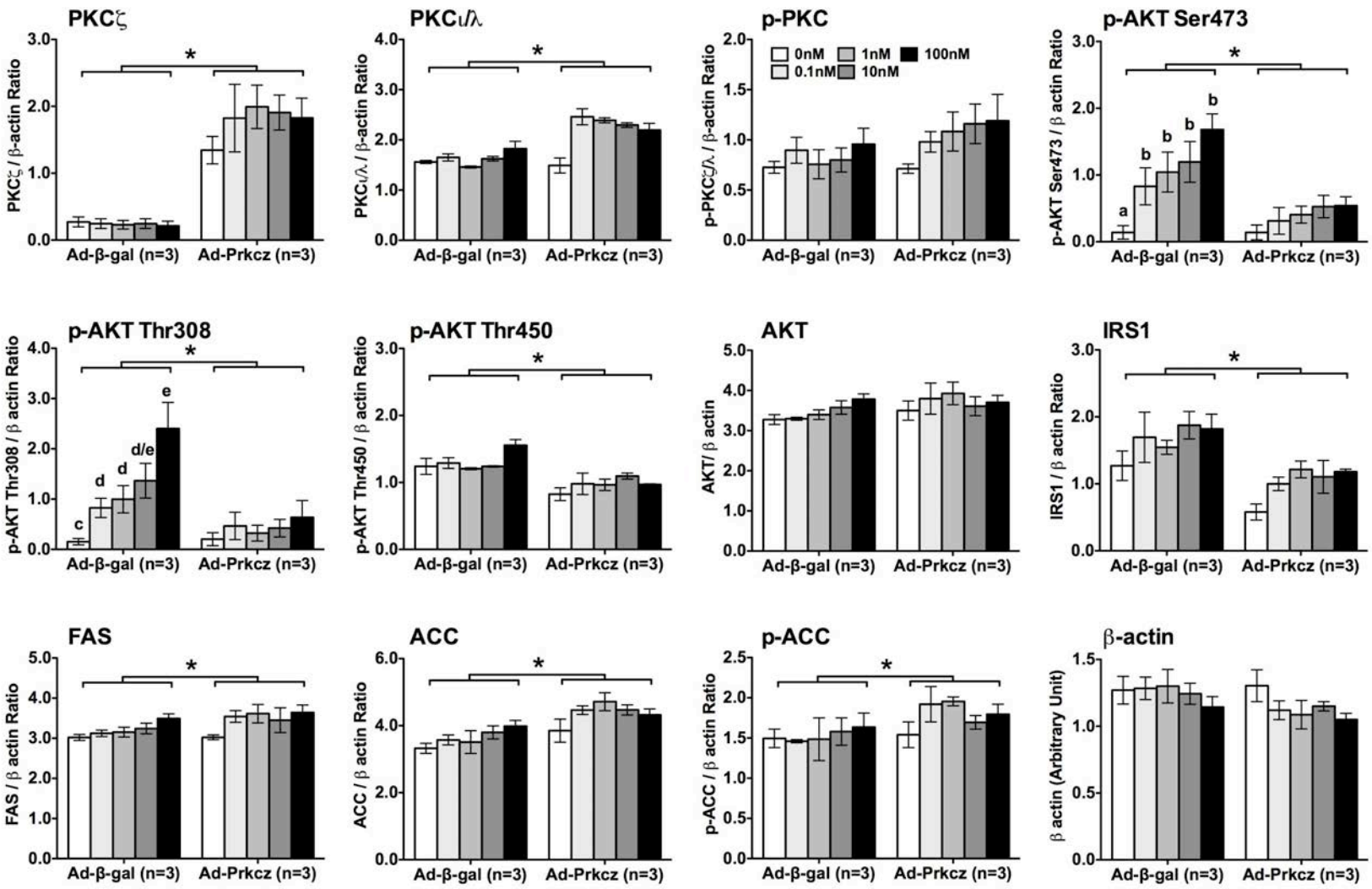

Figure 3-4 Continued

Figure 3-5: Overexpression of PKCι/λ attenuated the insulin signaling cascade in ZL primary rat hepatocytes. ZL rats were fed standard chow for eight weeks before primary hepatocytes were harvested. Purified Ad-Prkci was added in the medium A during the pretreatment period to allow the overexpression of PKCι/λ. Purified Ad-β-gal was used as a control recombinant adenovirus. The primary hepatocytes were then incubated in fresh medium A with increasing concentrations of insulin (0 nM to 100 nM) for 15 min before whole cell lysate preparation. The whole cell lysates were subjected to immunoblot analysis with antibodies indicated in the figure. The figure shows the representative result of three parallel experiments obtained from three sets of animals. (A) Immunoblot analysis of Ad-Prkci infected ZL primary hepatocytes treated with increasing concentrations of insulin for 15 min. (B) Densitometry analyses of the immunoblot results. Data are arbitrary intensity units expressed as mean ± SEM. All $p<0.05$; a<b, a'<b', c<d, e<f using one way ANOVA. * for comparing the difference between ZL and ZF using two way ANOVA.

(A)

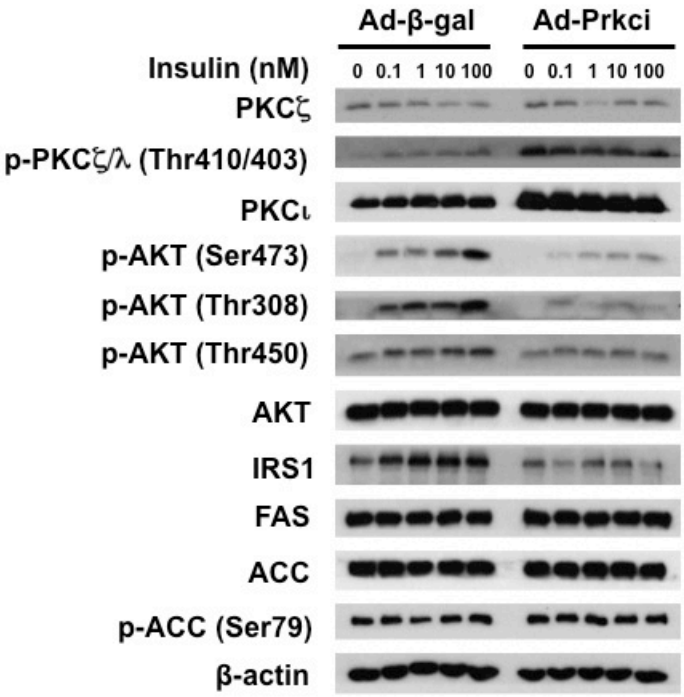
Ad-β-gal
Ad-Prkci
Insulin (nM)
0 0.1 1 10 100
0 0.1 1 10 100
PKCζ
p-PKCζ/λ (Thr410/403)
PKCι
p-AKT (Ser473)
p-AKT (Thr308)
p-AKT (Thr450)
AKT
IRS1
FAS
ACC
p-ACC (Ser79)
β-actin

Figure 3-5

(B)

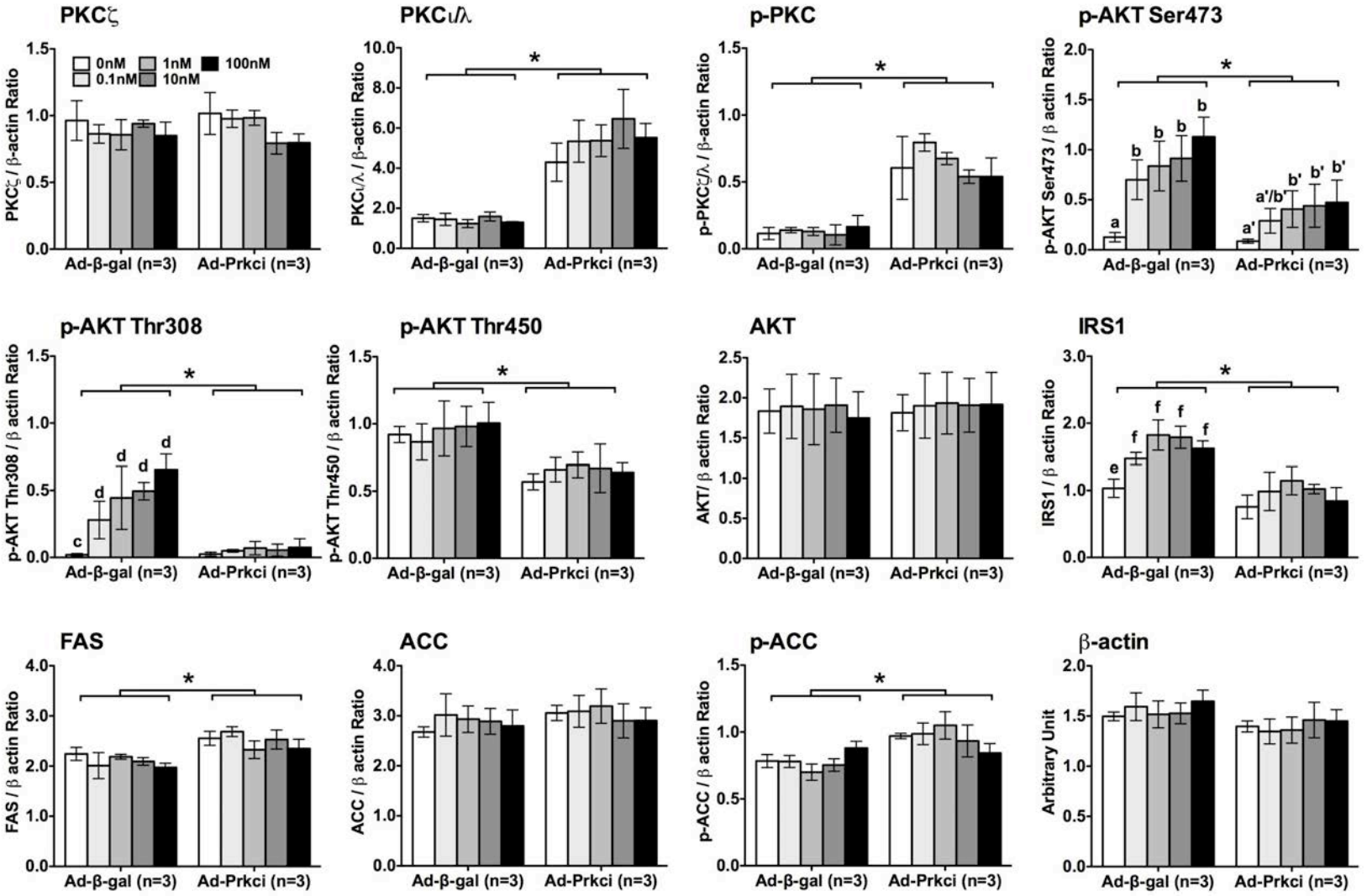

Figure 3-5 Continued

levels of IRS1. However, there was no significant difference between Ad-β-gal and Ad-Prkcz infected hepatocytes regarding FAS, ACC or phospho-ACC Ser79.

Overexpression of PKCι/λ did not significantly change the levels of PKCζ or ACC (Figure 3-5). However, there was a slight but significant elevation in the levels of FAS and phospho-ACC Ser79. Ad-Prkci infected hepatocytes showed similar level of total AKT to that of Ad-β-gal infected primary hepatocytes. But interestingly, the levels of IRS1, phospho-AKT Thr450, and insulin-induced phospho-AKT Ser473 and Thr308 were significantly decreased in primary rat hepatocytes overexpressing PKCι/λ.

These data collectively demonstrate that overexpression of aPKCs attenuates the insulin signaling cascade in ZL primary rat hepatocytes.

3.5 Overexpression of PKCζ and PKCι/λ impaired the insulin-regulated gene expression in ZL primary rat hepatocytes.

To investigate whether aPKCs affect hepatic insulin-regulated gene expression, we examined the transcript levels of *Gck*, *Pck1*, *Srebp-1c* and liver type pyruvate kinase gene (*Pklr*) in response to increasing concentrations of insulin treatments in ZL primary rat hepatocytes overexpressing PKCζ or PKCι/λ. Figure 3-6A showed that in hepatocytes overexpressing β-GAL, insulin dose-dependently induced the *Gck* expression. Overexpression of either PKCζ or PKCι/λ in ZL primary hepatocytes elevated the basal transcript level of *Gck*. Additionally, the fold inductions of *Gck* expression in response to 0.1-100 nM insulin treatments were abolished in hepatocytes overexpressing PKCζ or PKCι/λ.

Insulin at 0.1-100 nM dose-dependently suppressed the *Pck1* expression in hepatocytes overexpressing β-GAL by 80% (Figure 3-6B). At 0 nM insulin treatment, the transcript levels of *Pck1* in hepatocytes overexpressing PKCζ or PKCι/λ were about 3 times of that in hepatocytes overexpressing β-GAL. Moreover, the insulin-suppressed *Pck1* expression was abolished in hepatocytes overexpressing PKCζ or PKCι/λ.

Figure 3-6C showed that insulin dose-dependently induced the *Srebp-1c* expression in hepatocytes overexpressing β-GAL. Overexpression of either PKCζ or PKCι/λ in ZL primary hepatocytes elevated the basal transcript level of *Srebp-1c*. In addition, the

Figure 3-6: Overexpression of PKCζ and PKCι/λ impaired the insulin-regulated gene expression in ZL primary rat hepatocytes. ZL rats were fed standard chow for eight weeks before primary hepatocytes were harvested. Purified Ad-Prkcz and Ad-Prkci were added in the medium A during the pretreatment period to allow the overexpression of PKCζ and PKCι/λ. Purified Ad-β-gal was used as a control recombinant adenovirus. The primary hepatocytes were then incubated in fresh medium A with increasing concentrations of insulin (0 nM to 100 nM) for 6 hrs before total RNA extraction. Total mRNA was extracted, synthesized into cDNA, and then subjected to real time PCR analysis for the expression levels of *Gck* (A), *Pck1* (B), *Srebp-1c* (C), and *Pklr* (D). The data were expressed as fold induction. The gene transcript levels from Ad-β-gal infected primary hepatocytes with 0nM insulin treatment were arbitrarily set to 1. All $p<0.05$; for (A), a>b; for (B), c>d; for (C), e<f using one-way ANOVA; * for comparing fold inductions at corresponding treatments using one-way ANOVA.

(A) *Gck*

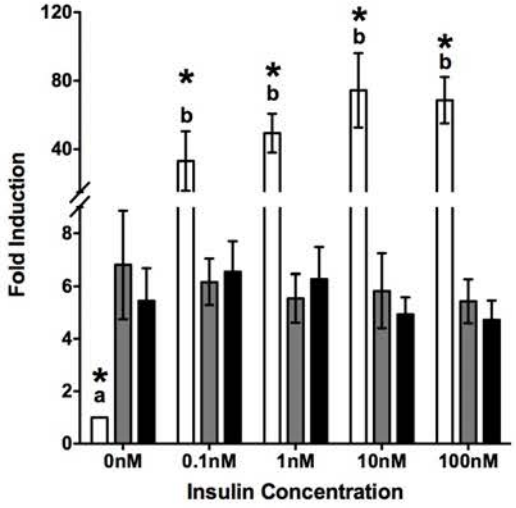

(B) *Pck1*

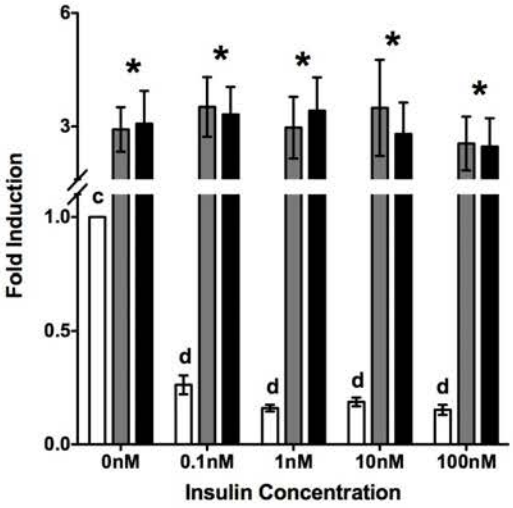

(C) *Srebp-1c*

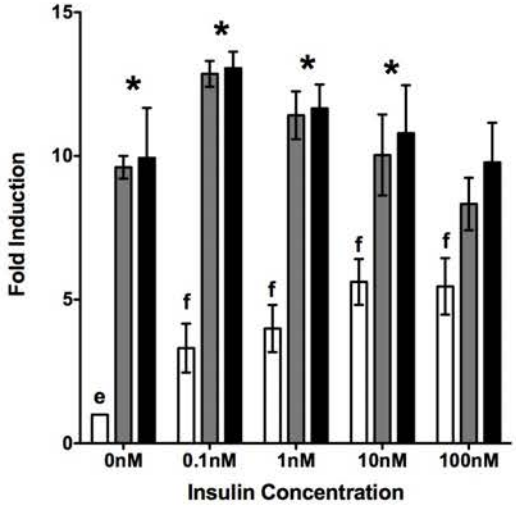

(D) *Pklr*

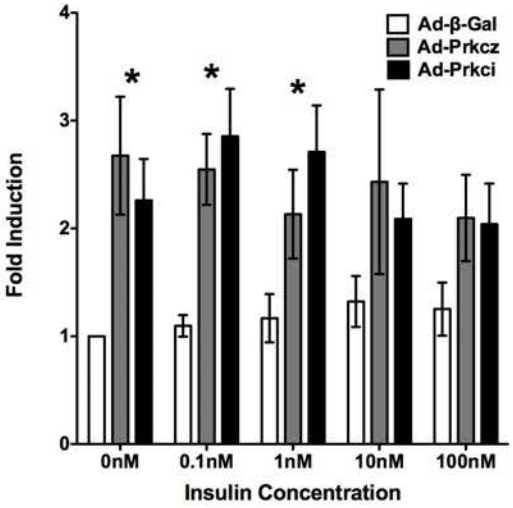

insulin-induced *Srebp-1c* expression was abolished in hepatocytes overexpressing PKCζ or PKCι/λ.

The mRNA levels of *Pklr* in ZL primary hepatocytes overexpressing β-GAL, PKCζ or PKCι/λ were not affected by insulin (Figure 3-6D). However, the expressions levels of *Pklr* were significantly higher at 0-1 nM insulin in hepatocytes overexpressing PKCζ or PKCι/λ than in hepatocytes overexpressing β-GAL.

4. Discussion

Here, we have shown that the expression levels of PKCζ, but not that of PKCι/λ, are higher in the livers of ZF rats than ZL rats. Since the insulin-regulated gene expression is impaired in primary hepatocytes from ZF, but not ZL rats fed ad libitum, we hypothesized that alteration of the aPKC expression in hepatocytes may play a role in the impairment. Therefore, PKCζ and PKCι/λ were successfully overexpressed using recombinant adenoviruses in ZL primary hepatocytes. It seems that the overexpression of either PKCζ or PKCι/λ is sufficient to alter basal and insulin-regulated gene expression in hepatocytes from ZL rats. We have tried and failed to detect the activities of the aPKC in both liver and primary hepatocyte samples, including those samples from hepatocytes with overexpression of PKCζ and PKCι/λ. The lack of antibody for immune-precipitation or a specific substrate peptide can be the reason. Further experiments are warranted when additional means become available for determination of their activities.

In this study, we demonstrate that adenoviral-mediated overexpression of PKCζ and PKCι/λ leads to the impairment of insulin-regulated *Gck*, *Srebp-1c*, and *Pck1* expressions in the ZL primary rat hepatocytes (Figure 3-6). At mRNA level, the observed impairment has two main characteristics: (1) the overexpression of either PKCζ or PKCι/λ causes the elevation of basal mRNA levels of *Gck*, *Srebp-1c*, *Pck1*, and *Pklr*; (2) the overexpression abrogates the insulin action to induce *Gck* and *Srebp-1c* expressions, and suppress *Pck1* expression in the primary hepatocytes.

The impairment of the insulin-regulated gene expression might be attributed to the reduced activation of AKT/PKB in cells with overexpression of PKCζ or PKCι/λ. In ZL hepatocytes infected with ad-β-GAL, insulin dose-dependently induces the activation of

AKT/PKB and protein levels of IRS1. On the other hand, PKCζ or PKCι/λ overexpression attenuates the insulin-induced phosphorylation of AKT, and decreases the protein level of IRS1 in the hepatocytes, which suggests a diminished IRS/PI3K/AKT signaling cascade (Figure 3-4 and 3-5). However, the expression levels of AKT/PKB and its activation status seem to be not different between the Ad-β-gal control groups and overexpression groups. It indicates that other mechanisms may contribute to the elevation of the basal expression of the same genes in hepatocytes with overexpression of PKCζ or PKCι/λ. Collectively, these data show that PKCζ and PKCι/λ are critical regulators of hepatic glucose and lipid metabolism.

GCK catalyzes the phosphorylation of glucose into glucose-6-phosphate in the rate-limiting step of glycolysis in the liver [310]. The hepatic regulation of the *Gck* expression depends on the insulin-mediated activation of IRS/PI3K/AKT pathway [324,328,329]. It has been shown that the *Gck* expression requires mammalian target of rapamycin complex 2 (mTORC2) induced phosphorylation of AKT at Ser473 [18]. In Figure 3-4 and 3-5, PKCζ or PKCι/λ overexpression diminished phosphorylation of AKT at Ser473 with decrease of the IRS1 protein expression. This is accord with previous reports that aPKCs act as negative feedback regulators of insulin signaling pathway by promoting serine phosphorylation and tyrosine de-phosphorylation of IRS proteins [330-332]. Thus, the possible reduction of the activation of IRS/PI3K/AKT pathway due to PKCζ or PKCι/λ overexpression may impair the insulin-regulated *Gck* expression. Additionally, insulin-induced *Gck* expression is mediated through a selection of transcription factors, including hepatocyte nuclear factor 4 (HNF4), forkhead box protein O1 (FOXO1), SREBP-1c, liver x receptor α (LXRα), and peroxisome proliferator-activated receptor γ (PPARγ) [24,333-335]. Since the knowledge about the non-kinase activities and endogenous substrates of PKCζ or PKCι/λ is limited, it is also possible that PKCζ or PKCι/λ directly regulate *Gck* expression through certain transcription factors, which increases its basal transcript level.

PEPCK catalyzes the rate limiting enzymatic reaction in gluconeogenesis, by which oxaloacetate is converted into phosphoenolpyruvate [336]. In the liver, the insulin-suppressed *Pck1* expression is purportedly mediated through three pathways: (1) the phosphorylation and inactivation of FOXO1 via IRS/PI3K/AKT [337,338]; (2)

antagonizing the glucagon-induced PPARγ co-activator 1 (PGC1α) expression [339]; (3) the phosphorylation of CREB binding protein (CBP) via IRS/PI3K/aPKCs [340,341]. Interestingly, despite the high levels of aPKCs to suppress *Pck1* expression via CBP, the diminished IRS/PI3K/AKT pathway plays a dominant role in the primary hepatocytes overexpressing aPKCs. It not only leads to an increase in the basal transcript of *Pck1* mRNA, but also abrogates the insulin-mediated *Pck1* suppression (Figure 3-6B). Incidentally, the activities of aPKC isoforms are elevated in the livers of type 2 diabetic individuals [31,35,36]. Treatment of hepatocytes from these individuals with aPKC inhibitors decreases the basal transcript levels of gluconeogenic genes [35,36]. These data suggest that aPKCs are prominent positive regulators of hepatic gluconeogenesis.

SREBP-1c is a master transcriptional factor for the expression of lipogenic genes in the liver [342]. The insulin-induced *Srebp-1c* expression requires the activation of PI3K/AKT, and the mTORC2-mediated phosphorylation of AKT at Ser473 [18,324]. With the help of pharmacological inhibitors, the activation of mTORC1 downstream of AKT is identified as an indispensible step in the induction of *Srebp-1c* [316]. On the other hand, the activation of PI3K subsequently activates aPKC in the liver, which promotes *Srebp-1c* expression and lipogenesis [30-34]. Despite the diminished IRS/PI3K/AKT signaling pathway and the abolished insulin-regulated *Srebp-1c* expression, PKCζ or PKCι/λ overexpression increases the basal transcript level of *Srebp-1c* in the hepatocytes (Figure 3-6C). Interestingly, PKCζ or PKCι/λ overexpression only slightly induced the protein levels of FAS and ACC (Figure 3-4 and 3-5). One possibility is that the induced transcripts might not have been translated in the presence of overexpression of PKCζ or PKCι/λ. Alternatively, diminished IRS/PI3K/AKT signaling pathway results in decreased activation of p70 S6-kinase (S6K), which is required for the SREBP-1c processing to generate nuclear SREBP-1c [343]. In this regard, the protein levels of FAS and ACC do not significantly increase due to unstimulated SREBP-1c processing. Moreover, there might be a lag time for us to see the elevation of mRNA to the protein, the down-stream targeted mRNA and proteins. Nevertheless, the protein levels of ACC and FAS are maintained at a high level in the hepatocytes and livers from ZF rats, demonstrating the metabolic defects associated with these insulin-resistant animals. Further investigations are needed to delineate the sequential events associated

with the elevation of the hepatic lipogenesis upon insulin stimulation and activation of AKT and aPKC isoforms.

It is interesting to note that the *Prkcz* mRNA and PKCζ protein, but not that of *Prkci* mRNA and PKCι/λ protein levels are elevated in the liver of ZF rats. Insulin at 1 nM and up significantly induces the expression levels of *Prkci* mRNA, a process that is blunted in the presence of PKCζ overexpression. On the other hand, insulin does not affect the expression of *Prkcz* mRNA. Additionally, PKCι/λ overexpression alone does not affect *Prkcz* mRNA expression. However, PKCι/λ overexpression introduced the insulin-mediated suppression of *Prkcz* mRNA expression. These data indicate that there are crosstalk between PKCζ and PKCι/λ pathways, which may mutually regulate the expression of each other at mRNA levels in response to hormonal or nutritional stimuli. The alteration of this mutual regulation mechanism probably is associated with the development of the impairment of insulin signaling. Further studies are warranted.

In summary, we have shown that aPKC overexpression in ZL primary hepatocytes impairs the insulin-regulated gene expression, and attenuates the IRS/PI3K/AKT part of the insulin signaling pathway. It demonstrates that the alteration of the expression levels of aPKC leads to reduction of the phosphorylation of AKT and its downstream pathways. These results demonstrate the critical roles of aPKCs in the regulation of hepatic glucose and lipid metabolism at gene expression level, and provide interesting insights into the development of the hepatic insulin resistance and type 2 diabetes.

CHAPTER IV. UNPUBLISHED DATA, CONCLUSION AND FUTURE DIRECTIONS

1. Unpublished data

1.1 The effect of retinoids on the glucose-stimulated insulin secretion from INS-1 cells.

1.1.1 Background summary

Islets of Langerhans, which account for less than 2% of the total pancreas mass, produce and secret anabolic hormone insulin from β-cells. The secretion of insulin is mainly stimulated by the influx of glucose into β-cells. It has been also shown that amino acid and neural stimuli can stimulate insulin secretion [274].

Glucose-stimulated insulin secretion (GSIS) from the pancreatic β-cells is a well characterized physiological event [344]. Upon entry into the pancreatic β cells, glucose will be broken down via the typical glycolysis and citric acid cycle, which results in the production of ATP. An elevated ATP:ADP ratio in the cytosol will inhibit the ATP-sensitive potassium ion channel in the cell membrane, which in turn facilitates the opening of the calcium ion channel. An influx of Ca^{2+} into the cell triggers the release of insulin [344].

Previous studies showed that VAD rats had impaired GSIS from isolated islets, but the insulin content and morphology of the islet cells were unchanged [278]. In comparison, VA deficiency reduces the β-cell mass in fetal islets by reducing the fetal β-cell replication [277]. On the other hand, the effects of VA and its metabolites on isolated islets and insulin secreting cells are both chemical- and dosage-dependent (See Chapter 1, section 9.4). In insulin-secreting RINm5F cells, both all-*trans*-RA and 9-*cis*-RA were found to increase insulin secretion. However, all-*trans*-RA could also inhibit cell growth and increase apoptosis [280]. Several proteins including nuclear receptors LXR, RARs and RXRs, and transglutaminase were hypothesized to mediate the effects of retinoids on the GSIS, However, the specific molecular mechanisms involved in the process are still unknown [281]. INS-1 cells are well established cell lines for the elucidation of GSIS mechanisms [345]. Here, standard GSIS assay was performed on INS-1 parental cells, 832/13, 833/15 and 833/117 cell lines to investigate the effects of retinal, retinal and RA on the GSIS.

1.1.2 All-*trans*-RA has divergent effects on the GSIS of different INS-1 cell lines

INS-1 parental cells, 832/13, and 833/117 cells were seeded in 12 well tissue culture plate and cultured in standard RPMI 1640 medium (supplemented with 10 mM glucose, 2 mM glutamine, 1 mM sodium pyruvate, 10%FBS, 10 mM HEPES, 1% penicillin/streptomycin, and 50 μM β-mercaptoethanol) at 37˚C and 5% CO_2 for 3 days to reach 70% confluency. The INS-1 cells were then treated with 5μM all-*trans*-RA in the same fresh RPMI 1649 medium at 37˚C and 5% overnight. After the removal of the medium, the cells were treated in secretion assay buffer (SAB, 114 mM NaCl, 4.7 mM KCl, 1.2 mM KH_2PO_4, 1.16 mM $MgSO_4$, 2.5 mM $CaCl_2$, 25 mM $NaHCO_3$, 20 mM HEPES, 1% BSA, pH 7.4) with either 3 mM or 15 mM glucose to measure insulin secretion. After incubation at 37˚C for 2 hrs, the supernatant SAB and the cells were collected into separate centrifuge tubes (Figure 4-1). The insulin content in the SAB was measured using the Siemens Insulin Coat-A-Count® Kit (06615423). The collected cells were lysed by 0.5% (v/v) Triton X-100. The total protein was measured using Pierce™ BCA Protein Assay Kit.

833/15 cells were used to examine the effects and difference between the pretreatment and the acute treatment of all-*trans*-RA on GSIS (Figure 4-1). The cells are cultured in RPMI 1640 medium containing 3 mM glucose. The experiment procedure is similar to the one described above, except that: (1) in the pretreatment condition, the cell are treated with 5μM all-*trans*-RA in the medium at 37˚C and 5% CO_2 overnight; (2) in the acute treatment condition, 5μM all-*trans*-RA is added to the SAB containing either 3 mM or 15 mM glucose, and incubated at 37˚C for 2 hrs.

The results (Figure 4-1) showed that 5μM all-*trans*-RA significantly enhanced the GSIS of 832/13 and 833/117 cells by 15 mM glucose, but not by 3 mM glucose. It suggests that all-*trans*-RA may potentiate the GSIS of INS-1 cells at the stimulatory concentrations of glucose. As expected, INS-1 parental cells did not show any response to either glucose stimulation or all-*trans*-RA treatment. One possible explanation is that the INS-1 parental cells a mixture of insulinoma cells. It is reported that most of the INS-1 parental cells have lost the GSIS [346].

All-*trans*-RA pretreatment of 833/15 cells caused a significant increase of insulin secretion by 3 mM glucose, but not by 15 mM glucose. Interestingly, this phenomenon

Figure 4-1: The effects of all-*trans* RA on the GSIS of INS-1 cells. INS-1 cells were cultured in standard RPMI 1640 medium at 37˚C for 3 days to reach 70% confluence. The cells were treated with 5 μM all-*trans* RA, and the insulin secretion assay was performed as indicated by the schematic graphs. The secreted insulin during 2 hrs is measured and the data were normalized to the protein content of the cells. The data are presented as mean ± SD. (A), the effect of all-*trans* RA on the GSIS of INS-1 parental, 832/13 and 832/117 cells**.** (B) The pretreatment and acute treatments of all-*trans* RA on the GSIS of 833/15 cells.

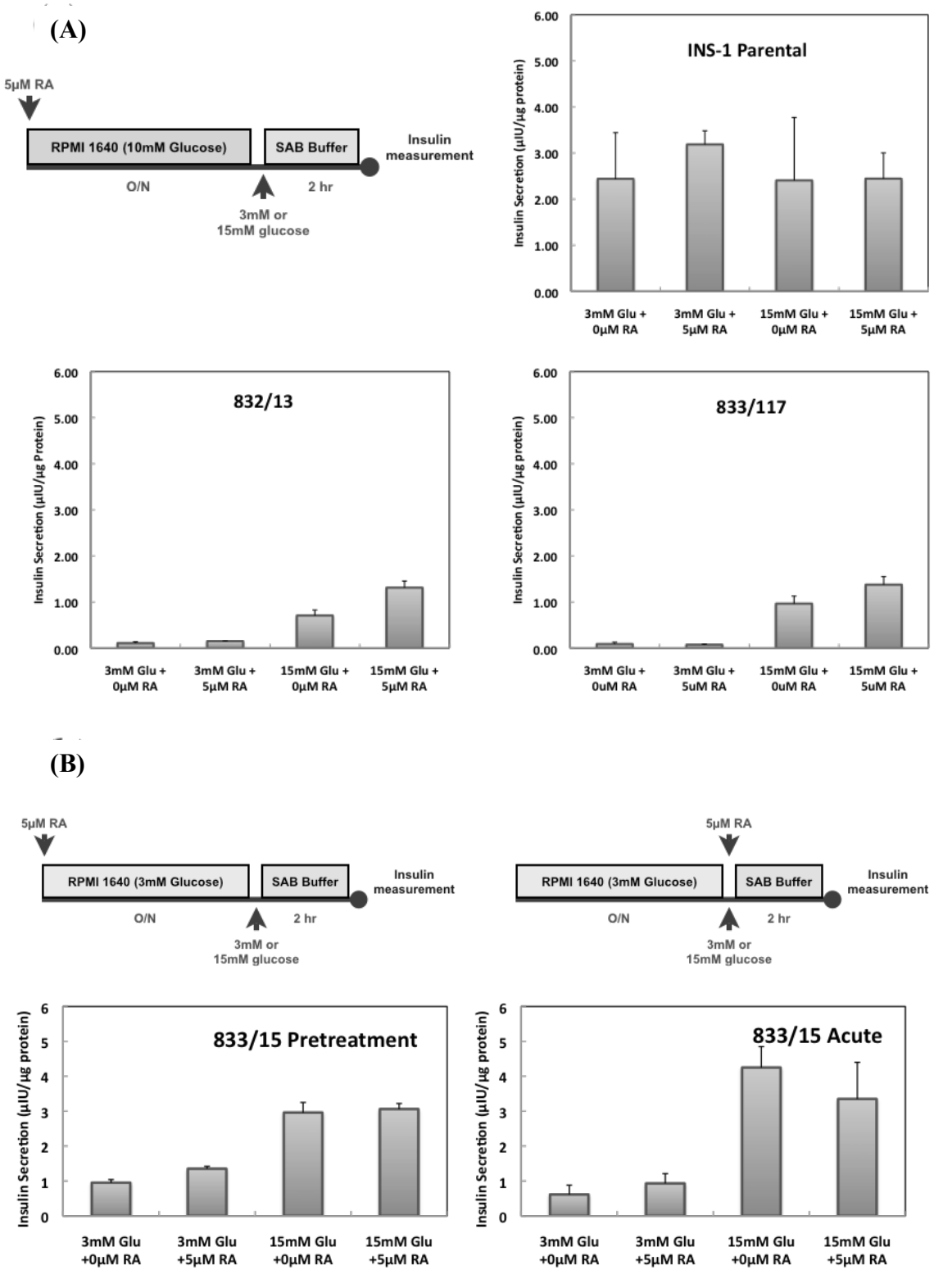
(A)
5μM RA
RPMI 1640 (10mM Glucose)
SAB Buffer
Insulin measurement
O/N
2 hr
3mM or 15mM glucose
INS-1 Parental
832/13
833/117
Insulin Secretion (μIU/μg protein)
Insulin Secretion (μIU/μg Protein)
3mM Glu + 0μM RA
3mM Glu + 5μM RA
15mM Glu + 0μM RA
15mM Glu + 5μM RA
(B)
RPMI 1640 (3mM Glucose)
833/15 Pretreatment
833/15 Acute

was not apparent in the acute treatment condition. These results collectively suggest that all-*trans*-RA has divergent effects on the GSIS of INS-1 cell lines.

1.1.3 The effects of retinoids on the GSIS from isolated subclones of INS-1 parental cells.

INS-1 cell lines 832/13, 833/15 and 833/117 contain exogenous human insulin gene [346,347]. To establish an INS-1 cell line without human insulin gene, INS-1 parental cells were trypsinized and subjected to serial dilutions with RPMI 1640 medium in a 96-well plate. After incubation at 37˚C and 5% CO_2, the INS-1 cells originated from a single cell from the dilution of the parental cells and maintained stable growth in culture were picked for further analyses. In particular, two isolated subclones, INS-1 6D and 8E manifested stable propagation properties and were used to investigate the effects of all-*trans*-retinol, retinal and RA on the GSIS (Figure 4-2). Standard insulin secretion assay showed that INS-1 8E manifested high basal insulin secretion when it was cultured in RPMI 1640 containing 10 mM glucose (Figure 4-2). INS-1 6D showed low basal insulin secretion, but high GSIS by 15 mM glucose (Figure 4-2). These data further confirmed that INS-1 parental cells are a mixture of subclones, which have diverse GSIS capacities.

The effects of retinoids on the GSIS were performed on INS-1 6D and INS-1 8E according to the procedures described above with RMPI 1640 medium containing 10 mM glucose. The results showed that 5μM all-*trans*-retinol and 5μM all-*trans*-retinal did not affect the GSIS of INS-1 6D cells. 5μM all-*trans*-RA, however, suppressed the GSIS of INS-1 6D cells (Figure 4-2). In addition, 5μM all-*trans*-retinol and 5μM all-*trans*-retinal and 5μM all-*trans*-RA did not affect the GSIS of INS-1 8E cells (Figure 4-2).

Interestingly, when INS-1 8E cells were cultured in RPMI1640 medium with 3 mM glucose, the cells regained the stimulatory response of insulin secretion pattern by 15 mM glucose (Figure 4-2). Furthermore, all-*trans*-RA significantly decreased GSIS by 15 mM glucose in INS-1 8E. In contrast, all-*trans*-RA only significantly decreased the GSIS by 15 mM glucose in INS-1 6D, when the cells were incubated in RMPI 1640 medium with all-*trans*-RA (Figure 4-2). These results showed that all-*trans*-RA had suppressive effect on the GSIS of INS-1 cells, which do not contain exogenous human insulin gene.

Figure 4-2: The effects of all-*trans* retinol, retinal and RA on the GSIS of INS-1 6D and 8E cell lines. INS-1 6D and 8E cells lines were obtained from isolation of single clones from parental cells. Insulin secretion assays were performed as indicated in the text. **(A)** Insulin secretion of INS-1 6D and 8E in response to 3 mM and 15 mM glucose stimulation. **(B and C)** The effects of all-*trans* retinol, retinal and RA on the GSIS by 3 mM and 15 mM glucose in INS-1 6D and 8E cells. **(D)** The differential all-*trans* RA treatments on the GSIS by 3 mM and 15 mM glucose in INS-1 6D and 8E cells.

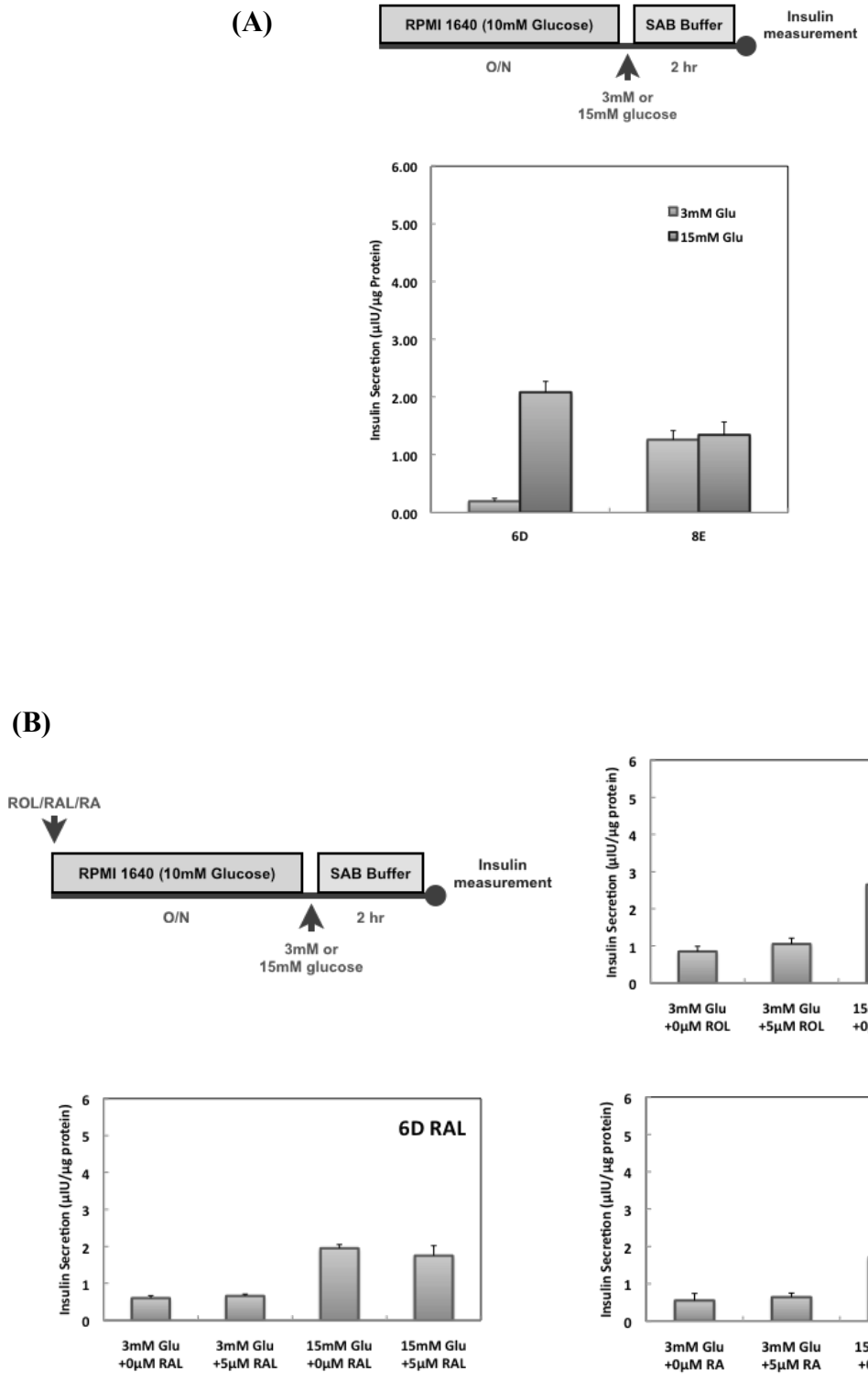
(A)
RPMI 1640 (10mM Glucose)
SAB Buffer
Insulin measurement
O/N
2 hr
3mM or 15mM glucose
Insulin Secretion (μIU/μg Protein)
3mM Glu
15mM Glu
6D
8E
(B)
ROL/RAL/RA
RPMI 1640 (10mM Glucose)
SAB Buffer
Insulin measurement
O/N
2 hr
3mM or 15mM glucose
6D ROL
Insulin Secretion (μIU/μg protein)
3mM Glu +0μM ROL
3mM Glu +5μM ROL
15mM Glu +0μM ROL
15mM Glu +5μM ROL
6D RAL
3mM Glu +0μM RAL
3mM Glu +5μM RAL
15mM Glu +0μM RAL
15mM Glu +5μM RAL
6D RA
3mM Glu +0μM RA
3mM Glu +5μM RA
15mM Glu +0μM RA
15mM Glu +5μM RA

Figure 4-2

(C)

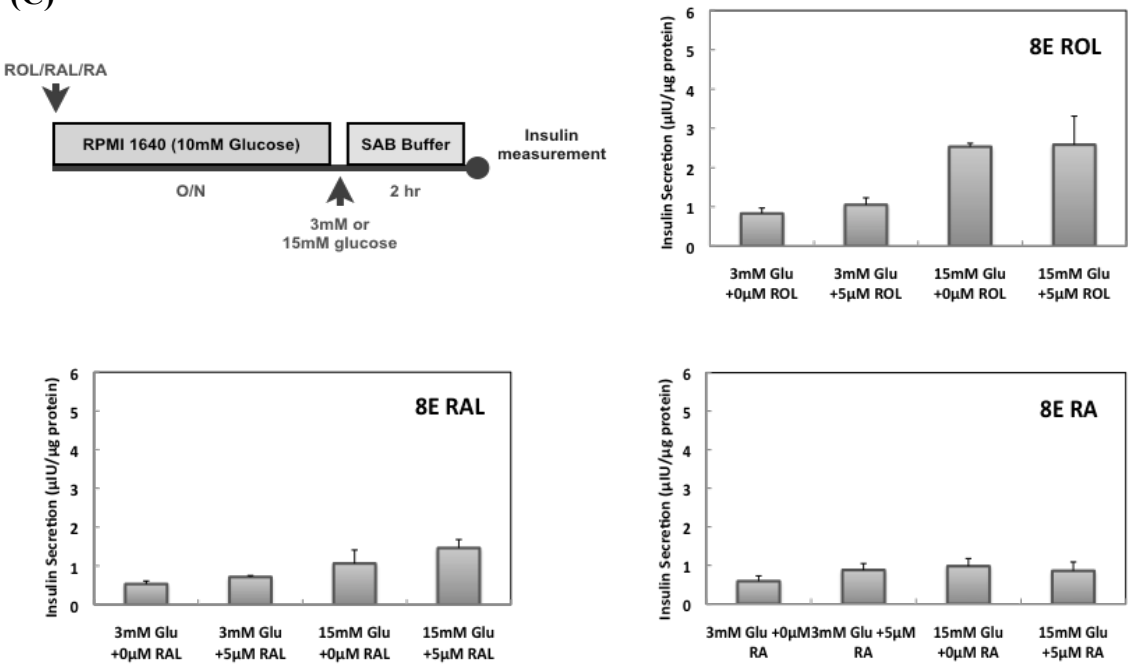

(D)

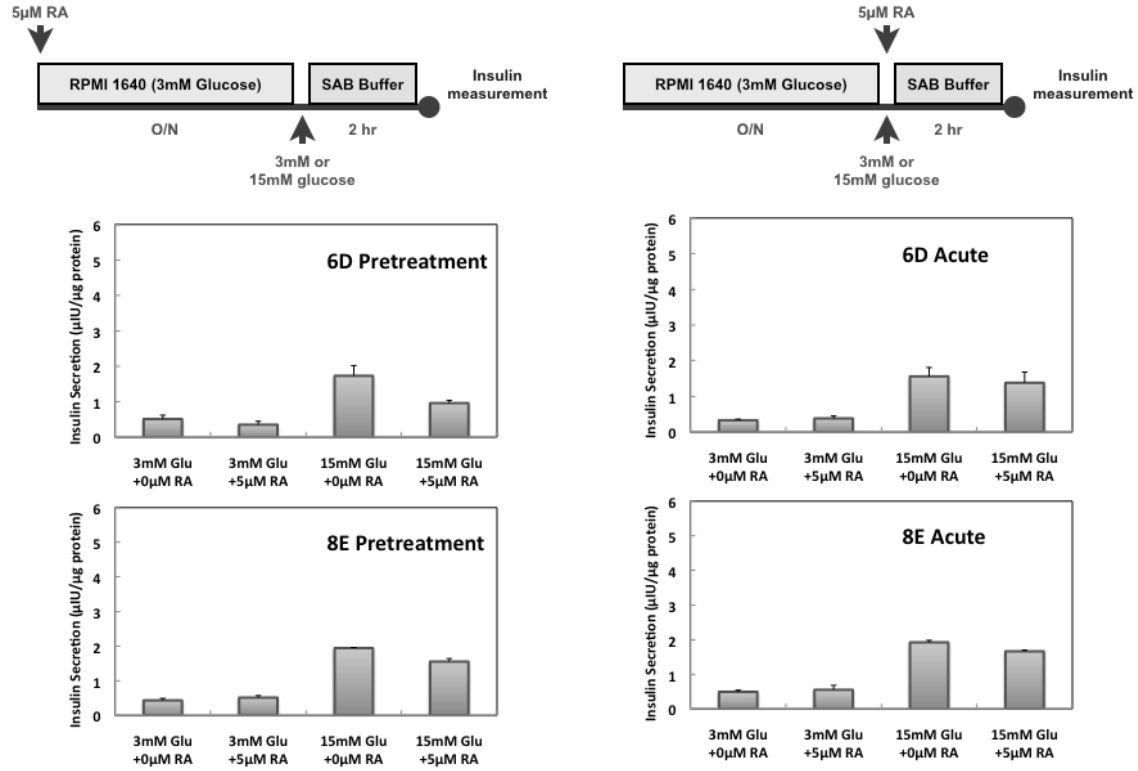

Figure 4-2 Continued

1.2 Chromatin immunoprecipitation analyses of the *Gck* gene promoter in primary hepatocytes

1.2.1 Background summary

Glucokinase (GCK, gene *Gck*), also known as hexokinase D, is a key enzyme in glucose metabolism. It catalyzes the irreversible conversion of glucose into glucose-6-phosphate [310]. Other hexoses such as fructose and mannose can also be phosphorylated by this enzyme, but to a lesser content [310]. Given its important role, *Gck* was proposed to be a gene involved in the pathogenesis of type 2 diabetes. Genetic studies have revealed several diseases, such as maturity onset of diabetes of the young (MODY) [348], persistent hyperinsulinemic hypoglycemia in infancy (PHHI) [349], that are associated with mutated *GCK* gene. The altered glucokinase activity directly leads to abnormal metabolic profile in these patients, demonstrating the central role of glucokinase in regulating glucose metabolism.

Even though glucokinase is expressed in multiple organs, including liver, pancreas, brain, intestine and gonads, its physiological role of maintaining glucose homeostasis is mainly carried out in the hepatocytes and pancreatic β-cells [310]. Studies in the 1960s and 1980s established that glucokinase in the former cell type helped remove glucose from the blood stream, whereas in the latter cell type it worked as a glucose sensor [350-352]. The differential functions of glucokinase in hepatocytes and pancreatic β-cells were mediated by different stimuli, with the former responding to insulin, and the latter to glucose [353]. Additionally, the transcription of glucokinase gene is regulated by tissue-specific enhancers, thereby providing molecular evidence to its differential functions [354-357]. In the hepatocytes, previous luciferase activity assay showed that an upstream region up to -1000bp relative to the transcription start site of *Gck* was able to retain maximal transcription ability of the intact promoter [357]. In order to investigate the transcriptional machinery at the promoter of *Gck* upon insulin and RA treatment, chromatin immunoprecipitation (ChIP) assay was performed.

1.2.2 Procedures of the ChIP assay.

Primary hepatocytes were isolated from ZL rats fed chow diet for 8 weeks according to the previously described protocol [235]. The cells were plated at the concentration of $1x10^7$ cells per 150mm cell culture dish, and pretreated with 100 nM triiodiothyronine

(T3), 100 nM dexamethasone and 1 nM insulin in M199 at 37˚C and 5% CO_2 overnight. After pretreatment, the primary hepatocytes were treated 2 nM insulin and 5μM RA for increasing time period (0, 0.5, 1, 2hr), and then cross-linked by formaldehyde (1% final concentration) for 10 min at room temperature. The cells were dounced by a Whitmann type B dounce to release nuclei. The nuclei were then sonicated with Branson M150 sonicator to generate DNA fragments of 100-1000bp. The fragmented chromatin was incubated with specific antibodies, including anti-Acetyl-histone H3 (Anti-AcH3, Cell Signaling, Danvers, MA, USA) and anti-Rpb1 (Cell Signaling). Normal Rabbit IgG (Millipore, Billerica, MA, USA and Cell Signaling) was used as non-specific control. Target chromatins were pulled down by Protein A or G beads, eluted, and subjected to de-crosslinking. The released DNA fragments were purified and tested by standard PCR with designed primer pairs. The amplicons were stained with ethidium bromide and visualized in 2% agarose gel with Kodak imaging system.

Semi-quantitative analysis was performed with ImageJ software (National Institute Health, MD), which measures the intensity of color of a given area in a picture. Black gives zero intensity by default. Gel images were thus loaded onto the software. A preset area was selected to cover a single DNA band on the gel. Then the brightness of the DNA band was measured and transformed into numbers by the software. The relative amount of the DNA, which corresponds to the brightness of the band, was expressed as the percentage compared to the amount of INPUT DNA.

1.2.3 Optimization of sonication condition

3×10^7 primary hepatocytes were suspended in 3 ml nuclei lysis buffer. (50 mM Tris-HCl, 10 mM EDTA, 1% SDS). Cells were sonicated using 35% power output with a 10 seconds ON/ 40 seconds OFF cycle. Total sonication time is showed in Figure 4-3. 100μl cell lysis was taken out at each time point. 10μl 5M NaCl were added to each sample, which was subjected to de-crosslinking at 65˚C overnight. Total DNA was then extracted with the phenol/chloroform extraction method. 5μg of DNA from each sample was loaded on a 2% agarose gel. As it shows in Figure 4-3, a total sonication time of 6 min was sufficient to break down DNA into 200bp fragments.

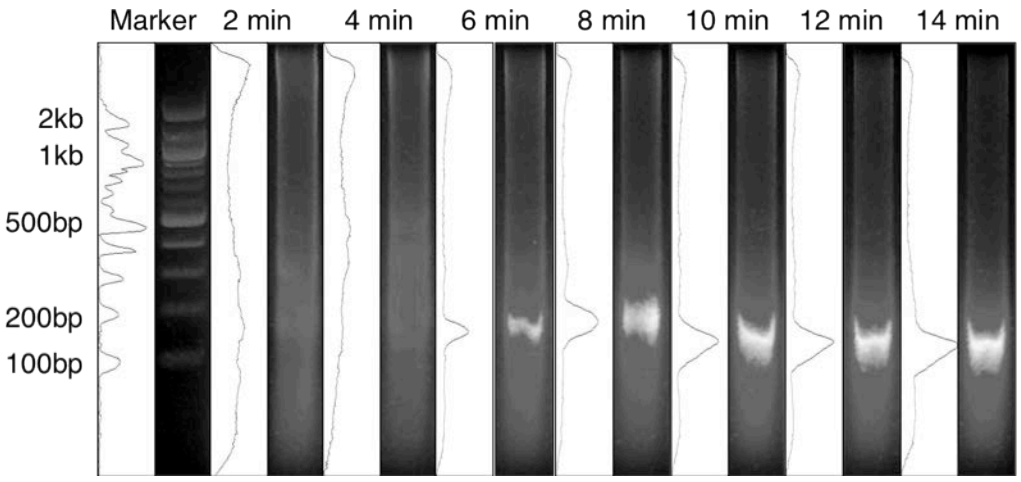

Figure 4-3: The optimization of sonication condition.

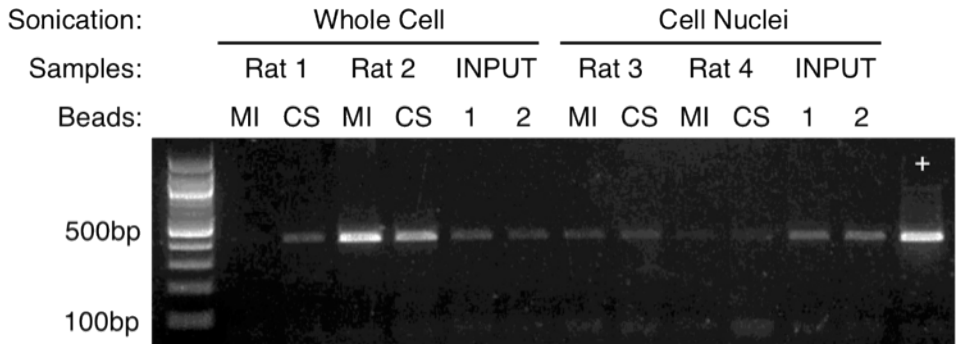

Figure 4-4: Comparison of whole cell and cell nuclei in the ChIP assay. "+" represents the positive control for PCR.

1.2.4 Test whether whole cells or nuclei should be used in the ChIP assay so that less background signal is obtained

Whole cell samples were acquired from two individual rats. Cell nuclei samples were acquired from two individual rats. All samples were sonicated at 35% power with 10 seconds ON/50 seconds OFF cycle for a total of 6 min. Chromatin was precleared with 20µl Santa Cruz protein A/G agarose beads for 2 hrs at 4˚C. Precleared chromatin was aliquoted 100µg DNA per IP. The IP was performed by adding 2µg rabbit IgG overnight and 10µl Millipore Protein A Magnetic Beads (MI) or 10µl Cell Signaling Protein G Agarose Beads (CS) for 2 hrs. The final elute was amplified with primer pairs oGC786/797 which target the *Gck* promoter. Figure 4-4 showed that using cell nuclei gave out less background signal. The graph also suggested that MI and CS beads gave out similar background signal.

1.2.5 Test the amount of chromatin needed for each IP

Decreasing amount of precleared chromatin (100µg, 50µg, 25µg, 10µg) was used for each IP. DynaBeads (Invitrogen) was either preblocked with 1 mg/ml BSA and 30 µg/ml pGL-Basic plasmid at 4˚C for 2 hrs. IP was done by adding 2µg rabbit IgG or 2µl anti-AcH3. ChIP assay was performed as described in the protocol. The final elute was amplified with primer pairs oGC788/794 which target *Gck* promoter. The result (Figure 4-5) showed that decreasing initial amount of chromatin for each IP would decrease the signal, thus decrease the resolution of the assay.

1.2.6 Test of preclearing condition

For each IP, 100 µg crude chromation is used. To test preclearing condition, two different chromatin samples were precleared by 20 µl Santa Cruz protein A/G beads with or without 2 µg Rabbit IgG overnight. Then IP was performed by using 2 µg Rabbit IgG. The final elute was amplified with primer pairs Cyp26a1-1/2. The result (Figure 4-6) showed that adding IgG at the preclearing step did not improve background signal.

1.2.7 Test of different beads and preblocking condition

100µg precleared chromatin was used for each IP. Millipore Magnetic Beads was either preblocked with 1 mg/ml BSA and 30 µg/ml pGL-Basic plasmid, or not blocked at 4˚C for 2 hrs. IP was done by adding no reagent or 2µg rabbit IgG or 2µl rat serum. ChIP assay was performed as described in the protocol. The final elute was amplified with

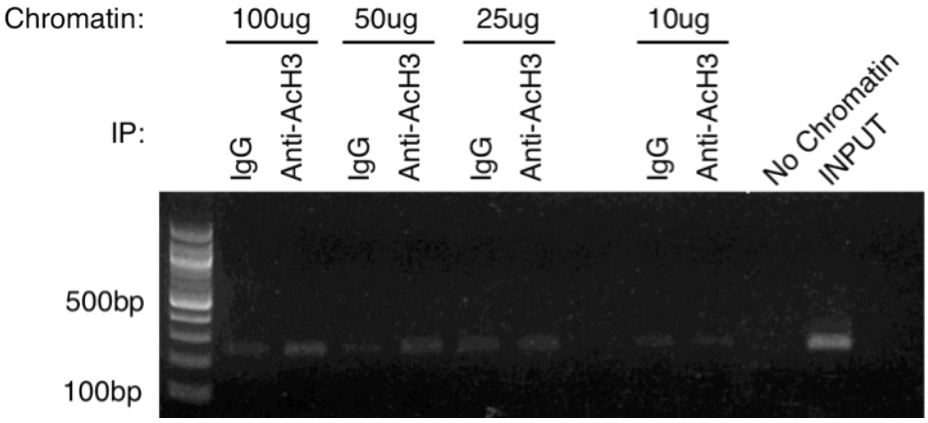

Figure 4-5: Test of the amount of chromatin needed for each IP.

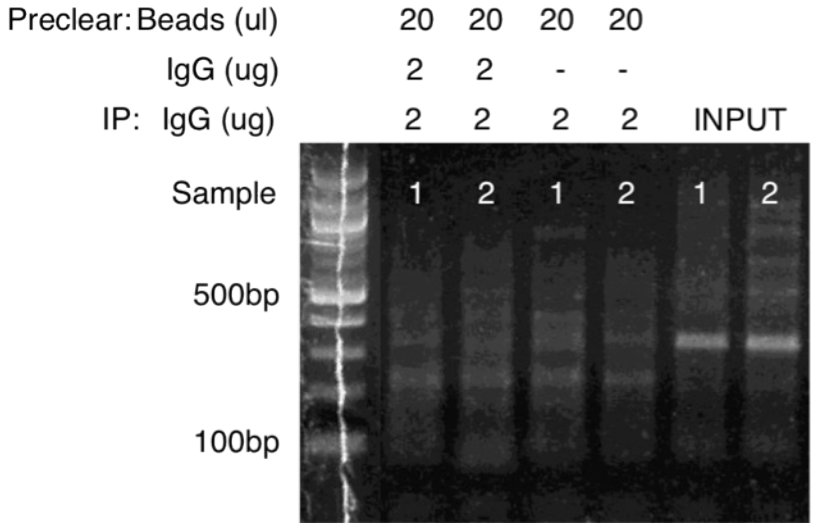

Figure 4-6: Test of the preclearing condition.

primer pairs oGC788/794 which target Gck promoter. Similar experiments were also performed for the Cell Signaling Protein G Beads and the Invitrogen DynaBeads. As we can see from Figure 4-7, the preblocking did not significantly reduce background signal.

1.2.8 Test beads amount and antibody amount

100µg precleared chromatin was used for each IP. DynaBeads was preblocked with 1 mg/ml BSA and 30 µg/ml pGL-Basic plasmid at 4˚C for 2 hrs. IP was done by adding decreasing amount of rabbit IgG or anti-AcH3 as shown in the Figure 4-8. ChIP assay was performed as described in the protocol. The final elute was amplified with primer pairs oGC788/794 which target *Gck* promoter. As we can see, the combination of fewer beads and antibody would lead to loss of signal.

1.2.9 Glycine interferes with the specific antibody-antigen binding

For each IP, 100µg precleared chromatin was used. In the IP system increasing amount of glycine (0 nM to 10 mM) was added. IP was performed by using 2µg rabbit IgG or 2µg anti-AcH3 antibodies overnight. The rest of the ChIP was performed according standard protocol. As Figure 4-9 suggests, glycine interferes with Ag-Ab binding at 0.1 mM and above without affecting non-specific binding.

1.2.10 No change of RNA polymerase II binding was observed at the hepatic *Gck* promoter 2 hrs after RA and Insulin treatment.

Primary hepatocytes were plated at the concentration of $1x10^7$ cells per 150mm cell culture dishes, and pretreated with 100 nM triiodiothyronine (T3), 100 nM dexamethasone and 1 nM insulin in M199 overnight. After pretreatment, the primary hepatocytes were exposed to 2 nM insulin and 5µM RA for increasing time period (0, 0.5, 1, 2hr), and then cross-linked by formaldehyde (1% final concentration) for 10min at room temperature. The nuclei of the cells were released by douncing with a type B douncer, and then sonicated at the 35% power output with 10sec ON/ 50sec OFF cycle for a total of 6min. The fragmented chromatin was incubated with 2µg Anti-AcH3, and 2µg anti-Rpb1. Normal rabbit IgG was used as non-specific control. Target chromatins were pulled down by 10µl Invitrogen Dynabeads, eluted, and subjected to de-crosslinking. The released DNA fragments were purified and tested by standard PCR with primer pair oGC788/794, which target the promoter region of hepatic *Gck*. The amplicons were stained with ethidium bromide and visualized in 2% agarose gel. The result (n=3) showed

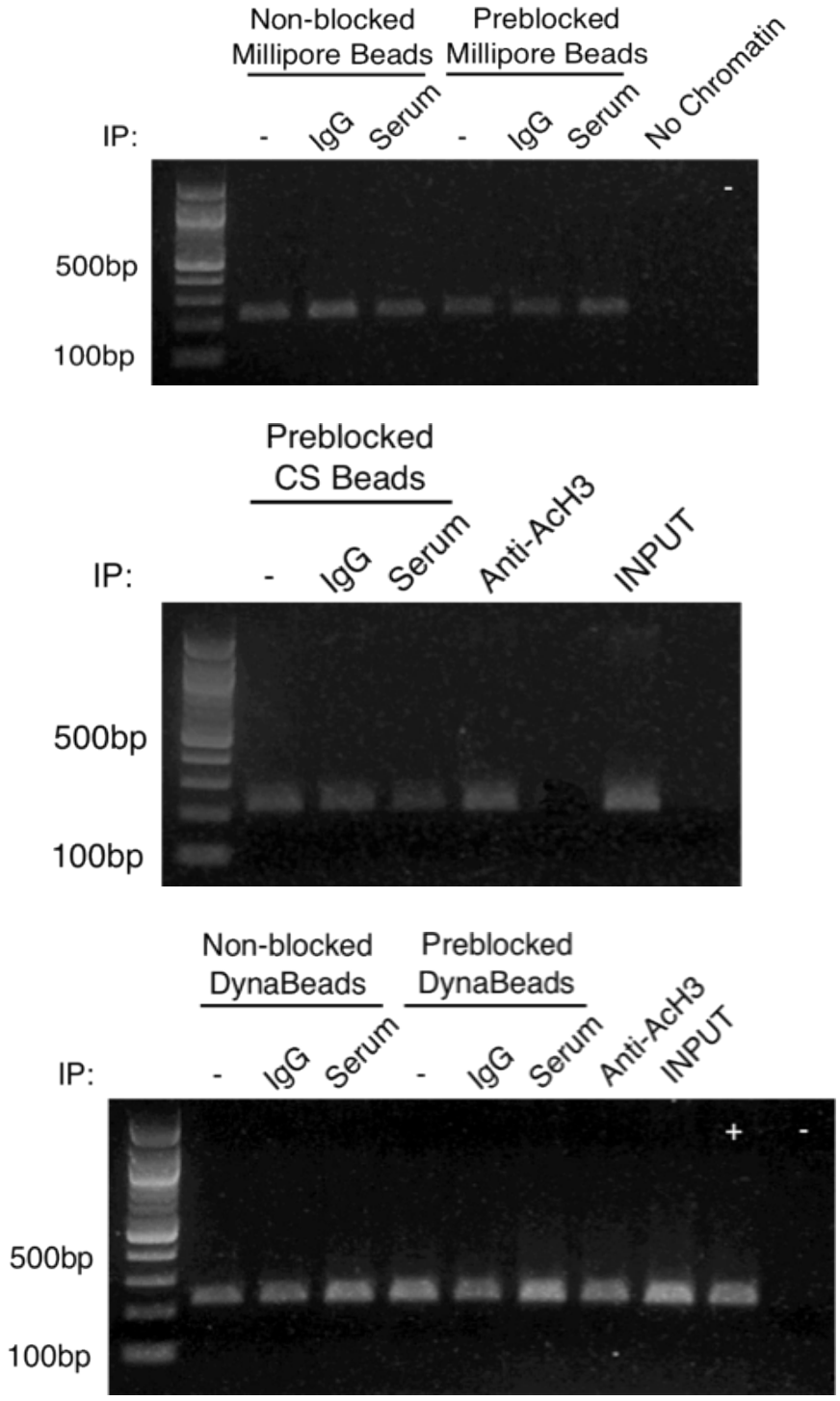

Figure 4-7: Test of different beads and the preblocking condition.

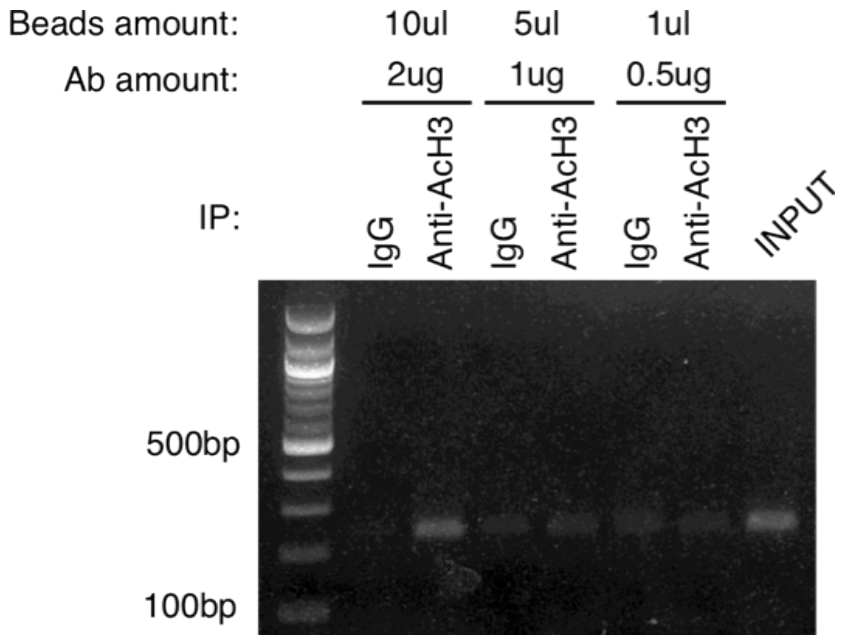

Fig. 4-8: Test of beads amount and antibody amount.

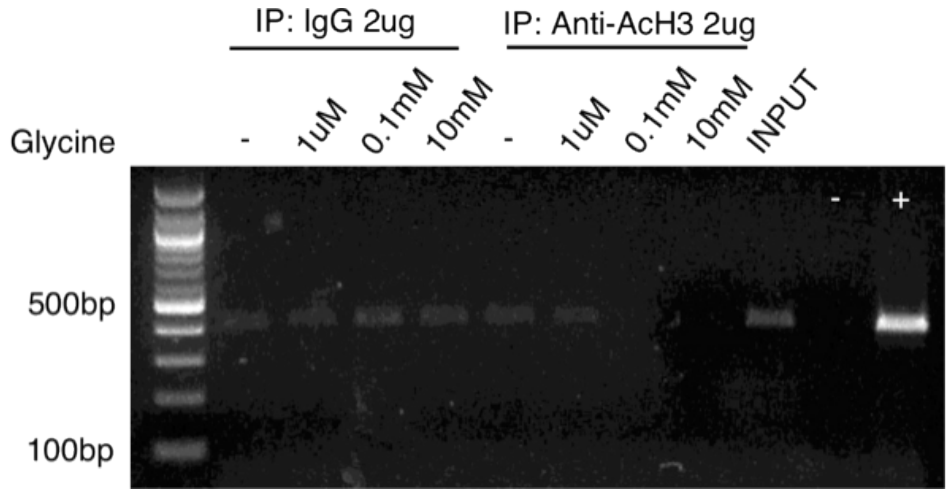

Figure 4-9: Glycine interferes with the specific antibody-antigen binding.

that within 2 hrs of treatment with 2 nM insulin and 5μM RA, the binding of RNA polymerase II to the promoter of hepatic *Gck* did not significantly change (Figure 4-10, Two-way ANOVA, $p>0.05$ for the time variable).

2. Conclusion and future directions

2.1 Conclusion

This dissertation explores the effects of hormonal and dietary factors on glucose and lipid metabolism in the liver. Specifically using ZF rats, a genetic model of obesity and insulin resistance, current research in the dissertation probes the molecular mechanisms underlying two study questions: (1) How does VA affect the hepatic glucose and lipid metabolism at the gene transcription level? (2) How does aPKC contribute to the hepatic insulin resistance in the liver of ZF rats? The answers to these two questions are delineated in the Chapters II and III, which provide insights into the development of hepatic insulin resistance and metabolic disease.

In Chapter II, we investigated the effects of food intake and VA status on the insulin-regulated gene expression in primary hepatocytes from ZL and ZF rats, and obtained the following results. First, the insulin-regulated *Gck*, *Pck1* and *Srebp-1c* expressions were impaired in the primary hepatocytes of the ZF rat fed chow diet ad libitum, confirming our previous observation [312]. The impairment was partially corrected if the ZF rats were fed a VAD diet ad libitum to induce VA deficiency, or they were pair-fed the same amount of a VAS diet in calories consumed by their VAD counterparts. Second, the ZL and ZF rats pair-fed the isocaloric VAS diet had higher body mass than those fed the VAD diet at the end of dietary manipulation. The pair-fed ZL and ZF rats tended to overeat when sufficient amount of food was provided at the end of the 8-week feeding paradigm. Third, transient over intake of the VAS diet for one day caused the impairment of insulin-regulated *Gck*, *Pck1* and *Srebp-1c* genes expression in the primary hepatocytes of both pair-fed ZL and ZF rats. Fourth, transient overeating for one day greatly affected the expression levels of genes involved in VA metabolism in response to insulin treatment in the hepatocytes of ZL and ZF rats. Taken together, these observations show that both food intake and VA status of rats affect hepatic insulin sensitivity at gene expression level in the hepatocytes.

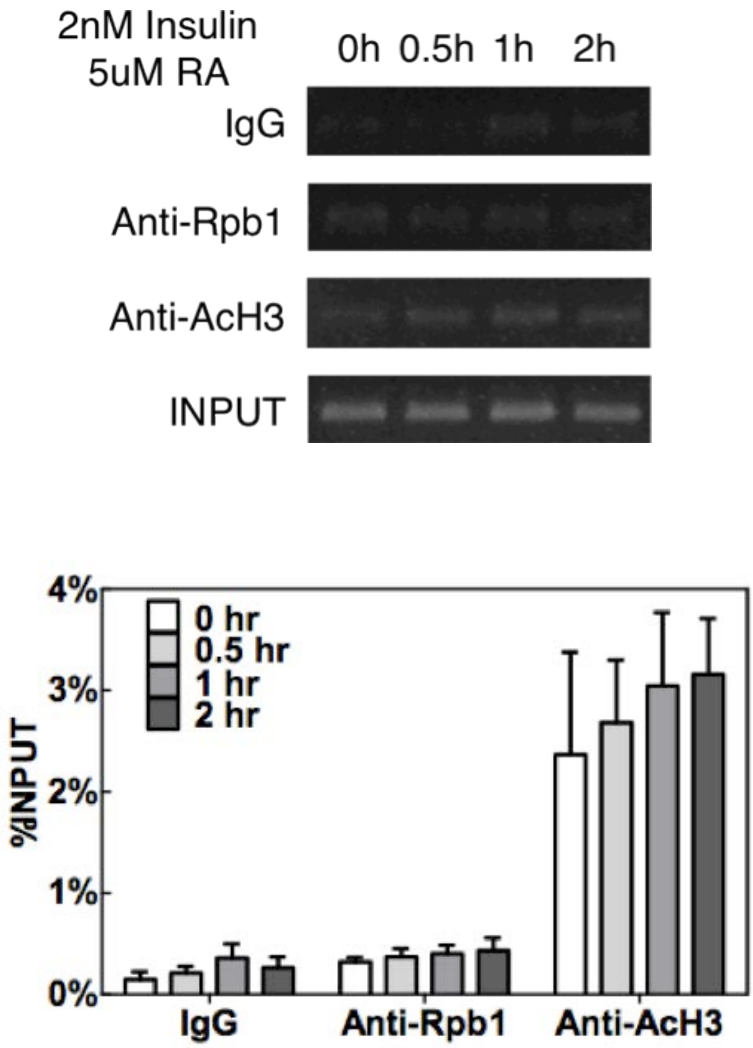

Figure 4-10: Representative ChIP assay results and the densitometry analysis of three independent experiments. The error bar represents S.E.M.

In Chapter III, we investigated the roles of PKCζ and PKCι/λ on the insulin-regulated gene expression in the liver tissues and primary hepatocytes of Zucker rats, which yielded the following findings. First, ZL and ZF rats exhibited similar mRNA and protein levels of PKCι/λ in the liver tissues and primary hepatocytes. The mRNA and protein levels of PKCζ, and the level of phosphorylated PKCζ/λ, on the other hand, were elevated in the liver tissues and primary hepatocytes of ZF rats. Second, the phosphorylation levels of AKT Ser473 were elevated in the liver tissues of ZF rats. However, this induction does not seem to affect the impairment of insulin-regulated gene expression in ZF hepatocytes. The basal level of AKT Ser473 phosphorylation in ZF primary hepatocytes dropped upon pretreatment, which was not associated with any return of insulin-regulated gene expression in the same cells, suggesting other factors probably play a role in the impairment. This conclusion is supported by the fact that the levels of lipogenic enzymes were still elevated in the primary hepatocytes of ZF rats after pretreatment. Third, adenoviral mediated PKCζ and PKCι/λ overexpression blunted the insulin-induced phosphorylation of AKT, and decreased the IRS1 level in the primary hepatocytes of ZL rats. Fourth, adenoviral mediated PKCζ and PKCι/λ overexpressions in the ZL primary hepatocytes attenuated the insulin-regulated *Gck*, *Pck1* and *Srebp-1c* genes expression. These findings collectively demonstrate that PKCζ and PKCι/λ serve as negative feedback regulators of hepatic insulin signaling cascade, and play critical roles in the regulation of hepatic glucose and lipid metabolism.

2.2 Future directions

Even though the results presented in this dissertation have provided ample evidence that both VA and aPKC affect insulin-regulated gene expression in the liver, future research questions can be extracted from the findings to help extend our understandings of the development of insulin resistance and its related metabolic diseases.

2.2.1 How does overeating for one day affect the metabolic profile of Zucker rats?

In this dissertation, we found that overeating of a VAS diet for one day altered the VA metabolic gene expression, and caused the impairment of insulin-regulated gene expression in the primary hepatocytes of ZL and ZF rats. It would be interesting to see if these gene expression changes lead to broader metabolic changes *in vivo*. For example, will the transient overeating lead to alterations of serum levels of insulin, glucagon and

leptin? Does dysregulated hepatic *Gck*, *Pck1* and *Srebp-1c* genes expression forebode increased serum glucose level, hepatic glucose production and hepatic lipogenesis? Answers to these questions will provide additional information about the development of insulin resistance by overnutrition.

2.2.2 How does RA regulate the hepatic expression of *Gck*, *Pck1* and *Srebp-1c*?

It is evident that RA, as a natural metabolite of VA, regulates the hepatic expression of *Gck*, *Pck1* and *Srebp-1c*. However, the knowledge about the transcriptional machinery that mediates the actions of RA in the expression of *Gck*, *Pck1* and *Srebp-1c* is still limited. More detail studies are needed to identify the transcription factors that are responsible for mediating both RA and insulin effects. By using biochemical and molecular research tools, such as ChIP and mobility shift assay, we should be able to delineate the components of transcriptional machinery in the promoters of those genes. The findings will help identify therapeutic targets to combat dysregulated metabolic gene expression in obesity and type 2 diabetes.

2.2.3 How is the gene expression of *Prkcz* and *Prkci* regulated?

One interesting finding in Chapter III was that insulin seemed to attenuate the expression of *Prkci* in the primary hepatocytes overexpressing *Prkcz*. This suggests that *Prkci* expression is regulated by both insulin and PKCζ. Given the fact that: (1) PKCζ and PKCι/λ share high homology; (2) PKCζ and PKCι/λ both attenuate the insulin signaling cascade in the hepatocytes when overexpressed, the investigation into how their gene expression is regulated will further delineate the roles of aPKC in the development of insulin resistance.

2.2.4 What are other downstream substrates of PKCζ and PKCι/λ in the regulation of hepatic gene expression?

In Chapter III, we demonstrated that PKCζ and PKCι/λ overexpressions increased the basal transcript levels of *Gck*, *Pck1* and *Srebp-1c*. It is possible that these increases are mediated through the modification of certain transcription factors or downstream proteins targeted by PKCζ and PKCι/λ. The discovery of these downstream substrates will provide new research ground for the understanding of hepatic insulin resistance and its related metabolic diseases.

LIST OF REFERENCES

1 Consultation, W. (2000) Obesity: preventing and managing the global epidemic. World Health Organization technical report series.

2 World Health Organization (Ed.). (2011) Chapter 1 Burden: mortality, morbidity and risk factors. In Global status report on noncommunicable diseases 2010 - Description of the global burden of NCDs, their risk factors and determinants, pp 1–23.

3 Jensen, M. D., Ryan, D. H., Apovian, C. M., Loria, C. M., Ard, J. D., Millen, B. E., Comuzzie, A. G., Nonas, C. A., Donato, K. A., Pi-Sunyer, F. X., et al. (2013) 2013 AHA/ACC/TOS Guideline for the Management of Overweight and Obesity in Adults: A Report of the American College of Cardiology/American Heart Association Task Force on Practice Guidelines and The Obesity Society. J. Am. Coll. Cardiol.

4 Gallagher, E. J., LeRoith, D. and Karnieli, E. (2008) The Metabolic Syndrome—from Insulin Resistance to Obesity and Diabetes. Endocrinology and Metabolism Clinics of North America **37**, 559–579.

5 Reaven, G. M. (1988) Banting lecture 1988. Role of insulin resistance in human disease. Diabetes **37**, 1595–1607.

6 Gallagher, E. J., LeRoith, D. and Karnieli, E. (2011) The Metabolic Syndrome—from Insulin Resistance to Obesity and Diabetes. Medical Clinics of NA, Elsevier Inc **95**, 855–873.

7 Malik, S., Wong, N. D., Franklin, S. S., Kamath, T. V., L'Italien, G. J., Pio, J. R. and Williams, G. R. (2004) Impact of the metabolic syndrome on mortality from coronary heart disease, cardiovascular disease, and all causes in United States adults. Circulation **110**, 1245–1250.

8 Girman, C. J., Rhodes, T., Mercuri, M., Pyörälä, K., Kjekshus, J., Pedersen, T. R., Beere, P. A., Gotto, A. M., Clearfield, M.4S Group and the AFCAPS/TexCAPS Research Group. (2004) The metabolic syndrome and risk of major coronary events in the Scandinavian Simvastatin Survival Study (4S) and the Air Force/Texas Coronary Atherosclerosis Prevention Study (AFCAPS/TexCAPS). Am. J. Cardiol. **93**, 136–141.

9 Rutter, M. K., Meigs, J. B., Sullivan, L. M., D'Agostino, R. B. and Wilson, P. W.

(2005) Insulin resistance, the metabolic syndrome, and incident cardiovascular events in the Framingham Offspring Study. Diabetes **54**, 3252–3257.

10 White, M. F. (2003) Insulin signaling in health and disease. Science **302**, 1710–1711.

11 Kasuga, M., Karlsson, F. A. and Kahn, C. R. (1982) Insulin stimulates the phosphorylation of the 95,000-dalton subunit of its own receptor. Science **215**, 185–187.

12 Petruzzelli, L. M., Ganguly, S., Smith, C. J., Cobb, M. H., Rubin, C. S. and Rosen, O. M. (1982) Insulin activates a tyrosine-specific protein kinase in extracts of 3T3-L1 adipocytes and human placenta. Proc. Natl. Acad. Sci. U.S.A. **79**, 6792–6796.

13 McKern, N. M., Lawrence, M. C., Streltsov, V. A., Lou, M.-Z., Adams, T. E., Lovrecz, G. O., Elleman, T. C., Richards, K. M., Bentley, J. D., Pilling, P. A., et al. (2006) Structure of the insulin receptor ectodomain reveals a folded-over conformation. Nature **443**, 218–221.

14 Cohen, P. (2006) The twentieth century struggle to decipher insulin signalling. Nat. Rev. Mol. Cell Biol. **7**, 867–873.

15 Taniguchi, C. M., Emanuelli, B. and Kahn, C. R. (2006) Critical nodes in signalling pathways: insights into insulin action. Nat. Rev. Mol. Cell Biol. **7**, 85–96.

16 Bellacosa, A., Chan, T. O., Ahmed, N. N., Datta, K., Malstrom, S., Stokoe, D., McCormick, F., Feng, J. and Tsichlis, P. (1998) Akt activation by growth factors is a multiple-step process: the role of the PH domain. Oncogene **17**, 313–325.

17 Sarbassov, D. D., Guertin, D. A., Ali, S. M. and Sabatini, D. M. (2005) Phosphorylation and regulation of Akt/PKB by the rictor-mTOR complex. Science **307**, 1098–1101.

18 Hagiwara, A., Cornu, M., Cybulski, N., Polak, P., Betz, C., Trapani, F., Terracciano, L., Heim, M. H., Rüegg, M. A. and Hall, M. N. (2012) Hepatic mTORC2 activates glycolysis and lipogenesis through Akt, glucokinase, and SREBP1c. Cell Metab. **15**, 725–738.

19 Laplante, M. and Sabatini, D. M. (2012) mTOR signaling in growth control and disease. Cell **149**, 274–293.

20 Pearce, L. R., Komander, D. and Alessi, D. R. (2010) The nuts and bolts of AGC protein kinases. Nat. Rev. Mol. Cell Biol. **11**, 9–22.

21 Cheatham, B. (2000) GLUT4 and company: SNAREing roles in insulin-regulated glucose uptake. Trends Endocrinol. Metab. **11**, 356–361.

22 Cross, D. A., Alessi, D. R., Cohen, P., Andjelkovich, M. and Hemmings, B. A. (1995) Inhibition of glycogen synthase kinase-3 by insulin mediated by protein kinase B. Nature **378**, 785–789.

23 Scott, P. H., Brunn, G. J., Kohn, A. D., Roth, R. A. and Lawrence, J. C. (1998) Evidence of insulin-stimulated phosphorylation and activation of the mammalian target of rapamycin mediated by a protein kinase B signaling pathway. Proc. Natl. Acad. Sci. U.S.A. **95**, 7772–7777.

24 Chen, G. (2013) Roles of Vitamin A Metabolism in the Development of Hepatic Insulin Resistance. ISRN Hepatology **2013**, 1–21.

25 Farese, R. V. and Sajan, M. P. (2010) Metabolic functions of atypical protein kinase C: "good" and “bad” as defined by nutritional status. Am. J. Physiol. Endocrinol. Metab. **298**, E385–94.

26 Stross, C., Keitel, V., Winands, E., Häussinger, D. and Kubitz, R. (2009) Expression and localization of atypical PKC isoforms in liver parenchymal cells. Biological Chemistry **390**, 235–244.

27 Standaert, M. L., Galloway, L., Karnam, P., Bandyopadhyay, G., Moscat, J. and Farese, R. V. (1997) Protein kinase C-zeta as a downstream effector of phosphatidylinositol 3-kinase during insulin stimulation in rat adipocytes. Potential role in glucose transport. J. Biol. Chem. **272**, 30075–30082.

28 Kotani, K., Ogawa, W., Matsumoto, M., Kitamura, T., Sakaue, H., Hino, Y., Miyake, K., Sano, W., Akimoto, K., Ohno, S., et al. (1998) Requirement of atypical protein kinase clambda for insulin stimulation of glucose uptake but not for Akt activation in 3T3-L1 adipocytes. Molecular and Cellular Biology **18**, 6971–6982.

29 Farese, R. V., Sajan, M. P., Yang, H., Li, P., Mastorides, S., Gower, W. R., Nimal, S., Choi, C. S., Kim, S., Shulman, G. I., et al. (2007) Muscle-specific knockout of PKC-lambda impairs glucose transport and induces metabolic and diabetic

syndromes. J. Clin. Invest. **117**, 2289–2301.

30 Matsumoto, M., Ogawa, W., Akimoto, K., Inoue, H., Miyake, K., Furukawa, K., Hayashi, Y., Iguchi, H., Matsuki, Y., Hiramatsu, R., et al. (2003) PKClambda in liver mediates insulin-induced SREBP-1c expression and determines both hepatic lipid content and overall insulin sensitivity. J. Clin. Invest. **112**, 935–944.

31 Standaert, M. L., Sajan, M. P., Miura, A., Kanoh, Y., Chen, H. C., Farese, R. V. and Farese, R. V. (2004) Insulin-induced activation of atypical protein kinase C, but not protein kinase B, is maintained in diabetic (ob/ob and Goto-Kakazaki) liver. Contrasting insulin signaling patterns in liver versus muscle define phenotypes of type 2 diabetic and high fat-induced insulin-resistant states. J. Biol. Chem. **279**, 24929–24934.

32 Taniguchi, C. M., Kondo, T., Sajan, M., Luo, J., Bronson, R., Asano, T., Farese, R., Cantley, L. C. and Kahn, C. R. (2006) Divergent regulation of hepatic glucose and lipid metabolism by phosphoinositide 3-kinase via Akt and PKClambda/zeta. Cell Metab. **3**, 343–353.

33 Sajan, M. P., Standaert, M. L., Nimal, S., Varanasi, U., Pastoor, T., Mastorides, S., Braun, U., Leitges, M. and Farese, R. V. (2009) The critical role of atypical protein kinase C in activating hepatic SREBP-1c and NF B in obesity. J. Lipid Res. **50**, 1133–1145.

34 Sajan, M. P., Standaert, M. L., Rivas, J., Miura, A., Kanoh, Y., Soto, J., Taniguchi, C. M., Kahn, C. R. and Farese, R. V. (2009) Role of atypical protein kinase C in activation of sterol regulatory element binding protein-1c and nuclear factor kappa B (NFkappaB) in liver of rodents used as a model of diabetes, and relationships to hyperlipidaemia and insulin resistance. Diabetologia **52**, 1197–1207.

35 Sajan, M. P. and Farese, R. V. (2012) Insulin signalling in hepatocytes of humans with type 2 diabetes: excessive production and activity of protein kinase C-ι (PKC-ι) and dependent processes and reversal by PKC-ι inhibitors. Diabetologia **55**, 1446–1457.

36 Sajan, M. P., Nimal, S., Mastorides, S., Acevedo-Duncan, M., Kahn, C. R., Fields, A. P., Braun, U., Leitges, M. and Farese, R. V. (2012) Correction of metabolic abnormalities in a rodent model of obesity, metabolic syndrome, and type 2

diabetes mellitus by inhibitors of hepatic protein kinase C-ι. Metab. Clin. Exp. **61**, 459–469.

37 Brown, M. S. and Goldstein, J. L. (2008) Selective versus total insulin resistance: a pathogenic paradox. Cell Metab. **7**, 95–96.

38 Johnson, A. M. F. and Olefsky, J. M. (2013) The Origins and Drivers of Insulin Resistance. Cell, Elsevier Inc. **152**, 673–684.

39 Hotamisligil, G. S., Shargill, N. S. and Spiegelman, B. M. (1993) Adipose expression of tumor necrosis factor-alpha: direct role in obesity-linked insulin resistance. Science **259**, 87–91.

40 Gregor, M. F. and Hotamisligil, G. S. (2011) Inflammatory mechanisms in obesity. Annu. Rev. Immunol. **29**, 415–445.

41 McGarry, J. D. (1992) What if Minkowski had been ageusic? An alternative angle on diabetes. Science **258**, 766–770.

42 Zhao, S., Li, R., Li, Y., Chen, W., Zhang, Y. and Chen, G. (2012) Roles of vitamin A status and retinoids in glucose and fatty acid metabolism. Biochem. Cell Biol. **90**, 142–152.

43 Fall, T. and Ingelsson, E. (2014) Genome-wide association studies of obesity and metabolic syndrome. Mol. Cell. Endocrinol. **382**, 740–757.

44 Kopelman, P. (2010) Symposium 1: Overnutrition: consequences and solutions. Foresight Report: the obesity challenge ahead. Proc Nutr Soc **69**, 80–85.

45 Key, T. J., Spencer, E. A. and Reeves, G. K. (2010) Symposium 1: Overnutrition: consequences and solutions. Obesity and cancer risk. Proc Nutr Soc **69**, 86–90.

46 IARC. (1999) IARC Handbooks of Cancer Prevention, IARC Scientific Publications.

47 Wolf, G. (1996) A history of vitamin A and retinoids. FASEB J. **10**, 1102–1107.

48 Wolf, G. (2002) The experimental induction of vitamin A deficiency in humans. J. Nutr. **132**, 1805–1811.

49 Moore, T. (1957) Vitamin A., Elsevier Publishing Company.

50 Moore, T. (1930) Vitamin A and carotene: The absence of the liver oil vitamin A from carotene. VI. The conversion of carotene to vitamin A in vivo. Biochem. J. **24**, 692–702.

51 Stipanuk, M. H. and Caudill, M. A. (2012) Biochemical, Physiological, and Molecular Aspects of Human Nutrition 3rd ed., Elsevier.

52 Skibsted, L. H. (2012) Carotenoids in antioxidant networks. Colorants or radical scavengers. J. Agric. Food Chem. **60**, 2409–2417.

53 Edisbury, J. R., Morton, R. A. and Simpkins, G. W. (1937) A Possible Vitamin A2. Nature **140**, 234–234.

54 Rigopoulos, D., Ioannides, D., Kalogeromitros, D. and Katsambas, A. D. (2004) Comparison of topical retinoids in the treatment of acne. Clin. Dermatol. **22**, 408–411.

55 Haushalter, K., Murad, E. J., Dabade, T. S., Rowell, R., Pearce, D. J. and Feldman, S. R. (2012) Efficacy of low-dose acitretin in the treatment of psoriasis. J Dermatolog Treat **23**, 400–403.

56 Bettoli, V., Zauli, S. and Virgili, A. (2013) Retinoids in the chemoprevention of non-melanoma skin cancers: why, when and how. J Dermatolog Treat.

57 Saari, J. C. (2012) Vitamin A metabolism in rod and cone visual cycles. Annu. Rev. Nutr. **32**, 125–145.

58 Robeson, C. and Baxter, J. (1947) Neovitamin A. J. Am. Chem. Soc. **69**, 136–141.

59 Harris, P. L., Ames, S. R. and Brinkman, J. H. (1951) Biochemical studies on vitamin A. IX. Biopotency of neovitamin A in the rat. J. Am. Chem. Soc., ACS Publications **73**, 1252–1254.

60 Sporn, M. B. and Roberts, A. B. (1994) The Retinoids 2nd ed., Raven Press, New York.

61 Noy, N. (1992) The ionization behavior of retinoic acid in aqueous environments and bound to serum albumin. Biochim. Biophys. Acta **1106**, 151–158.

62 Dingle, J. T. and Lucy, J. A. (1965) Vitamin A, Carotinoids and Cell Function. Biol Rev Camb Philos Soc **40**, 422–461.

63 Tsukida, K., Ito, M. and Ikeda, F. (1971) Vitamin A degradation products encountered on vitamin A analysis. I. The structures of retrovitamin A, anhydrovitamin A, and isoanhydrovitamin A. Int J Vitam Nutr Res **41**, 158–170.

64 Hickman, K. C. D., Harris, P. L. and Woodside, M. R. (1942) Interrelationship of Vitamins A and E. Nature **150**, 91–92.

65 Drummond, J. C., Bell, M. E. and Palmer, E. T. (1935) Observations on the Absorption of Carotene and Vitamin A. Br Med J **1**, 1208–1210.

66 Rigtrup, K. M. and Ong, D. E. (1992) A retinyl ester hydrolase activity intrinsic to the brush border membrane of rat small intestine. Biochemistry **31**, 2920–2926.

67 Rigtrup, K. M., Kakkad, B. and Ong, D. E. (1994) Purification and partial characterization of a retinyl ester hydrolase from the brush border of rat small intestine mucosa: probable identity with brush border phospholipase B. Biochemistry **33**, 2661–2666.

68 Dew, S. E. and Ong, D. E. (1994) Specificity of the retinol transporter of the rat small intestine brush border. Biochemistry **33**, 12340–12345.

69 Erdman, J. W., Bierer, T. L. and Gugger, E. T. (1993) Absorption and transport of carotenoids. Ann. N. Y. Acad. Sci. **691**, 76–85.

70 Parker, R. S. (1996) Absorption, metabolism, and transport of carotenoids. FASEB J. **10**, 542–551.

71 Fidge, N. H., Shiratori, T., Ganguly, J. and Goodman, D. S. (1968) Pathways of absorption of retinal and retinoic acid in the rat. J. Lipid Res. **9**, 103–109.

72 Zimmerman, C. L., Han, S. and Wiedmann, T. S. (2001) The absorption of retinoic acids from the gastrointestinal tract is dependent upon chemical structure. Cancer Chemother. Pharmacol. **47**, 27–33.

73 Goodman, D. S. and Huang, A. S. (1965) Biosynthesis of vitamin A with rat intestinal enzymes. Science **149**, 879–880.

74 Wyss, A., Wirtz, G., Woggon, W., Brugger, R., Wyss, M., Friedlein, A., Bachmann, H. and Hunziker, W. (2000) Cloning and expression of beta,beta-carotene 15,15'-dioxygenase. Biochem. Biophys. Res. Commun. **271**, 334–336.

75 Wyss, A., Wirtz, G. M., Woggon, W. D., Brugger, R., Wyss, M., Friedlein, A., Riss, G., Bachmann, H. and Hunziker, W. (2001) Expression pattern and localization of beta,beta-carotene 15,15'-dioxygenase in different tissues. Biochem. J. **354**, 521–529.

76 Wang, X. D., Russell, R. M., Liu, C., Stickel, F., Smith, D. E. and Krinsky, N. I. (1996) Beta-oxidation in rabbit liver in vitro and in the perfused ferret liver contributes to retinoic acid biosynthesis from beta-apocarotenoic acids. J. Biol.

Chem. **271**, 26490–26498.

77 Kiefer, C., Hessel, S., Lampert, J. M., Vogt, K., Lederer, M. O., Breithaupt, D. E. and Lintig, von, J. (2001) Identification and characterization of a mammalian enzyme catalyzing the asymmetric oxidative cleavage of provitamin A. J. Biol. Chem. **276**, 14110–14116.

78 Harrison, E. H. (2005) Mechanisms of digestion and absorption of dietary vitamin A. Annu. Rev. Nutr. **25**, 87–103.

79 MacDonald, P. N. and Ong, D. E. (1987) Binding specificities of cellular retinol-binding protein and cellular retinol-binding protein, type II. J. Biol. Chem. **262**, 10550–10556.

80 MacDonald, P. N. and Ong, D. E. (1988) Evidence for a lecithin-retinol acyltransferase activity in the rat small intestine. J. Biol. Chem. **263**, 12478–12482.

81 Helgerud, P., Petersen, L. B. and Norum, K. R. (1982) Acyl CoA:retinol acyltransferase in rat small intestine: its activity and some properties of the enzymic reaction. J. Lipid Res. **23**, 609–618.

82 Eden, E. and Sellers, K. C. (1949) The absorption of vitamin A in ruminants and rats. Biochem. J. **44**, 264–267.

83 Nayak, N., Harrison, E. H. and Hussain, M. M. (2001) Retinyl ester secretion by intestinal cells: a specific and regulated process dependent on assembly and secretion of chylomicrons. J. Lipid Res. **42**, 272–280.

84 During, A. and Harrison, E. H. (2007) Mechanisms of provitamin A (carotenoid) and vitamin A (retinol) transport into and out of intestinal Caco-2 cells. J. Lipid Res. **48**, 2283–2294.

85 Cooper, A. D. (1997) Hepatic uptake of chylomicron remnants. J. Lipid Res.

86 Tall, A. (1995) Plasma lipid transfer proteins. Annu. Rev. Biochem. **64**, 235–257.

87 Lemieux, S., Fontani, R., Uffelman, K. D., Lewis, G. F. and Steiner, G. (1998) Apolipoprotein B-48 and retinyl palmitate are not equivalent markers of postprandial intestinal lipoproteins. J. Lipid Res. **39**, 1964–1971.

88 Mahley, R. W. (1996) Heparan sulfate proteoglycan/low density lipoprotein receptor-related protein pathway involved in type III hyperlipoproteinemia and Alzheimer's disease. Isr. J. Med. Sci. **32**, 414–429.

89 Gad, M. Z. and Harrison, E. H. (1991) Neutral and acid retinyl ester hydrolases associated with rat liver microsomes: relationships to microsomal cholesteryl ester hydrolases. J. Lipid Res. **32**, 685–693.

90 Sun, G., Alexson, S. E. and Harrison, E. H. (1997) Purification and characterization of a neutral, bile salt-independent retinyl ester hydrolase from rat liver microsomes. Relationship To rat carboxylesterase ES-2. J. Biol. Chem. **272**, 24488–24493.

91 Schreiber, R., Taschler, U., Preiss-Landl, K., Wongsiriroj, N., Zimmermann, R. and Lass, A. (2012) Retinyl ester hydrolases and their roles in vitamin A homeostasis. Biochim. Biophys. Acta **1821**, 113–123.

92 Harrison, E. H., Gad, M. Z. and Ross, A. C. (1995) Hepatic uptake and metabolism of chylomicron retinyl esters: probable role of plasma membrane/endosomal retinyl ester hydrolases. J. Lipid Res. **36**, 1498–1506.

93 Blaner, W. S., Hendriks, H. F., Brouwer, A., de Leeuw, A. M., Knook, D. L. and Goodman, D. S. (1985) Retinoids, retinoid-binding proteins, and retinyl palmitate hydrolase distributions in different types of rat liver cells. J. Lipid Res. **26**, 1241–1251.

94 Nau, H. and Blaner, W. S. (1999) Retinoids, Springer.

95 Blomhoff, R., Rasmussen, M., Nilsson, A., Norum, K. R., Berg, T., Blaner, W. S., Kato, M., Mertz, J. R., Goodman, D. S. and Eriksson, U. (1985) Hepatic retinol metabolism. Distribution of retinoids, enzymes, and binding proteins in isolated rat liver cells. J. Biol. Chem. **260**, 13560–13565.

96 Hendriks, H. F., Elhanany, E., Brouwer, A., de Leeuw, A. M. and Knook, D. L. (1988) Uptake and processing of [3H]retinoids in rat liver studied by electron microscopic autoradiography. Hepatology **8**, 276–285.

97 Senoo, H., Kojima, N. and Sato, M. (2007) Vitamin A-storing cells (stellate cells). Vitam. Horm. **75**, 131–159.

98 Azaïs-Braesco, V., Dodeman, I., Delpal, S., Alexandre-Gouabau, M. C., Partier, A., Borel, P. and Grolier, P. (1995) Vitamin A contained in the lipid droplets of rat liver stellate cells is substrate for acid retinyl ester hydrolase. Biochim. Biophys. Acta **1259**, 271–276.

99 Harrison, E. H., Blaner, W. S., Goodman, D. S. and Ross, A. C. (1987) Subcellular localization of retinoids, retinoid-binding proteins, and acyl-CoA:retinol acyltransferase in rat liver. J. Lipid Res. **28**, 973–981.

100 Napoli, J. L. (2012) Physiological insights into all-trans-retinoic acid biosynthesis. Biochim. Biophys. Acta **1821**, 152–167.

101 Boerman, M. H. and Napoli, J. L. (1991) Cholate-independent retinyl ester hydrolysis. Stimulation by Apo-cellular retinol-binding protein. J. Biol. Chem. **266**, 22273–22278.

102 Herr, F. M. and Ong, D. E. (1992) Differential interaction of lecithin-retinol acyltransferase with cellular retinol binding proteins. Biochemistry **31**, 6748–6755.

103 Yang, Q., Graham, T. E., Mody, N., Preitner, F., Peroni, O. D., Zabolotny, J. M., Kotani, K., Quadro, L. and Kahn, B. B. (2005) Serum retinol binding protein 4 contributes to insulin resistance in obesity and type 2 diabetes. Nature **436**, 356–362.

104 Graham, T. E., Yang, Q., Blüher, M., Hammarstedt, A., Ciaraldi, T. P., Henry, R. R., Wason, C. J., Oberbach, A., Jansson, P.-A., Smith, U., et al. (2006) Retinol-binding protein 4 and insulin resistance in lean, obese, and diabetic subjects. N. Engl. J. Med. **354**, 2552–2563.

105 Newcomer, M. E., Jones, T. A., Aqvist, J., Sundelin, J., Eriksson, U., Rask, L. and Peterson, P. A. (1984) The three-dimensional structure of retinol-binding protein. EMBO J. **3**, 1451–1454.

106 Monaco, H. L., Rizzi, M. and Coda, A. (1995) Structure of a complex of two plasma proteins: transthyretin and retinol-binding protein. Science **268**, 1039–1041.

107 Kawaguchi, R., Yu, J., Honda, J., Hu, J., Whitelegge, J., Ping, P., Wiita, P., Bok, D. and Sun, H. (2007) A membrane receptor for retinol binding protein mediates cellular uptake of vitamin A. Science **315**, 820–825.

108 Szeto, W., Jiang, W., Tice, D. A., Rubinfeld, B., Hollingshead, P. G., Fong, S. E., Dugger, D. L., Pham, T., Yansura, D. G., Wong, T. A., et al. (2001) Overexpression of the retinoic acid-responsive gene Stra6 in human cancers and its synergistic induction by Wnt-1 and retinoic acid. Cancer Res. **61**, 4197–4205.

109 Berry, D. C., O'Byrne, S. M., Vreeland, A. C., Blaner, W. S. and Noy, N. (2012)

Cross talk between signaling and vitamin A transport by the retinol-binding protein receptor STRA6. Molecular and Cellular Biology **32**, 3164–3175.

110 Berry, D. C., Croniger, C. M., Ghyselinck, N. B. and Noy, N. (2012) Transthyretin blocks retinol uptake and cell signaling by the holo-retinol-binding protein receptor STRA6. Molecular and Cellular Biology **32**, 3851–3859.

111 Alapatt, P., Guo, F., Komanetsky, S. M., Wang, S., Cai, J., Sargsyan, A., Rodríguez Díaz, E., Bacon, B. T., Aryal, P. and Graham, T. E. (2013) Liver retinol transporter and receptor for serum retinol-binding protein (RBP4). Journal of Biological Chemistry **288**, 1250–1265.

112 Moore, T. (1937) Vitamin A and carotene: The vitamin A reserve of the adult human being in health and disease. Biochem. J. **31**, 155–164.

113 Jeans, P. C. and Zentmire, Z. (1934) A clinical method for determining moderate degrees of vitamin A deficiency. JAMA, American Medical Association **102**, 892–895.

114 Tanumihardjo, S. A. (2004) Assessing vitamin A status: past, present and future. J. Nutr. **134**, 290S–293S.

115 Pilch, S. M. (1985) Assessment of the Vitamin A Nutritional Status of the U.S. Population Based on Data Collected in the Health and Nutrition Examination Surveys (Pilch, S. M., ed.), Life Sciences Research Office, Federation of American Societies for Experimental Biology, Bethesda, MD.

116 Combs, G. F. (2012) Chapter 5. Vitamin A. The Vitamins Fourth Edition. pp 93–138, Elsevier Inc.

117 Huang, J.-F., Dai, C.-Y., Yu, M.-L., Shin, S.-J., Hsieh, M.-Y., Huang, C.-F., Lee, L.-P., Lin, K.-D., Lin, Z.-Y., Chen, S.-C., et al. (2009) Serum retinol-binding protein 4 is inversely correlated with disease severity of chronic hepatitis C. J. Hepatol. **50**, 471–478.

118 Amédée-Manesme, O., Anderson, D. and Olson, J. A. (1984) Relation of the relative dose response to liver concentrations of vitamin A in generally well-nourished surgical patients. Am. J. Clin. Nutr. **39**, 898–902.

119 West, K. P. (2003) Vitamin A deficiency disorders in children and women. Food Nutr Bull **24**, S78–90.

120 West, K. P. (2002) Extent of vitamin A deficiency among preschool children and women of reproductive age. J. Nutr. **132**, 2857S–2866S.

121 Arlappa, N. (2013) Vitamin A deficiency control measures: Importance of vitamin A supplementation as a public health policy in the Indian context. J Public Health Policy.

122 Olson, J. A. (1987) Recommended dietary intakes (RDI) of vitamin A in humans. Am. J. Clin. Nutr. **45**, 704–716.

123 Ramakrishnan, U. and Darnton-Hill, I. (2002) Assessment and control of vitamin A deficiency disorders. J. Nutr. **132**, 2947S–2953S.

124 Penniston, K. L. and Tanumihardjo, S. A. (2006) The acute and chronic toxic effects of vitamin A. Am. J. Clin. Nutr. **83**, 191–201.

125 Olson, J. A. (1983) Adverse effects of large doses of vitamin A and retinoids. Semin. Oncol. **10**, 290–293.

126 Chambon, P. (1994) The retinoid signaling pathway: molecular and genetic analyses. Semin. Cell Biol. **5**, 115–125.

127 Lefebvre, P., Martin, P. J., Flajollet, S., Dedieu, S., Billaut, X. and Lefebvre, B. (2005) Transcriptional activities of retinoic acid receptors. Vitam. Horm. **70**, 199–264.

128 Lehmann, J. M., Dawson, M. I., Hobbs, P. D., Husmann, M. and Pfahl, M. (1991) Identification of retinoids with nuclear receptor subtype-selective activities. Cancer Res. **51**, 4804–4809.

129 Napoli, J. L. (1986) Retinol metabolism in LLC-PK1 Cells. Characterization of retinoic acid synthesis by an established mammalian cell line. J. Biol. Chem. **261**, 13592–13597.

130 Ottonello, S., Scita, G., Mantovani, G., Cavazzini, D. and Rossi, G. L. (1993) Retinol bound to cellular retinol-binding protein is a substrate for cytosolic retinoic acid synthesis. J. Biol. Chem. **268**, 27133–27142.

131 Zhang, M., Hu, P. and Napoli, J. L. (2004) Elements in the N-terminal signaling sequence that determine cytosolic topology of short-chain dehydrogenases/reductases. Studies with retinol dehydrogenase type 1 and cis-retinol/androgen dehydrogenase type 1. J. Biol. Chem. **279**, 51482–51489.

132 Boerman, M. H. and Napoli, J. L. (1995) Effects of sulfhydryl reagents, retinoids, and solubilization on the activity of microsomal retinol dehydrogenase. Arch. Biochem. Biophys. **321**, 434–441.

133 Akawi, el, Z. and Napoli, J. L. (1994) Rat liver cytosolic retinal dehydrogenase: comparison of 13-cis-, 9-cis-, and all-trans-retinal as substrates and effects of cellular retinoid-binding proteins and retinoic acid on activity. Biochemistry **33**, 1938–1943.

134 Matt, N., Dupé, V., Garnier, J.-M., Dennefeld, C., Chambon, P., Mark, M. and Ghyselinck, N. B. (2005) Retinoic acid-dependent eye morphogenesis is orchestrated by neural crest cells. Development **132**, 4789–4800.

135 Lassen, N., Bateman, J. B., Estey, T., Kuszak, J. R., Nees, D. W., Piatigorsky, J., Duester, G., Day, B. J., Huang, J., Hines, L. M., et al. (2007) Multiple and additive functions of ALDH3A1 and ALDH1A1: cataract phenotype and ocular oxidative damage in Aldh3a1(-/-)/Aldh1a1(-/-) knock-out mice. J. Biol. Chem. **282**, 25668–25676.

136 Ziouzenkova, O., Orasanu, G., Sharlach, M., Akiyama, T. E., Berger, J. P., Viereck, J., Hamilton, J. A., Tang, G., Dolnikowski, G. G., Vogel, S., et al. (2007) Retinaldehyde represses adipogenesis and diet-induced obesity. Nat. Med. **13**, 695–702.

137 Reichert, B., Yasmeen, R., Jeyakumar, S. M., Yang, F., Thomou, T., Alder, H., Duester, G., Maiseyeu, A., Mihai, G., Harrison, E. H., et al. (2011) Concerted action of aldehyde dehydrogenases influences depot-specific fat formation. Mol. Endocrinol. **25**, 799–809.

138 Elizondo, G., Corchero, J., Sterneck, E. and Gonzalez, F. J. (2000) Feedback inhibition of the retinaldehyde dehydrogenase gene ALDH1 by retinoic acid through retinoic acid receptor alpha and CCAAT/enhancer-binding protein beta. J. Biol. Chem. **275**, 39747–39753.

139 Elizondo, G., Medina-Díaz, I. M., Cruz, R., Gonzalez, F. J. and Vega, L. (2009) Retinoic acid modulates retinaldehyde dehydrogenase 1 gene expression through the induction of GADD153-C/EBPbeta interaction. Biochem. Pharmacol. **77**, 248–257.

140 Zhai, Y., Sperkova, Z. and Napoli, J. L. (2001) Cellular expression of retinal dehydrogenase types 1 and 2: effects of vitamin A status on testis mRNA. J. Cell. Physiol. **186**, 220–232.

141 Lin, M., Zhang, M., Abraham, M., Smith, S. M. and Napoli, J. L. (2003) Mouse retinal dehydrogenase 4 (RALDH4), molecular cloning, cellular expression, and activity in 9-cis-retinoic acid biosynthesis in intact cells. J. Biol. Chem. **278**, 9856–9861.

142 Sima, A., Parisotto, M., Mader, S. and Bhat, P. V. (2009) Kinetic characterization of recombinant mouse retinal dehydrogenase types 3 and 4 for retinal substrates. Biochim. Biophys. Acta **1790**, 1660–1664.

143 Roberts, A. B., Nichols, M. D., Newton, D. L. and Sporn, M. B. (1979) In vitro metabolism of retinoic acid in hamster intestine and liver. J. Biol. Chem. **254**, 6296–6302.

144 Fujii, H., Sato, T., Kaneko, S., Gotoh, O., Fujii-Kuriyama, Y., Osawa, K., Kato, S. and Hamada, H. (1997) Metabolic inactivation of retinoic acid by a novel P450 differentially expressed in developing mouse embryos. EMBO J. **16**, 4163–4173.

145 Wang, Y., Zolfaghari, R. and Ross, A. C. (2002) Cloning of rat cytochrome P450RAI (CYP26) cDNA and regulation of its gene expression by all-trans-retinoic acid in vivo. Arch. Biochem. Biophys. **401**, 235–243.

146 Ray, W. J., Bain, G., Yao, M. and Gottlieb, D. I. (1997) CYP26, a novel mammalian cytochrome P450, is induced by retinoic acid and defines a new family. J. Biol. Chem. **272**, 18702–18708.

147 Abu-Abed, S., Dollé, P., Metzger, D., Beckett, B., Chambon, P. and Petkovich, M. (2001) The retinoic acid-metabolizing enzyme, CYP26A1, is essential for normal hindbrain patterning, vertebral identity, and development of posterior structures. Genes Dev. **15**, 226–240.

148 Kane, M. A., Folias, A. E., Pingitore, A., Perri, M., Obrochta, K. M., Krois, C. R., Cione, E., Ryu, J. Y. and Napoli, J. L. (2010) Identification of 9-cis-retinoic acid as a pancreas-specific autacoid that attenuates glucose-stimulated insulin secretion. Proceedings of the National Academy of Sciences **107**, 21884–21889.

149 Kane, M. A. (2012) Analysis, occurrence, and function of 9-cis-retinoic acid.

Biochim. Biophys. Acta **1821**, 10–20.

150 Urbach, J. and Rando, R. R. (1994) Isomerization of all-trans-retinoic acid to 9-cis-retinoic acid. Biochem. J. **299 (Pt 2)**, 459–465.

151 Hébuterne, X., Wang, X. D., Johnson, E. J., Krinsky, N. I. and Russell, R. M. (1995) Intestinal absorption and metabolism of 9-cis-beta-carotene in vivo: biosynthesis of 9-cis-retinoic acid. J. Lipid Res. **36**, 1264–1273.

152 Mangelsdorf, D. J., Thummel, C., Beato, M., Herrlich, P., Schütz, G., Umesono, K., Blumberg, B., Kastner, P., Mark, M., Chambon, P., et al. (1995) The nuclear receptor superfamily: the second decade. Cell **83**, 835–839.

153 Nagpal, S., Friant, S., Nakshatri, H. and Chambon, P. (1993) RARs and RXRs: evidence for two autonomous transactivation functions (AF-1 and AF-2) and heterodimerization in vivo. EMBO J. **12**, 2349–2360.

154 Katahira, M., Knegtel, R. M., Boelens, R., Eib, D., Schilthuis, J. G., van der Saag, P. T. and Kaptein, R. (1992) Homo- and heteronuclear NMR studies of the human retinoic acid receptor beta DNA-binding domain: sequential assignments and identification of secondary structure elements. Biochemistry **31**, 6474–6480.

155 Mader, S., Chen, J. Y., Chen, Z., White, J., Chambon, P. and Gronemeyer, H. (1993) The patterns of binding of RAR, RXR and TR homo- and heterodimers to direct repeats are dictated by the binding specificites of the DNA binding domains. EMBO J. **12**, 5029–5041.

156 Mader, S., Kumar, V., de Verneuil, H. and Chambon, P. (1989) Three amino acids of the oestrogen receptor are essential to its ability to distinguish an oestrogen from a glucocorticoid-responsive element. Nature **338**, 271–274.

157 Bourguet, W., Vivat, V., Wurtz, J. M., Chambon, P., Gronemeyer, H. and Moras, D. (2000) Crystal structure of a heterodimeric complex of RAR and RXR ligand-binding domains. Mol. Cell **5**, 289–298.

158 Graupner, G., Wills, K. N., Tzukerman, M., Zhang, X. K. and Pfahl, M. (1989) Dual regulatory role for thyroid-hormone receptors allows control of retinoic-acid receptor activity. Nature **340**, 653–656.

159 Glass, C. K. (1994) Differential recognition of target genes by nuclear receptor monomers, dimers, and heterodimers. Endocr. Rev. **15**, 391–407.

160 Hu, X. and Lazar, M. A. (1999) The CoRNR motif controls the recruitment of corepressors by nuclear hormone receptors. Nature **402**, 93–96.

161 Wagner, R. L., Apriletti, J. W., McGrath, M. E., West, B. L., Baxter, J. D. and Fletterick, R. J. (1995) A structural role for hormone in the thyroid hormone receptor. Nature **378**, 690–697.

162 Holm, E. (1929) Demonstration of vitamin A in retinal tissue and a comparison with the vitamin content of brain tissue. Acta Ophthalm **7**, 146–161.

163 Yudkin, A. M. (1931) The Presence of Vitamin A in the Retina. Trans Am Ophthalmol Soc **29**, 263–272.

164 Collins, F. D. and Morton, R. A. (1950) Studies on rhodopsin. I. Methods of extraction and the absorption spectrum. Biochem. J. **47**, 3–10.

165 Collins, F. D. and Morton, R. A. (1950) Studies on rhodopsin. 2. Indicator yellow. Biochem. J. **47**, 10–18.

166 Collins, F. D. and Morton, R. A. (1950) Studies in rhodopsin. 3. Rhodopsin and transient orange. Biochem. J. **47**, 18–24.

167 Wald, G. (1951) The chemistry of rod vision. Science **113**, 287–291.

168 Rattner, A., Smallwood, P. M. and Nathans, J. (2000) Identification and characterization of all-trans-retinol dehydrogenase from photoreceptor outer segments, the visual cycle enzyme that reduces all-trans-retinal to all-trans-retinol. J. Biol. Chem. **275**, 11034–11043.

169 Haeseleer, F., Jang, G.-F., Imanishi, Y., Driessen, C. A. G. G., Matsumura, M., Nelson, P. S. and Palczewski, K. (2002) Dual-substrate specificity short chain retinol dehydrogenases from the vertebrate retina. J. Biol. Chem. **277**, 45537–45546.

170 Ruiz, A. and Bok, D. (2010) Focus on molecules: lecithin retinol acyltransferase. Exp. Eye Res. **90**, 186–187.

171 Trehan, A., Cañada, F. J. and Rando, R. R. (1990) Inhibitors of retinyl ester formation also prevent the biosynthesis of 11-cis-retinol. Biochemistry **29**, 309–312.

172 Collins, C. E. and Koay, P. (2010) Xerophthalmia because of dietary-induced vitamin a deficiency in a young Scottish man. Cornea **29**, 828–829.

173 Basti, S. and Schmidt, C. (2008) Vitamin a deficiency. Cornea **27**, 973–author reply 973.

174 Green, H. N. and Mellanby, E. (1928) Vitamin A as an anti-infective agent. Br Med J **2**, 691–696.

175 Stephensen, C. B. (2001) Vitamin A, infection, and immune function. Annu. Rev. Nutr. **21**, 167–192.

176 West, C. E., Sijtsma, S. R., Kouwenhoven, B., Rombout, J. H. and van der Zijpp, A. J. (1992) Epithelia-damaging virus infections affect vitamin A status in chickens. J. Nutr. **122**, 333–339.

177 Martorell, R., Yarbrough, C., Yarbrough, S. and Klein, R. E. (1980) The impact of ordinary illnesses on the dietary intakes of malnourished children. Am. J. Clin. Nutr. **33**, 345–350.

178 Duggan, M. B. and Milner, R. D. (1986) Composition of weight gain by Kenyan children during recovery from measles. Hum Nutr Clin Nutr **40**, 173–183.

179 Duggan, M. B. and Milner, R. D. (1986) Energy cost of measles infection. Arch. Dis. Child. **61**, 436–439.

180 Mata, L. (1992) Diarrheal disease as a cause of malnutrition. Am. J. Trop. Med. Hyg. **47**, 16–27.

181 Solomons, N. W. (1993) Pathways to the impairment of human nutritional status by gastrointestinal pathogens. Parasitology **107 Suppl**, S19–35.

182 Mitra, A. K., Alvarez, J. O., Guay-Woodford, L., Fuchs, G. J., Wahed, M. A. and Stephensen, C. B. (1998) Urinary retinol excretion and kidney function in children with shigellosis. Am. J. Clin. Nutr. **68**, 1095–1103.

183 Spencer, S. P. and Belkaid, Y. (2012) Dietary and commensal derived nutrients: shaping mucosal and systemic immunity. Curr. Opin. Immunol. **24**, 379–384.

184 Huang, M. E., Ye, Y. C., Chen, S. R., Chai, J. R., Lu, J. X., Zhoa, L., Gu, L. J. and Wang, Z. Y. (1988) Use of all-trans retinoic acid in the treatment of acute promyelocytic leukemia. Blood **72**, 567–572.

185 Smith, S. M., Levy, N. S. and Hayes, C. E. (1987) Impaired immunity in vitamin A-deficient mice. J. Nutr. **117**, 857–865.

186 Wiedermann, U., Tarkowski, A., Bremell, T., Hanson, L. A., Kahu, H. and

Dahlgren, U. I. (1996) Vitamin A deficiency predisposes to Staphylococcus aureus infection. Infect. Immun. **64**, 209–214.

187 Ross, A. C. (2012) Vitamin A and retinoic acid in T cell-related immunity. Am. J. Clin. Nutr. **96**, 1166S–72S.

188 Orr, J. B. and Richards, M. B. (1934) Growth and vitamin A deficiency. Biochem. J. **28**, 1259–1273.

189 Anzano, M. A., Lamb, A. J. and Olson, J. A. (1979) Growth, appetite, sequence of pathological signs and survival following the induction of rapid, synchronous vitamin A deficiency in the rat. J. Nutr. **109**, 1419–1431.

190 Sherbet, G. V. (1997) Retinoids: Their Physiological Function and Therapeutic Potential, Elsevier.

191 Collins, M. D. and Mao, G. E. (1999) Teratology of retinoids. Annu. Rev. Pharmacol. Toxicol. **39**, 399–430.

192 Howell, J. M., Thompson, J. N. and Pitt, G. A. (1963) Histology of the lesions produced in the reproductive tract of animals fed a diet deficient in vitamin A alcohol but containing vitamin A acid. I. The male rat. J. Reprod. Fertil. **5**, 159–167.

193 Lufkin, T., Lohnes, D., Mark, M., Dierich, A., Gorry, P., Gaub, M. P., LeMeur, M. and Chambon, P. (1993) High postnatal lethality and testis degeneration in retinoic acid receptor alpha mutant mice. Proc. Natl. Acad. Sci. U.S.A. **90**, 7225–7229.

194 Lohnes, D., Kastner, P., Dierich, A., Mark, M., LeMeur, M. and Chambon, P. (1993) Function of retinoic acid receptor gamma in the mouse. Cell **73**, 643–658.

195 Kastner, P., Mark, M., Leid, M., Gansmuller, A., Chin, W., Grondona, J. M., Décimo, D., Krezel, W., Dierich, A. and Chambon, P. (1996) Abnormal spermatogenesis in RXR beta mutant mice. Genes Dev. **10**, 80–92.

196 Breitman, T. R., Selonick, S. E. and Collins, S. J. (1980) Induction of differentiation of the human promyelocytic leukemia cell line (HL-60) by retinoic acid. Proc. Natl. Acad. Sci. U.S.A. **77**, 2936–2940.

197 Breitman, T. R., Collins, S. J. and Keene, B. R. (1981) Terminal differentiation of human promyelocytic leukemic cells in primary culture in response to retinoic acid. Blood **57**, 1000–1004.

198 Mangiarotti, R., Danova, M., Alberici, R. and Pellicciari, C. (1998) All-trans retinoic acid (ATRA)-induced apoptosis is preceded by G1 arrest in human MCF-7 breast cancer cells. Br. J. Cancer **77**, 186–191.

199 Si, S. P., Tsou, H. C., Lee, X. and Peacocke, M. (1995) Effect of cellular senescence and retinoic acid on the expression of cellular retinoic acid binding proteins in skin fibroblasts. Exp. Cell Res. **219**, 243–248.

200 Swisshelm, K., Ryan, K., Lee, X., Tsou, H. C., Peacocke, M. and Sager, R. (1994) Down-regulation of retinoic acid receptor beta in mammary carcinoma cell lines and its up-regulation in senescing normal mammary epithelial cells. Cell Growth Differ. **5**, 133–141.

201 Cheung, B., Hocker, J. E., Smith, S. A., Reichert, U., Norris, M. D., Haber, M., Stewart, B. W. and Marshall, G. M. (1996) Retinoic acid receptors beta and gamma distinguish retinoid signals for growth inhibition and neuritogenesis in human neuroblastoma cells. Biochem. Biophys. Res. Commun. **229**, 349–354.

202 Noy, N. (2010) Between death and survival: retinoic acid in regulation of apoptosis. Annu. Rev. Nutr. **30**, 201–217.

203 Mrass, P., Rendl, M., Mildner, M., Gruber, F., Lengauer, B., Ballaun, C., Eckhart, L. and Tschachler, E. (2004) Retinoic acid increases the expression of p53 and proapoptotic caspases and sensitizes keratinocytes to apoptosis: a possible explanation for tumor preventive action of retinoids. Cancer Res. **64**, 6542–6548.

204 Mayer, J. and Krehl, W. A. (1948) Influence of vitamin A deficiency on the gross efficiency of growth of rats. Yale J Biol Med **20**, 403–405.

205 Sampson, M. M. and Korenchevsky, V. (1932) The influence of vitamin A deficiency on male rats in paired feeding experiments. Biochem. J. **26**, 1322–1339.

206 Zhang, Y., Li, R., Li, Y., Chen, W., Zhao, S. and Chen, G. (2012) Vitamin A status affects obesity development and hepatic expression of key genes for fuel metabolism in Zucker fatty rats. Biochem. Cell Biol. **90**, 548–557.

207 Rogers, W. E. and Bieri, J. G. (1969) Vitamin A deficiency in the rat prior to weaning. Proc. Soc. Exp. Biol. Med. **132**, 622–624.

208 McCarthy, P. T. and Cerecedo, L. R. (1952) Vitamin A deficiency in the mouse. J. Nutr. **46**, 361–376.

209 Sagazio, A., Piantedosi, R., Alba, M., Blaner, W. S. and Salvatori, R. (2007) Vitamin A deficiency does not influence longitudinal growth in mice. Nutrition **23**, 483–488.

210 Friedman, J. M. and Halaas, J. L. (1998) Leptin and the regulation of body weight in mammals. Nature **395**, 763–770.

211 Kumar, M. V., Sunvold, G. D. and Scarpace, P. J. (1999) Dietary vitamin A supplementation in rats: suppression of leptin and induction of UCP1 mRNA. J. Lipid Res. **40**, 824–829.

212 Hollung, K., Rise, C. P., Drevon, C. A. and Reseland, J. E. (2004) Tissue-specific regulation of leptin expression and secretion by all-trans retinoic acid. J. Cell. Biochem. **92**, 307–315.

213 Felipe, F., Mercader, J., Ribot, J., Palou, A. and Bonet, M. L. (2005) Effects of retinoic acid administration and dietary vitamin A supplementation on leptin expression in mice: lack of correlation with changes of adipose tissue mass and food intake. Biochim. Biophys. Acta **1740**, 258–265.

214 Bernard, R. A. and Halpern, B. P. (1968) Taste changes in vitamin A deficiency. J. Gen. Physiol. **52**, 444–464.

215 Reifen, R., Agami, O., Weiser, H., Biesalski, H. and Naim, M. (1998) Impaired responses to sweet taste in vitamin A-deficient rats. Metab. Clin. Exp. **47**, 1–2.

216 Garrett-Laster, M., Russell, R. M. and Jacques, P. F. (1984) Impairment of taste and olfaction in patients with cirrhosis: the role of vitamin A. Hum Nutr Clin Nutr **38**, 203–214.

217 Boeck, W. C. and Yater, W. M. (1929) Xanthemia and xanthosis (carotinemia): clinical study. Journal of the Laboratory & Clinical Medicine **14**, 1129–1143.

218 Rabinowitch, I. M. (1930) Carotinemia and diabetes: II. The relationship between the sugar, cholesterol and carotin contents of blood plasma. Archives of Internal Medicine, JAMA **45**, 586–592.

219 Mosenthal, H. O. and Loughlin, W. C. (1944) Vitamins A, B and C in diabetic children. Archives of Internal Medicine, JAMA **73**, 391–396.

220 Basu, T. K., Tze, W. J. and Leichter, J. (1989) Serum vitamin A and retinol-binding protein in patients with insulin-dependent diabetes mellitus. Am. J. Clin.

Nutr. **50**, 329–331.

221 Bershad, S., Rubinstein, A., Paterniti, J. R., Le, N. A., Poliak, S. C., Heller, B., Ginsberg, H. N., Fleischmajer, R. and Brown, W. V. (1985) Changes in plasma lipids and lipoproteins during isotretinoin therapy for acne. N. Engl. J. Med. **313**, 981–985.

222 Tallman, M. S. and Kwaan, H. C. (1992) Reassessing the hemostatic disorder associated with acute promyelocytic leukemia. Blood **79**, 543–553.

223 Miller, V. A., Rigas, J. R., Muindi, J. R., Tong, W. P., Venkatraman, E., Kris, M. G. and Warrell, R. P. (1994) Modulation of all-trans retinoic acid pharmacokinetics by liarozole. Cancer Chemother. Pharmacol. **34**, 522–526.

224 Vu-Dac, N., Gervois, P., Torra, I. P., Fruchart, J. C., Kosykh, V., Kooistra, T., Princen, H. M., Dallongeville, J. and Staels, B. (1998) Retinoids increase human apo C-III expression at the transcriptional level via the retinoid X receptor. Contribution to the hypertriglyceridemic action of retinoids. J. Clin. Invest. **102**, 625–632.

225 Shachter, N. S. (2001) Apolipoproteins C-I and C-III as important modulators of lipoprotein metabolism. Curr. Opin. Lipidol. **12**, 297–304.

226 Preitner, F., Mody, N., Graham, T. E., Peroni, O. D. and Kahn, B. B. (2009) Long-term Fenretinide treatment prevents high-fat diet-induced obesity, insulin resistance, and hepatic steatosis. Am. J. Physiol. Endocrinol. Metab. **297**, E1420–9.

227 Mcilroy, G. D., Delibegovic, M., Owen, C., Stoney, P. N., Shearer, K. D., McCaffery, P. J. and Mody, N. (2013) Fenretinide treatment prevents diet-induced obesity in association with major alterations in retinoid homeostatic gene expression in adipose, liver, and hypothalamus. Diabetes **62**, 825–836.

228 Wolf, G., Lane, M. D. and Johnson, B. C. (1957) Studies on the function of vitamin A in metabolism. J. Biol. Chem. **225**, 995–1008.

229 Johnson, B. C. and Wolf, G. (1960) The function of vitamin A in carbohydrate metabolism; its role in adrenocorticoid production. Vitam. Horm. **18**, 457–483.

230 Ray, A. and Sadhu, D. P. (1959) Carbohydrate metabolism in hypervitaminosis A. Nature **184(Suppl 17)**, 1323.

231 Singh, M., Singh, V. N. and Venkitasubramanian, T. A. (1968) Early effects of

feeding excess vitamin A: hepatic glycogen, blood lactic acid, plasma NEFA and glucose tolerance in rats. Life Sci. **7**, 239–247.

232 Singh, M., Singh, V. N. and Venkitasubramanian, T. A. (1976) Early effects of excessive retinol intake on hepatic glycogen metabolism. Arch. Biochem. Biophys. **173**, 93–99.

233 Shankar, S., Creek, K. E. and De Luca, L. M. (1990) The effect of the progression of vitamin A deficiency on glucose, galactose and mannose incorporation into sugar phosphates and sugar nucleotides in hamster liver. J. Nutr. **120**, 361–374.

234 Singh, V. N., Singh, M. and Dileepan, K. N. (1978) Early effects of vitamin A toxicity on hepatic glycolysis in rat. J. Nutr. **108**, 1959–1962.

235 Chen, G., Zhang, Y., Lu, D., Li, N.-Q. and Ross, A. C. (2009) Retinoids synergize with insulin to induce hepatic Gck expression. Biochem. J. **419**, 645–653.

236 Dileepan, K. N., Singh, V. N. and Ramachandran, C. K. (1981) Decreased hepatic gluconeogenesis in vitamin A-deficient rats. Proc. Soc. Exp. Biol. Med. **167**, 248–253.

237 Singh, M., Ningh, V. N. and Venkitasubramanian, T. A. (1975) Role of adrenals in the vitamin A-mediated increase in the activities of gluconeogenic enzymes of rat liver. Life Sci. **17**, 859–865.

238 Dileepan, K. N., Singh, V. N. and Ramachandran, C. K. (1977) Early effects of hypervitaminosis A on gluconeogenic activity and amino acid metabolizing enzymes of rat liver. J. Nutr. **107**, 1809–1815.

239 Singh, M., Singh, V. N. and Venkitasubramanian, T. A. (1976) Early effects of excessive retinol intake on gluconeogenesis. Involvement of adrenals in the increased activities on Gluconeogenic Enzymes of rat. Arch. Biochem. Biophys. **173**, 82–92.

240 Zhang, Y., Li, R., Chen, W., Li, Y. and Chen, G. (2011) Retinoids induced Pck1 expression and attenuated insulin-mediated suppression of its expression via activation of retinoic acid receptor in primary rat hepatocytes. Mol. Cell. Biochem. **355**, 1–8.

241 Shin, D.-J., Odom, D. P., Scribner, K. B., Ghoshal, S. and McGrane, M. M. (2002) Retinoid regulation of the phosphoenolpyruvate carboxykinase gene in liver. Mol.

Cell. Endocrinol. **195**, 39–54.

242 Scribner, K. B., Odom, D. P. and McGrane, M. M. (2007) Nuclear receptor binding to the retinoic acid response elements of the phosphoenolpyruvate carboxykinase gene in vivo: effects of vitamin A deficiency. J. Nutr. Biochem. **18**, 206–214.

243 Sampson, M. M., Dennison, M. and Korenchevsky, V. (1932) The absorption of nitrogen and of fat from the alimentary canal of rats kept on a vitamin A-deficient diet. Biochem. J. **26**, 1315–1321.

244 Brown, E. F. and Morgan, A. F. (1948) The effect of vitamin A deficiency upon the nitrogen metabolism of the rat. J. Nutr. **35**, 425–438.

245 Esteban-Pretel, G., Marín, M. P., Cabezuelo, F., Moreno, V., Renau-Piqueras, J., Timoneda, J. and Barber, T. (2010) Vitamin A deficiency increases protein catabolism and induces urea cycle enzymes in rats. J. Nutr. **140**, 792–798.

246 John, A. and Sivakumar, B. (1989) Effect of vitamin A deficiency on nitrogen balance and hepatic urea cycle enzymes and intermediates in rats. J. Nutr. **119**, 29–35.

247 Rao, B. S. N. (1966) Effect of vitamin A deficiency on the incorporation of 14C-Leucine into tissue proteins of rats. Nature **210**, 306–307.

248 Tryfiates, G. P. and Krause, R. F. (1971) Effect of vitamin A deficiency on the protein synthetic activity of rat liver ribosomes. Proc. Soc. Exp. Biol. Med. **136**, 946–948.

249 Nerurkar, M. K. and Sahasrabudhe, M. B. (1956) Metabolism of calcium, phosphorus and nitrogen in hypervitaminosis A in young rats. Biochem. J. **63**, 344–349.

250 Gerber, L. E. and Erdman, J. W. (1982) Changes in lipid metabolism during retinoid administration. J. Am. Acad. Dermatol. **6**, 664–674.

251 Ellis, C. N., Kang, S., Vinik, A. I., Grekin, R. C., Cunningham, W. J. and Voorhees, J. J. (1987) Glucose and insulin responses are improved in patients with psoriasis during therapy with etretinate. Arch Dermatol **123**, 471–475.

252 Yehya, A., Baer, J. T., Smiley, W., Dollar, A. and Sperling, L. (2009) Hypervitaminosis A altering the lipid profile in a hypercholesterolemic patient. J

Clin Lipidol **3**, 205–207.

253 Ellis, J. K., Russell, R. M., Makrauer, F. L. and Schaefer, E. J. (1986) Increased risk for vitamin A toxicity in severe hypertriglyceridemia. Ann. Intern. Med. **105**, 877–879.

254 Lettinga, K. D., Gutter, W., Van Noorden, C. J., Schellens, J. P. and Frederiks, W. M. (1996) Early effects of high doses of retinol (vitamin A) on the in situ cellular metabolism in rat liver. Liver **16**, 1–11.

255 Misra, U. K. (1965) Hypervitaminosis A and tissue fatty acids. Can. J. Biochem. **43**, 1885–1886.

256 Singh, V. N., Singh, M. and Venkitasubramanian, T. A. (1969) Early effects of feeding excess vitamin A: mechanism of fatty liver production in rats. J. Lipid Res. **10**, 395–401.

257 Ramachandran, C. K., Dileepan, K. N., Singh, V. and Venkitasubramanian, T. A. (1975) Effect of excess and deficiency of vitamin A on the utilization of FFA by liver and skeletal muscle. Environ Physiol Biochem **5**, 208–214.

258 Singh, M. and Singh, V. N. (1978) Fatty liver in hypervitaminosis A: synthesis and release of hepatic triglycerides. Am. J. Physiol. **234**, E511–4.

259 Oliveros, L. B., Domeniconi, M. A., Vega, V. A., Gatica, L. V., Brigada, A. M. and Gimenez, M. S. (2007) Vitamin A deficiency modifies lipid metabolism in rat liver. Br. J. Nutr. **97**, 263–272.

260 Khanna, A. and Reddy, T. S. (1983) Effect of undernutrition and vitamin A deficiency on the phospholipid composition of rat tissues at 21 days of age. -- I. Liver, spleen and kidney. Int J Vitam Nutr Res **53**, 3–8.

261 Green, B., Lowe, J. S. and Morton, R. A. (1955) The effect of vitamin A deficiency on the cholesterol levels of the plasma and liver of the rat. Biochem. J. **61**, 447–453.

262 Wiss, O. and Wiss, V. (1980) Alterations of the lipid metabolism of rat liver as early symptoms of vitamin A deficiency. Int J Vitam Nutr Res **50**, 233–237.

263 Green, H. N. (1934) Fat metabolism in vitamin A deficiency: the utilisation of fat and the desaturation of fat in the liver. Biochem. J. **28**, 25–30.

264 Horton, J. D., Goldstein, J. L. and Brown, M. S. (2002) SREBPs: activators of the

complete program of cholesterol and fatty acid synthesis in the liver. J. Clin. Invest. **109**, 1125–1131.

265 Chen, G., Liang, G., Ou, J., Goldstein, J. L. and Brown, M. S. (2004) Central role for liver X receptor in insulin-mediated activation of Srebp-1c transcription and stimulation of fatty acid synthesis in liver. Proc. Natl. Acad. Sci. U.S.A. **101**, 11245–11250.

266 Li, R., Chen, W., Li, Y., Zhang, Y. and Chen, G. (2011) Retinoids synergized with insulin to induce Srebp-1c expression and activated its promoter via the two liver X receptor binding sites that mediate insulin action. Biochem. Biophys. Res. Commun. **406**, 268–272.

267 Deluca, H. F., Manatt, M. R., Madsen, N. and Olson, E. B. (1963) Action of vitamin A on liver homogenate oxidation of tricarboxylic acid cycle intermediates. J. Nutr. **81**, 383–386.

268 Seward, C. R., Vaughan, G. and Hove, E. L. (1964) Respiratory activities of hypo- and hypervitaminotic A rat liver homogenates. Proc. Soc. Exp. Biol. Med. **117**, 477–480.

269 Seward, C. R., Vaughan, G. and Hove, E. L. (1966) Effect of vitamin A deficiency or excess on the oxidative phosphorylation by rat liver mitochondria. J. Biol. Chem. **241**, 1229–1232.

270 Brissova, M., Fowler, M. J., Nicholson, W. E., Chu, A., Hirshberg, B., Harlan, D. M. and Powers, A. C. (2005) Assessment of human pancreatic islet architecture and composition by laser scanning confocal microscopy. J. Histochem. Cytochem. **53**, 1087–1097.

271 Andralojc, K. M., Mercalli, A., Nowak, K. W., Albarello, L., Calcagno, R., Luzi, L., Bonifacio, E., Doglioni, C. and Piemonti, L. (2009) Ghrelin-producing epsilon cells in the developing and adult human pancreas. Diabetologia **52**, 486–493.

272 Unger, R. H. and Cherrington, A. D. (2012) Glucagonocentric restructuring of diabetes: a pathophysiologic and therapeutic makeover. J. Clin. Invest. **122**, 4–12.

273 Gylfe, E. and Gilon, P. (2013) Glucose regulation of glucagon secretion. Diabetes Res. Clin. Pract.

274 Jensen, M. V., Joseph, J. W., Ronnebaum, S. M., Burgess, S. C., Sherry, A. D. and

Newgard, C. B. (2008) Metabolic cycling in control of glucose-stimulated insulin secretion. Am. J. Physiol. Endocrinol. Metab. **295**, E1287–97.

275 Chertow, B. S., Driscoll, H. K., Blaner, W. S., Meda, P., Cordle, M. B. and Matthews, K. A. (1994) Effects of vitamin A deficiency and repletion on rat glucagon secretion. Pancreas **9**, 475–484.

276 Chertow, B. S., Driscoll, H. K., Primerano, D. A., Cordle, M. B. and Matthews, K. A. (1996) Retinoic acid receptor transcripts and effects of retinol and retinoic acid on glucagon secretion from rat islets and glucagon-secreting cell lines. Metab. Clin. Exp. **45**, 300–305.

277 Matthews, K. A., Rhoten, W. B., Driscoll, H. K. and Chertow, B. S. (2004) Vitamin A deficiency impairs fetal islet development and causes subsequent glucose intolerance in adult rats. J. Nutr. **134**, 1958–1963.

278 Chertow, B. S., Blaner, W. S., Baranetsky, N. G., Sivitz, W. I., Cordle, M. B., Thompson, D. and Meda, P. (1987) Effects of vitamin A deficiency and repletion on rat insulin secretion in vivo and in vitro from isolated islets. J. Clin. Invest. **79**, 163–169.

279 Chertow, B. S. and Baker, G. R. (1978) The effects of vitamin A on insulin release and glucose oxidation in isolated rat islets. Endocrinology **103**, 1562–1572.

280 Chertow, B. S., Goking, N. Q., Driscoll, H. K., Primerano, D. A. and Matthews, K. A. (1997) Effects of all-trans-retinoic acid (ATRA) and retinoic acid receptor (RAR) expression on secretion, growth, and apoptosis of insulin-secreting RINm5F cells. Pancreas **15**, 122–131.

281 Driscoll, H. K., Adkins, C. D., Chertow, T. E., Cordle, M. B., Matthews, K. A. and Chertow, B. S. (1997) Vitamin A stimulation of insulin secretion: effects on transglutaminase mRNA and activity using rat islets and insulin-secreting cells. Pancreas **15**, 69–77.

282 Cabrera-Valladares, G., German, M. S., Matschinsky, F. M., Wang, J. and Fernandez-Mejia, C. (1999) Effect of retinoic acid on glucokinase activity and gene expression and on insulin secretion in primary cultures of pancreatic islets. Endocrinology **140**, 3091–3096.

283 Kane, M. A., Folias, A. E., Pingitore, A., Perri, M., Krois, C. R., Ryu, J. Y., Cione,

E. and Napoli, J. L. (2011) CrbpI modulates glucose homeostasis and pancreas 9-cis-retinoic acid concentrations. Molecular and Cellular Biology **31**, 3277–3285.

284 Ramachandran, C. K., Dileepan, K. N., Singh, V. N. and Venkitasubramanian, T. A. (1986) Metabolic potential of the adipose tissue of rats during hyper- and hypovitaminosis A. Proc. Soc. Exp. Biol. Med. **182**, 73–78.

285 Ribot, J., Felipe, F., Bonet, M. L. and Palou, A. (2001) Changes of Adiposity in Response to Vitamin A Status Correlate with Changes of PPARγ2 Expression. Obesity **9**, 500–509.

286 de Souza Valente da Silva, L., Valeria da Veiga, G. and Ramalho, R. A. (2007) Association of serum concentrations of retinol and carotenoids with overweight in children and adolescents. Nutrition **23**, 392–397.

287 Zulet, M. A., Puchau, B., Hermsdorff, H. H. M., Navarro, C. and Martínez, J. A. (2008) Vitamin A intake is inversely related with adiposity in healthy young adults. J. Nutr. Sci. Vitaminol. **54**, 347–352.

288 Berry, D. C. and Noy, N. (2009) All-trans-retinoic acid represses obesity and insulin resistance by activating both peroxisome proliferation-activated receptor beta/delta and retinoic acid receptor. Molecular and Cellular Biology **29**, 3286–3296.

289 Mercader, J., Ribot, J., Murano, I., Felipe, F., Cinti, S., Bonet, M. L. and Palou, A. (2006) Remodeling of white adipose tissue after retinoic acid administration in mice. Endocrinology **147**, 5325–5332.

290 Murholm, M., Isidor, M. S., Basse, A. L., Winther, S., Sørensen, C., Skovgaard-Petersen, J., Nielsen, M. M., Hansen, A. S., Quistorff, B. and Hansen, J. B. (2013) Retinoic acid has different effects on UCP1 expression in mouse and human adipocytes. BMC Cell Biol. **14**, 41.

291 Kiefer, F. W., Vernochet, C., O'Brien, P., Spoerl, S., Brown, J. D., Nallamshetty, S., Zeyda, M., Stulnig, T. M., Cohen, D. E., Kahn, C. R., et al. (2012) Retinaldehyde dehydrogenase 1 regulates a thermogenic program in white adipose tissue. Nat. Med. **18**, 918–925.

292 Dimaculangan, D. D., Chawla, A., Boak, A., Kagan, H. M. and Lazar, M. A. (1994) Retinoic acid prevents downregulation of ras recision gene/lysyl oxidase

early in adipocyte differentiation. Differentiation **58**, 47–52.

293 Berry, D. C., Soltanian, H. and Noy, N. (2010) Repression of cellular retinoic acid-binding protein II during adipocyte differentiation. Journal of Biological Chemistry **285**, 15324–15332.

294 Xue, J. C., Schwarz, E. J., Chawla, A. and Lazar, M. A. (1996) Distinct stages in adipogenesis revealed by retinoid inhibition of differentiation after induction of PPARgamma. Molecular and Cellular Biology **16**, 1567–1575.

295 Safonova, I., Darimont, C., Amri, E. Z., Grimaldi, P., Ailhaud, G., Reichert, U. and Shroot, B. (1994) Retinoids are positive effectors of adipose cell differentiation. Mol. Cell. Endocrinol. **104**, 201–211.

296 Cannon, B. and Nedergaard, J. (2004) Brown adipose tissue: function and physiological significance. Physiol. Rev. **84**, 277–359.

297 Bonet, M. L., Oliver, J., Picó, C., Felipe, F., Ribot, J., Cinti, S. and Palou, A. (2000) Opposite effects of feeding a vitamin A-deficient diet and retinoic acid treatment on brown adipose tissue uncoupling protein 1 (UCP1), UCP2 and leptin expression. J. Endocrinol. **166**, 511–517.

298 Puigserver, P., Vázquez, F., Bonet, M. L., Picó, C. and Palou, A. (1996) In vitro and in vivo induction of brown adipocyte uncoupling protein (thermogenin) by retinoic acid. Biochem. J. **317 (Pt 3)**, 827–833.

299 Alvarez, R., de Andrés, J., Yubero, P., Viñas, O., Mampel, T., Iglesias, R., Giralt, M. and Villarroya, F. (1995) A novel regulatory pathway of brown fat thermogenesis. Retinoic acid is a transcriptional activator of the mitochondrial uncoupling protein gene. J. Biol. Chem. **270**, 5666–5673.

300 Larose, M., Cassard-Doulcier, A. M., Fleury, C., Serra, F., Champigny, O., Bouillaud, F. and Ricquier, D. (1996) Essential cis-acting elements in rat uncoupling protein gene are in an enhancer containing a complex retinoic acid response domain. J. Biol. Chem. **271**, 31533–31542.

301 Ribot, J., Felipe, F., Bonet, M. L. and Palou, A. (2004) Retinoic acid administration and vitamin A status modulate retinoid X receptor alpha and retinoic acid receptor alpha levels in mouse brown adipose tissue. Mol. Cell. Biochem. **266**, 25–30.

302 Pedersen, B. K. (2011) Muscles and their myokines. J. Exp. Biol. **214**, 337–346.

303 Sundeen, G., Richards, J. F. and Bragg, D. B. (1980) The effect of vitamin A deficiency on some postmortem parameters of avian muscle. Poult. Sci. **59**, 2225–2236.

304 Lee, Y. M., Lee, J. O., Jung, J.-H., Kim, J. H., Park, S.-H., Park, J. M., Kim, E.-K., Suh, P.-G. and Kim, H. S. (2008) Retinoic acid leads to cytoskeletal rearrangement through AMPK-Rac1 and stimulates glucose uptake through AMPK-p38 MAPK in skeletal muscle cells. J. Biol. Chem. **283**, 33969–33974.

305 Narbonne, J. F., Daubeze, M. and Bonmort, F. (1978) [Protein metabolism in vitamin A deficient rats. II. Protein synthesis in striated muscle]. Ann Nutr Aliment **32**, 59–75.

306 Hillgartner, F. B., Morin, D. and Hansen, R. J. (1982) Effect of excessive vitamin A intake on muscle protein turnover in the rat. Biochem. J. **202**, 499–508.

307 Amengual, J., Ribot, J., Bonet, M. L. and Palou, A. (2008) Retinoic acid treatment increases lipid oxidation capacity in skeletal muscle of mice. Obesity (Silver Spring) **16**, 585–591.

308 Angulo, P. (2002) Nonalcoholic fatty liver disease. N. Engl. J. Med. **346**, 1221–1231.

309 O'Brien, R. M. and Granner, D. K. (1996) Regulation of gene expression by insulin. Physiol. Rev. **76**, 1109–1161.

310 Iynedjian, P. B. (2009) Molecular physiology of mammalian glucokinase. Cell. Mol. Life Sci. **66**, 27–42.

311 Brown, M. S. and Goldstein, J. L. (1997) The SREBP pathway: regulation of cholesterol metabolism by proteolysis of a membrane-bound transcription factor. Cell **89**, 331–340.

312 Zhang, Y., Chen, W., Li, R., Li, Y., Ge, Y. and Chen, G. (2011) Insulin-regulated Srebp-1c and Pck1 mRNA expression in primary hepatocytes from zucker fatty but not lean rats is affected by feeding conditions. PLoS ONE **6**, e21342.

313 Li, Y., Zhang, Y., Li, R., Chen, W., Howell, M., Zhang, R. and Chen, G. (2012) The hepatic Raldh1 expression is elevated in Zucker fatty rats and its over-expression introduced the retinal-induced Srebp-1c expression in INS-1 cells.

PLoS ONE **7**, e45210.

314 Phillips, M. S., Liu, Q., Hammond, H. A., Dugan, V., Hey, P. J., Caskey, C. T. and Hess, J. F. (1996) Leptin receptor missense mutation in the fatty Zucker rat. Nature Genetics, Nature Publishing Group **13**, 18–19.

315 Clark, J. B., Keen, S. and Clark, C. M. (1982) Studies on the regulation of insulin binding by liver plasma membranes from Zucker fatty rats. Diabetes **31**, 867–873.

316 Li, S., Brown, M. S. and Goldstein, J. L. (2010) Bifurcation of insulin signaling pathway in rat liver: mTORC1 required for stimulation of lipogenesis, but not inhibition of gluconeogenesis. Proceedings of the National Academy of Sciences **107**, 3441–3446.

317 Moon, Y.-A., Liang, G., Xie, X., Frank-Kamenetsky, M., Fitzgerald, K., Koteliansky, V., Brown, M. S., Goldstein, J. L. and Horton, J. D. (2012) The Scap/SREBP pathway is essential for developing diabetic fatty liver and carbohydrate-induced hypertriglyceridemia in animals. Cell Metab. **15**, 240–246.

318 Heilbronn, L. K., Coster, A. C. F., Campbell, L. V., Greenfield, J. R., Lange, K., Christopher, M. J., Meikle, P. J. and Samocha-Bonet, D. (2013) The effect of short-term overfeeding on serum lipids in healthy humans. Obesity (Silver Spring).

319 Magkos, F., Smith, G. I., Reeds, D. N., Okunade, A., Patterson, B. W. and Mittendorfer, B. (2013) One day of overfeeding impairs nocturnal glucose but not fatty acid homeostasis in overweight men. Obesity (Silver Spring).

320 Lecoultre, V., Egli, L., Carrel, G., Theytaz, F., Kreis, R., Schneiter, P., Boss, A., Zwygart, K., Lê, K.-A., Bortolotti, M., et al. (2013) Effects of fructose and glucose overfeeding on hepatic insulin sensitivity and intrahepatic lipids in healthy humans. Obesity (Silver Spring) **21**, 782–785.

321 Cahill, F., Amini, P., Wadden, D., Khalili, S., Randell, E., Vasdev, S., Gulliver, W. and Sun, G. (2013) Short-term overfeeding increases circulating adiponectin independent of obesity status. PLoS ONE **8**, e74215.

322 Wadden, D., Cahill, F., Amini, P., Randell, E., Vasdev, S., Yi, Y., Church, J. and Sun, G. (2013) Circulating glucagon-like peptide-1 increases in response to short-term overfeeding in men. Nutr Metab (Lond) **10**, 33.

323 Sajan, M. P., Standaert, M. L., Miura, A., Kahn, C. R. and Farese, R. V. (2004)

Tissue-specific differences in activation of atypical protein kinase C and protein kinase B in muscle, liver, and adipocytes of insulin receptor substrate-1 knockout mice. Mol. Endocrinol. **18**, 2513–2521.

324 Iynedjian, P. B., Roth, R. A., Fleischmann, M. and Gjinovci, A. (2000) Activation of protein kinase B/cAkt in hepatocytes is sufficient for the induction of expression of the gene encoding glucokinase. Biochem. J. **351 Pt 3**, 621–627.

325 Farese, R. V. and Sajan, M. P. (2012) Atypical protein kinase C in cardiometabolic abnormalities. Curr. Opin. Lipidol. **23**, 175–181.

326 Sajan, M. P., Ivey, R. A. and Farese, R. V. (2013) Metformin action in human hepatocytes: coactivation of atypical protein kinase C alters 5'-AMP-activated protein kinase effects on lipogenic and gluconeogenic enzyme expression. Diabetologia **56**, 2507–2516.

327 Zucker, L. M. and Antoniades, H. N. (1972) Insulin and obesity in the Zucker genetically obese rat "fatty". Endocrinology **90**, 1320–1330.

328 Ribaux, P. G. and Iynedjian, P. B. (2003) Analysis of the role of protein kinase B (cAKT) in insulin-dependent induction of glucokinase and sterol regulatory element-binding protein 1 (SREBP1) mRNAs in hepatocytes. Biochem. J. **376**, 697–705.

329 Iynedjian, P. B. (2005) Lack of evidence for a role of TRB3/NIPK as an inhibitor of PKB-mediated insulin signalling in primary hepatocytes. Biochem. J. **386**, 113–118.

330 Ravichandran, L. V., Esposito, D. L., Chen, J. and Quon, M. J. (2001) Protein kinase C-zeta phosphorylates insulin receptor substrate-1 and impairs its ability to activate phosphatidylinositol 3-kinase in response to insulin. J. Biol. Chem. **276**, 3543–3549.

331 Liu, Y. F., Paz, K., Herschkovitz, A., Alt, A., Tennenbaum, T., Sampson, S. R., Ohba, M., Kuroki, T., LeRoith, D. and Zick, Y. (2001) Insulin stimulates PKCzeta -mediated phosphorylation of insulin receptor substrate-1 (IRS-1). A self-attenuated mechanism to negatively regulate the function of IRS proteins. J. Biol. Chem. **276**, 14459–14465.

332 Moeschel, K., Beck, A., Weigert, C., Lammers, R., Kalbacher, H., Voelter, W.,

Schleicher, E. D., Häring, H.-U. and Lehmann, R. (2004) Protein kinase C-zeta-induced phosphorylation of Ser318 in insulin receptor substrate-1 (IRS-1) attenuates the interaction with the insulin receptor and the tyrosine phosphorylation of IRS-1. J. Biol. Chem. **279**, 25157–25163.

333 Hirota, K., Sakamaki, J.-I., Ishida, J., Shimamoto, Y., Nishihara, S., Kodama, N., Ohta, K., Yamamoto, M., Tanimoto, K. and Fukamizu, A. (2008) A combination of HNF-4 and Foxo1 is required for reciprocal transcriptional regulation of glucokinase and glucose-6-phosphatase genes in response to fasting and feeding. J. Biol. Chem. **283**, 32432–32441.

334 Kim, T.-H., Kim, H., Park, J.-M., Im, S.-S., Bae, J.-S., Kim, M.-Y., Yoon, H.-G., Cha, J.-Y., Kim, K.-S. and Ahn, Y.-H. (2009) Interrelationship between liver X receptor alpha, sterol regulatory element-binding protein-1c, peroxisome proliferator-activated receptor gamma, and small heterodimer partner in the transcriptional regulation of glucokinase gene expression in liver. J. Biol. Chem. **284**, 15071–15083.

335 Roth, U., Curth, K., Unterman, T. G. and Kietzmann, T. (2004) The transcription factors HIF-1 and HNF-4 and the coactivator p300 are involved in insulin-regulated glucokinase gene expression via the phosphatidylinositol 3-kinase/protein kinase B pathway. J. Biol. Chem. **279**, 2623–2631.

336 Yang, J., Reshef, L., Cassuto, H., Aleman, G. and Hanson, R. W. (2009) Aspects of the control of phosphoenolpyruvate carboxykinase gene transcription. Journal of Biological Chemistry **284**, 27031–27035.

337 Barthel, A. and Schmoll, D. (2003) Novel concepts in insulin regulation of hepatic gluconeogenesis. Am. J. Physiol. Endocrinol. Metab. **285**, E685–92.

338 Matsumoto, M., Pocai, A., Rossetti, L., Depinho, R. A. and Accili, D. (2007) Impaired regulation of hepatic glucose production in mice lacking the forkhead transcription factor Foxo1 in liver. Cell Metab. **6**, 208–216.

339 Puigserver, P., Rhee, J., Donovan, J., Walkey, C. J., Yoon, J. C., Oriente, F., Kitamura, Y., Altomonte, J., Dong, H., Accili, D., et al. (2003) Insulin-regulated hepatic gluconeogenesis through FOXO1-PGC-1alpha interaction. Nature **423**, 550–555.

340 Zhou, X. Y., Shibusawa, N., Naik, K., Porras, D., Temple, K., Ou, H., Kaihara, K., Roe, M. W., Brady, M. J. and Wondisford, F. E. (2004) Insulin regulation of hepatic gluconeogenesis through phosphorylation of CREB-binding protein. Nat. Med. **10**, 633–637.

341 He, L., Sabet, A., Djedjos, S., Miller, R., Sun, X., Hussain, M. A., Radovick, S. and Wondisford, F. E. (2009) Metformin and insulin suppress hepatic gluconeogenesis through phosphorylation of CREB binding protein. Cell **137**, 635–646.

342 Horton, J. D., Goldstein, J. L. and Brown, M. S. (2002) SREBPs: transcriptional mediators of lipid homeostasis. Cold Spring Harb. Symp. Quant. Biol. **67**, 491–498.

343 Owen, J. L., Zhang, Y., Bae, S.-H., Farooqi, M. S., Liang, G., Hammer, R. E., Goldstein, J. L. and Brown, M. S. (2012) Insulin stimulation of SREBP-1c processing in transgenic rat hepatocytes requires p70 S6-kinase. Proceedings of the National Academy of Sciences **109**, 16184–16189.

344 Langin, D. (2001) Diabetes, insulin secretion, and the pancreatic beta-cell mitochondrion. N. Engl. J. Med. **345**, 1772–1774.

345 Asfari, M., Janjic, D., Meda, P., Li, G., Halban, P. A. and Wollheim, C. B. (1992) Establishment of 2-mercaptoethanol-dependent differentiated insulin-secreting cell lines. Endocrinology **130**, 167–178.

346 Hohmeier, H. E., Mulder, H., Chen, G., Henkel-Rieger, R., Prentki, M. and Newgard, C. B. (2000) Isolation of INS-1-derived cell lines with robust ATP-sensitive K+ channel-dependent and -independent glucose-stimulated insulin secretion. Diabetes **49**, 424–430.

347 Chen, G., Hohmeier, H. E., Gasa, R., Tran, V. V. and Newgard, C. B. (2000) Selection of insulinoma cell lines with resistance to interleukin-1beta- and gamma-interferon-induced cytotoxicity. Diabetes **49**, 562–570.

348 Velho, G., Blanché, H., Vaxillaire, M., Bellanné-Chantelot, C., Pardini, V. C., Timsit, J., Passa, P., Deschamps, I., Robert, J. J., Weber, I. T., et al. (1997) Identification of 14 new glucokinase mutations and description of the clinical profile of 42 MODY-2 families. Diabetologia **40**, 217–224.

349 Cuesta-Muñoz, A. L., Huopio, H., Otonkoski, T., Gomez-Zumaquero, J. M., Näntö-Salonen, K., Rahier, J., López-Enriquez, S., García-Gimeno, M. A., Sanz, P., Soriguer, F. C., et al. (2004) Severe persistent hyperinsulinemic hypoglycemia due to a de novo glucokinase mutation. Diabetes **53**, 2164–2168.

350 Walker, D. G. and Rao, S. (1964) The role of glucokinase in the phosphorylation of glucose by rat liver. Biochem. J. **90**, 360–368.

351 Matschinsky, F. M. and Ellerman, J. E. (1968) Metabolism of glucose in the islets of Langerhans. J. Biol. Chem. **243**, 2730–2736.

352 Trus, M. D., Zawalich, W. S., Burch, P. T., Berner, D. K., Weill, V. A. and Matschinsky, F. M. (1981) Regulation of glucose metabolism in pancreatic islets. Diabetes **30**, 911–922.

353 Bedoya, F. J., Matschinsky, F. M., Shimizu, T., O'Neil, J. J. and Appel, M. C. (1986) Differential regulation of glucokinase activity in pancreatic islets and liver of the rat. J. Biol. Chem. **261**, 10760–10764.

354 Iynedjian, P. B., Pilot, P. R., Nouspikel, T., Milburn, J. L., Quaade, C., Hughes, S., Ucla, C. and Newgard, C. B. (1989) Differential expression and regulation of the glucokinase gene in liver and islets of Langerhans. Proc. Natl. Acad. Sci. U.S.A. **86**, 7838–7842.

355 Magnuson, M. A. and Shelton, K. D. (1989) An alternate promoter in the glucokinase gene is active in the pancreatic beta cell. J. Biol. Chem. **264**, 15936–15942.

356 Hayzer, D. J. and Iynedjian, P. B. (1990) Alternative splicing of glucokinase mRNA in rat liver. Biochem. J. **270**, 261–263.

357 Iynedjian, P. B., Marie, S., Wang, H., Gjinovci, A. and Nazaryan, K. (1996) Liver-specific enhancer of the glucokinase gene. J. Biol. Chem. **271**, 29113–29120.

APPENDIX

Table 1-5: List of real time PCR primers used in the dissertation.

Gene	Real-time PCR primers
Gck	5′-CGAGATGCTATCAAGAGGAGAG-3′
	5′-TCACATTGGCGGTCTTCATAG-3′
Pck1	5′-AGTCACCATCACTTCCTGGAAGA-3′
	5′-GGTGCAGAATCGCGAGTTG-3′
Srebp-1c	5′-GGAGCCATGGATTGCACATT-3′
	5′-AGGCCAGGGAAGTCACTGTCT-3′
Pklr	5′-CGTTTGTGCCACACAGATGCT-3′
	5′-CATTGGCCACATCGCTTGTCT-3′
Rdh2	5′-CAAGTTCTTCTACCTCCCCATGA-3′
	5′-TCCAGTAGAAAAGGGCATCCA-3′
Raldh1	5′-ATGGTCTAGCAGCAGGAGT-3′
	5′-CCAGACATCTTGAATCCACCGAA-3′
Raldh4	5′-TGACCCAAGAAATAGCCAAAGAA-3′
	5′-CTAGGCAACTGCCAGCACTTTT-3′
Cyp26a1	5′-AGTGATGGGCGCGGATAAT-3′
	5′-TGCACTGACACCAACCGGT-3′
Rbpr2	5′-GTCAGCTCCATCTTGGGCTT-3′
	5′-ACCTCCCTAGAAACTGCCCA-3′

Table 1-6: List of ChIP PCR primers used in the dissertation.

No.	ChIP PCR primers
oGC786	5′-GGCCAAACCCAAAGAAAGGAT-3′
oGC797	5′-CTGCGGAGGGGTTGACGAT-3′
oGC788	5′-CCCACGAGGATCCCCCACTA -3′
oGC794	5′-GGTTTGACAAAGGCCACAG -3′

VITA

Wei Chen was born on Mar. 19th 1984 to Qinji Chen and Cuixiang Li in Xi'an, Shaanxi, China. He received his elementary education at the University Road Elementary School from 1990 to 1996 in Xi'an. He then attended the Middle School Attached to Northwestern Polytechnical University in Xi'an and received his high school diploma in June of 2002. He completed his Bachelor of Science degree in biology at Wuhan University in June of 2006. In the fall of same year, he entered the graduate program at the College of Life Sciences of Wuhan University, where he studied the mechanisms of cell polarity establishment under the guidance of Dr. Xiangdong Gao. He received his Master of Science degree in microbiology in June of 2008. He was then admitted to the PhD program at the University of Tennessee in January of 2009, and joined Dr. Guoxun Chen's lab to study the roles of vitamin A and atypical protein kinase in the regulation of hepatic glucose and lipid metabolism. He defended his dissertation on May 6th, 2014. During his time at UTK, he served as a graduate assistant and completed the dietetic internship program.